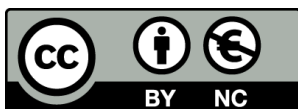


IMPORTANCE OF HYDROGEN-MEDIATED
MECHANISMS FOR MICROBIAL
ELECTROSYNTHESIS: REGULATION AT THE
MOLECULAR LEVEL

Elisabet Perona Vico

Per citar o enllaçar aquest document:
Para citar o enlazar este documento:
Use this url to cite or link to this publication:
<http://hdl.handle.net/10803/674124>



<http://creativecommons.org/licenses/by-nc/4.0/deed.ca>

Aquesta obra està subjecta a una llicència Creative Commons Reconeixement-
NoComercial

Esta obra está bajo una licencia Creative Commons Reconocimiento-NoComercial

This work is licensed under a Creative Commons Attribution-NonCommercial licence



DOCTORAL THESIS

**Importance of hydrogen-mediated mechanisms for microbial
electrosynthesis: regulation at the molecular level**

Elisabet Perona Vico

2021



DOCTORAL THESIS

**Importance of hydrogen-mediated mechanisms for microbial
electrosynthesis: regulation at the molecular level**

Elisabet Perona Vico

2021

Doctoral program in Water Science and Technology

Thesis supervisors

Dr. Lluís Bañeras Vives

Dr. Sebastià Puig Broch

PhD candidate

Elisabet Perona Vico

This thesis is submitted in fulfilment of the requirements to obtain the doctoral degree from the Universitat de Girona



Certificate of thesis direction

Hereby, Dr. Lluís Bañeras and Dr. Sebastià Puig, from the Universitat de Girona

CERTIFY:

That this doctoral thesis entitled: *“Importance of hydrogen-mediated mechanisms for microbial electrosynthesis: regulation at the molecular level”*, that Elisabet Perona Vico submitted to obtain the doctoral degree from Universitat de Girona, has been completed under their supervision and meets the requirements opt for the International Doctor mention.

In witness whereof and for such purposes as may arise, the following certification is signed:

Dr. Lluís Bañeras Vives

Dr. Sebastià Puig Broch

Girona, 26th of July of 2021

Papa, Mama,
Albert, Lourdes, María, Josep i Tura
A vosaltres que m'heu acompanyat,
moltes gràcies per ser-hi sempre.

LIST OF PUBLICATIONS

Part of this Ph.D. Thesis has been published in scientific journals:

Perona-Vico, E., Feliu-Paradedá, L., Puig, S, Bañeras, L. (2020) Bacteria coated cathodes as an *in-situ* hydrogen evolving platform for microbial electrosynthesis. Scientific Reports. 10 – 19852. Nature Publishing Group. ISSN 2045-2322. DOI: <https://doi.org/10.1038/s41598-020-76694-y>. Impact factor: 4.379. Open access.

Perona-Vico, E., Blasco-Gómez, R., Colprim, J., Puig S., Bañeras, L. (2019) [NiFe]-hydrogenases are constitutively expressed in an enriched *Methanobacterium* sp. population during electromethanogenesis. PLoS One 14(4): e0215029. Public Library of Science. ISSN 1932-6203 <https://doi.org/10.1371/journal.pone.0215029>. Impact factor: 2.740. Open access.

FUNDING AND ACKNOWLEDGEMENTS

This thesis was financially supported by the University of Girona (predoctoral grant IFUdG2018 ref.52 and mobility grant IF-MOB2020), and the European Union's Horizon 2020 research and innovation program under the grant agreement n° 760431 (BioReCO₂ver; <http://bioreco2ver.eu/>). LEQUIA and EcoAqua have been recognized as consolidated groups by the Catalan Government with codes 2017-SGR-1552 and 2017-SGR-548, respectively.

I would like to thank Prof. Dr. Miriam Agler-Rosenbaum for giving me the opportunity of being part of her research group at Leibniz Institute for Natural Product Research and Infection Biology – Hans Knöll Institute during my secondment in Jena (Germany).

LIST OF ABBREVIATIONS

Abbreviation	Description
16S rRNA	rRNA 16S ribosomal ribonucleic acid gene
Ag/AgCl	Silver chloride electrode
AEM	Anion exchange membrane
ADP	Adenosine diphosphate
ATP	Adenosine triphosphate
BES	Bioelectrochemical systems
BLAST	Basic Local Alignment Search Tool
bp	Base pair
cDNA	Complementary Deoxyribonucleic Acid
CA	Chronoamperometry
CE	Coulombic efficiency
CEM	Cationic exchange membrane
Chao1	Maximum richness index
CH ₄	Methane
CO ₂	Carbon dioxide
CTAB	Cetyltrimethylammonium bromide
CV	Cyclic voltammetry
dET	Direct interspecies electron transfer
DNA	Deoxyribonucleic Acid
DIET	Direct interspecies electron transfer
E	Energy
e ⁻	Electrons
EAB	Electroactive bacteria
EET	Extracellular electron transfer
E _f	Mid-point potential
FAD	Flavin adenine dinucleotide
Fd	Ferredoxin
FID	Flame ionization detector
GC	Gas chromatograph
GOIs	Genes of interest
H ⁰	Shannon diversity index
H ⁺	Protons
H ₂	Hydrogen
H ₂ ase	Hydrogenase
I	Intensity
IEM	Ionic exchange membrane
iET	Indirect Electron Transfer
MDC	Microbial desalination cell
MEC	Microbial electrolysis cell
MES	Microbial electrosynthesis
mET	Mediated electron transfer

Abbreviation	Description
METs	Microbial electrochemical technologies
MFC	Microbial fuel cell
MRC	Microbial remediation cell
N ₂	Nitrogen
NAD	Nicotinamide adenine dinucleotide
NADP	Nicotinamide adenine dinucleotide phosphate
NCBI	National Center for Biotechnology Information
NH ₃	Ammonia
OCV	Open circuit voltage
OD	Optical density
OTU	Operational Taxonomic Unit
P	Power
P _i	Inorganic phosphate
PD	Phylodiversity
PCoA	Principal Coordinates Analysis
PCR	Polymerase chain reaction
qPCR	Quantitative polymerase chain reaction
PHB	Polyhydroxy butyrate
PNS	Purple non-sulfur bacteria
RT-PCR	Reverse transcription-polymerase chain reaction
RNA	Ribonucleic Acid
SRB	Sulphate-reducing bacteria
SEM	Scanning electron microscopy
SHE	Standard hydrogen electrode
Sobs	Observed richness
V	Voltage
VFA	Volatile fatty acid
WLP	Wood Ljungdahl pathway

LIST OF FIGURES

INTRODUCTION

- Figure 1. Basic applications of microbial electrochemical technologies. **2**
- Figure 2. Wood-Ljungdahl pathway (A) and Wolfe cycle (B) for the reduction of CO₂. **5**
- Figure 3. Extracellular electron transfer mechanisms in biocathodes. **7**

MATERIALS AND METHODS

- Figure 4. Three-neck round flask BES configuration. **15**
- Figure 5. H-type BES configuration. **16**

CHAPTER 1

- Figure 6. Time course of state variables during the operation time of the BES reactor. **35**
- Figure 7. Electrochemical performance. **36**
- Figure 8. Scanning electron micrograph of the biofilm attached to the cathodes. **38**
- Figure 9. Microbial community composition in inoculum, bulk, and biofilm samples. **38**
- Figure 10. Changes in the DNA and cDNA-based microbial community structures of cathodes. **40**
- Figure 11. Relative content, number of target gene copies/number of copies of 16S rRNA or *ftsZ* gene of *Methanobacterium* sp. hydrogenases related genes. **42**

CHAPTER 2

- Figure 12. Abundance of 16S rRNA genes into biofilm and bulk samples. **49**
- Figure 13. Hydrogen production rates ($\mu\text{M}\cdot\text{min}^{-1}$) of monospecific biofilms of purple non sulphur (PNS) bacteria after successive CO₂ feeding in BES reactors. **50**
- Figure 14. Hydrogen production rates ($\mu\text{M}\cdot\text{min}^{-1}$) using *S. ovata* DSM 2662 (A) and *Desulfovibrio* strains (B). **54**
- Figure 15. Cyclic voltammeteries (CV) for *Rhodobacter*, *Rhodopseudomonas*, *Rhodocyclus tenuis*, *Sporomusa ovata*, and *Desulfovibrio* strains. **57**

CHAPTER 3

- Figure 16. Vector constructions for the two *Desulfovibrio* spp. **65**

LIST OF TABLES

MATERIALS AND METHODS

Table 1. Medium DSM 27	12
Table 2. Medium DSM 311	13
Table 3. Medium DSM 63	13
Table 4. Composition of trace element solutions	13
Table 5. Composition of vitamins solution	14
Table 6. Modified ATCC 1754 PETC medium used in BES	17
Table 7. Modified trace element solution and vitamin solution based on ATCC 1754 PETC medium	17
Table 8. Modifications of basal medium DSM 27 composition	18
Table 9. Modifications of basal medium DSM 311 composition	18
Table 10. Medium based on Aulenta et al., 2012 and modifications during biofilm formation and BES operation	19
Table 11. Designed primers for <i>Methanobacterium</i> sp.	26
Table 12. Primer design for <i>Desulfovibrio</i> spp. vectors construction.	29

CHAPTER 1

Table 13. Richness and diversity indicators according to sample type	37
Table 14. Most probable identification (BLAST, RefSeq RNA database), and relative abundance of the two most abundant archaeal 16S rRNA sequences in the electromethanogenic reactor	39

CHAPTER 2

Table 15. Hydrogen production rates, current demand, and energy consumption in abiotic conditions at different cathode potentials	47
Table 16. Ionic losses (mV) for each of the three used media modified for BES operation	48
Table 17. pH during BES operation	51
Table 18. pH values recorded after ten minutes of CO ₂ bubbling for each medium used for BES operation	51
Table 19. Maximum H ₂ accumulated, H ₂ production rate, H ₂ net production rate, current demand, energy, and coulombic efficiencies (CE%)	58

CHAPTER 3

Table 20. Characteristics of the available plasmids for SBR strains	62
Table 21. Genes of interest in <i>D. vulgaris</i> DSM 644 (NCBI accession number NC_002937) and presence of analogues in <i>D. paquesii</i> DSM 16681 (IMG Genome ID 2571042346)	63
Table 22. Changes on the main parameters of tested protocols to transform <i>D. paquesii</i> and <i>D. vulgaris</i> cells.	68
Table 23. Summary of the results obtained for the different transformations performed with both <i>D. paquesii</i> and <i>D. vulgaris</i> cells	69

TABLE OF CONTENTS

LIST OF PUBLICATIONS	i
FUNDING AND ACKNOWLEDGEMENTS	ii
LIST OF ABBREVIATIONS	iii
LIST OF FIGURES	v
LIST OF TABLES	vi
TABLE OF CONTENTS	viii
ABSTRACT	xi
RESUM	xiii
RESUMEN	xv
INTRODUCTION	1
1. Complex microbial populations and pure cultures for microbial electrosynthesis	3
2. Extracellular electron transfer mechanisms	5
3. Better together: synergic consortia	8
OBJECTIVES	11
MATERIALS AND METHODS	12
1. Bacterial strains and maintenance conditions	12
2. Configuration of bioelectrochemical systems	14
2.1. Three-neck flask BES	14
2.2. H-type reactors	15
3. Operation of bioelectrochemical systems	16
3.1. Electromethanogenesis	16
3.2. Electromicrobiology towards hydrogen evolution	17
4. Chemical analyses	20
5. Calculations	21
6. Electrochemical characterization	21
7. Nucleic acids (DNA and RNA) extractions	21
7.1. Electromethanogenesis	21
7.2. Electromicrobiology towards hydrogen evolution	22
8. Microbial community structure determination	23

9.	qPCR analyses	24
10.	Gene selection, primer design, and RT-PCR analyses	24
11.	Scanning electron microscopy (SEM)	27
12.	Plasmid construction for <i>Desulfovibrio</i> strains	27
13.	Transformation in <i>Desulfovibrio</i> strains	30
CHAPTER 1		31
1.	Background	32
2.	Results and Discussion	34
2.1.	Bioelectrochemical performance and methane production	34
2.2.	DNA based microbial community structure	37
2.3.	Determination of active members of the microbial community by RNA analysis	39
2.4.	Changes in the expression of <i>Methanobacterium</i> sp. [NiFe]-hydrogenases	41
CHAPTER 2		44
1.	Background	45
2.	Results and Discussion	47
2.1.	Electrocatalytic H ₂ production at carbon cloth electrodes	47
2.2.	Formation of monospecific biofilms and stability	48
2.3.	Bioelectrochemical production of H ₂ in purple non-sulphur (PNS) bacteria	49
2.4.	Bioelectrochemical production of H ₂ in <i>Sporomusa ovata</i>	53
2.5.	Bioelectrochemical production of H ₂ in sulphate-reducing bacteria	53
2.6.	Electrochemical characterization	55
CHAPTER 3		59
1.	Background	60
2.	Results and discussion	62
2.1.	Selection of genes of interest and vector construction	62
2.2.	Protocol assessment to transform the two <i>Desulfovibrio</i> spp.	66
2.3.	Proposal for improvements and future perspectives	70
GENERAL DISCUSSION		73
1.	Understanding EET: a higher ambition race	73
2.	Hydrogen is the key element in microbial electrosynthesis	76
3.	Putting all elements together: The <i>Desulfovibrio</i> scenario	78

4. Outlook and future perspectives	80
CONCLUDING REMARKS	81
REFERENCES	83

ABSTRACT

Microbial electrosynthesis (MES) is engineered to use electric power and carbon dioxide (CO₂) as the only energy and carbon sources in reductive bioelectrochemical processes for biosynthesis. This technology is conducted in bioelectrochemical systems (BES) and takes advantage of electroactive microorganisms. In MES, hydrogen (H₂) has been highlighted as the key intermediate element involved in a whole range of microbial metabolisms for the reduction of CO₂. A proper understanding of the role of H₂, its production, and availability in MES might reinforce the overall productivity and applicability of the technology.

Basic processes in MES rely on the transformation of electric power (electrons) into chemical energy in a process called electron transfer. The study of extracellular electron transfer (EET) mechanisms can help to understand the integration of microbes and electrode materials in an operative tandem, and to elucidate the participation of intermediate molecules, such as H₂, as opposed to direct electron transfer events for electrosynthesis. An electromethanogenic reactor conducting the reduction of CO₂ to methane (CH₄) was used to study putative genes taking part in EET. We aimed at determining short-time changes in the gene expression levels of [NiFe]-hydrogenases (Eha, Ehb, and Mvh), heterodisulfide reductase (Hdr), coenzyme F₄₂₀-reducing [NiFe]-hydrogenase (Frh), and hydrogenase maturation protein (HypD) according to the electron flow (closed and open electric circuits). Microbial community composition analysis through both DNA and cDNA signatures revealed that electromethanogenesis was conducted by *Methanobacterium* sp. being the main archaeon present in the system. According to RT-PCR data, suspected mechanisms in electron transfer events were not regulated at the transcriptional level when exposing *Methanobacterium* sp. cells to short-time open/closed electric circuits.

Since H₂ is the most relevant electron donor among microbial metabolisms, cathodic potentials generally used for CO₂ recycling are characterised to ensure no H₂ limitation. However, some microorganisms could serve as potentially interesting sustainable H₂ producers in biocathodes. We have studied the biological H₂ production in biocathodes operated at -1.0 V *vs.* Ag/AgCl, using a highly comparable technology and using CO₂ as the sole carbon feedstock. Ten different bacterial strains were chosen from genera *Rhodobacter*, *Rhodospseudomonas*, *Rhodocyclus*, *Desulfovibrio*, and *Sporomusa*, all described as hydrogen-producing candidates. Monospecific biofilms were formed on carbon cloth cathodes and hydrogen evolution was monitored over time using a microsensor. Eight over ten bacterial strains showed electroactivity and H₂ production rates increased significantly (2 to 8-fold)

compared to abiotic conditions for two of them (*Desulfovibrio paquesii* DSM 16681 and *Desulfovibrio desulfuricans* DSM 642). *D. paquesii* DSM 16681 exhibited the highest production rate ($45.6 \pm 18.8 \mu\text{M}\cdot\text{min}^{-1}$) compared to abiotic conditions ($5.5 \pm 0.6 \mu\text{M}\cdot\text{min}^{-1}$), although specific production rates (per unit biomass) were similar to those observed for other strains. Our results demonstrated many microorganisms are suspected to participate in hydrogen production, but inherent differences among strains did occur. These differences have to be considered for future developments of resilient biofilm coated cathodes as a stable hydrogen production platform in microbial electrosynthesis.

The application of bacteria-coated cathodes for sustainable H₂ production may not be efficient enough to maintain H₂ biosynthetic requirements for highly efficient producing strains. Here, we applied genetic engineering tools intending to further increase the H₂ production ability of *D. paquesii*. [Fe]-only hydrogenase and tetraheme cytochrome *c3* were selected as genes of interest to be overexpressed in *D. vulgaris* DSM 644 and *D. paquesii* DSM 16681. Different conditions and described protocols were tested towards implementing the proper mechanisms to ensure overexpression of the selected genes, but no successful results were obtained by the time of completion of this Ph.D. Thesis. Even though, an extensive and critical revision of the key factors to be controlled was done to address the existing limitations of the process.

Following an architecture analogy, studying H₂ production in BES has been the keystone of this Thesis, and model processes (such as methanogenesis, bioelectro-H₂ production, and homoacetogenesis) the needed rib-vaults to complete the desired structure. Different methods have been used throughout. In the process of completion of the dome, the presented approaches might have contributed to a better understanding of the key role of H₂ during microbial electrosynthesis and derive some conclusions. First, enhancing the current knowledge of extracellular electron transfer may lead to better control of reductive BES. Second, the required H₂ supply for sustainable electrochemical bioprocesses may be provided in a more efficient way using bio-H₂ evolving microorganisms. Finally, the application of synthetic biology and defined consortia should be considered for new and promising contributions in the MET's field.

RESUM

L'electrosíntesi microbiana (MES en anglès) utilitza l'electricitat i el diòxid de carboni (CO_2) com a única font d'energia i carboni durant els processos bioelectroquímics per a la biosíntesis. Aquest procés es duu a terme en sistemes bioelectroquímics (BES en anglès) aprofitant els microorganismes coneguts com electroactius. Durant l'electrosíntesi microbiana, l'hidrogen (H_2) ha estat destacat com a intermediari clau involucrat en varietat de metabolismes microbians durant la reducció del CO_2 . Entendre millor el paper de l' H_2 en l'electrosíntesi microbiana (producció i disponibilitat) pot reforçar la productivitat i aplicabilitat d'aquesta tecnologia.

Els processos bàsics en el MES depenen de la transformació de l'electricitat (electrons) en energia química en el procés anomenat transferència d'electrons. L'estudi dels mecanismes de transferència d'electrons (EET en anglès) en els sistemes bioelectroquímics pot ajudar a entendre les interaccions que es donen entre els microorganismes i els elèctrodes, i a determinar la participació de molècules intermediàries com l' H_2 , com a mecanisme oposat a la transferència directa d'electrons per l'electrosíntesi. Per estudiar els gens possiblement implicats en els esdeveniments d'EET es va utilitzar un reactor electrometanogènic en el que es promovia la reducció del CO_2 a metà (CH_4) amb l'objectiu de determinar canvis a curt termini en l'expressió gènica de [NiFe]-hidrogenases (Eha, Ehb i Mvh), heterodisulfur reductasa (Hdr), coenzim F_{420} [NiFe]-hidrogenasa (Frh) i la proteïna de maduració HypD segons el flux d'electrons (circuit elèctric obert o tancat). L'anàlisi de la composició de la comunitat microbiana, utilitzant com a aproximacions l'ADN i l'ADN complementari, van destacar *Methanobacterium* sp. com el principal arqueu responsable de l'electrometanogènesis. Els resultats obtinguts amb RT-PCR suggerien que els mecanismes implicats en la transferència d'electrons no es troben regulats a nivell transcripcional un cop les cèl·lules de *Methanobacterium* sp. s'exposen a períodes de circuit elèctric obert/tancat.

Tenint en compte que l' H_2 es destaca com una molècula donadora d'electrons important en el metabolisme microbià, els potencials catòdics usats pel reciclatge del CO_2 asseguren que l' H_2 no sigui un factor limitant. No obstant, alguns microorganismes poden servir com a potencials bio-productors d' H_2 en els biocàtodes. En aquest treball s'estudia la producció biològica d' H_2 en biocàtodes operats a $-1.0 \text{ V vs. Ag/AgCl}$, emprant una metodologia comparable i CO_2 com a font de carboni. Es van escollir deu soques bacterianes dels gèneres *Rhodobacter*, *Rhodospseudomonas*, *Rhodocyclus*, *Desulfovibrio* i *Sporomusa*, totes elles descrites com a candidats per a la producció d' H_2 . En totes les soques es va promoure la formació de biofilms

monoespecífics sobre la superfície dels càtodes, i es va controlar l'evolució d'H₂ constantment amb un microsensor. Vuit de les deu soques testades van mostrar electroactivitat i les taxes de producció d'H₂ van ser significativament superiors respecte a les condicions abiòtiques (de 2 a 8 vegades) en dues d'elles (*Desulfovibrio paquesii* DSM 16681 i *Desulfovibrio desulfuricans* DSM 642). *D. paquesii* va exhibir la major taxa de producció en comparació amb les condicions abiòtiques, encara que les taxes de producció específiques (per unitat de biomassa) van resultar molt similars a les d'altres soques analitzades. Els resultats van demostrar que, tot i que molts microorganismes han estat suggerits per la seva directa implicació amb la producció neta d'H₂, hi ha diferències inherents entre soques. Aquestes diferències han de ser considerades pel futur desenvolupament de biofilms estables en càtodes per a la producció eficient d'H₂ durant l'electrosíntesi microbiana.

L'aplicació de biocàtodes per a la producció sostinguda d'H₂ pot ser que no sigui prou eficient per a mantenir els requeriments que han de permetre incentivar el metabolisme d'altres soques microbianes. En conseqüència, hem aplicat tècniques d'enginyeria genètica per incrementar l'habilitat de *D. paquesii* per a la producció d'H₂. Els gens seleccionats per ser sobre-expressats van ser la [Fe]-hidrogenasa i el citocrom *c3* en dues soques, *D. vulgaris* DSM 644 i *D. paquesii* DSM 16681. Es van testar diverses condicions i protocols experimentals per la implementació dels mecanismes adients que assegurassin la sobre-expressió dels gens seleccionats, però no es van obtenir els resultats desitjats en el moment de la finalització d'aquesta Tesi Doctoral. Tanmateix, s'ha pogut dur a terme una revisió crítica i exhaustiva dels factors que cal controlar per tal de poder controlar les limitacions d'aquest procés.

Seguint una analogia arquitectònica, l'estudi de la producció d'H₂ en els sistemes bioelectroquímics és la peça clau d'aquesta Tesi, i els processos model (com la metanogènesis, la bio-producció d'H₂ i l'homoacetogènesis) les voltes de creueria necessàries per completar l'estructura desitjada. Per això, s'han emprat diferents metodologies. En el procés de finalització de la cúpula, les aproximacions presentades han contribuït a entendre millor el paper clau de l'H₂ durant l'electrosíntesi microbiana i han derivat en diverses conclusions. La primera és que expandir el coneixement sobre els mecanismes de transferència d'electrons ha de permetre un millor control dels sistemes bioelectroquímics. La segona és que el requeriment d'H₂ per poder operar de manera sostinguda els processos bioelectroquímics pot subministrar-se d'una manera eficient usant microorganismes amb la capacitat de produir H₂. I per últim, que l'aplicació de la biologia sintètica així com dels co-cultius definits han de ser considerades dues contribucions prometedores en el camp de les tecnologies bioelectroquímiques.

RESUMEN

La electrosíntesis microbiana (en inglés MES) usa la electricidad y el dióxido de carbono (CO_2) como únicas fuentes de energía y carbono durante los procesos bioelectroquímicos para la biosíntesis. Esta tecnología se desarrolla en sistemas bioelectroquímicos (en inglés BES) que sacan partido de microorganismos conocidos como electroactivos. Durante la electrosíntesis microbiana, el hidrógeno (H_2) se destaca como intermediario clave, involucrado en variedad de metabolismos microbianos durante la reducción del CO_2 . Entender mejor el papel del H_2 en la electrosíntesis microbiana (producción y disponibilidad) puede reforzar la productividad y aplicabilidad de esta tecnología.

Los procesos básicos en el MES requieren de la transformación de la electricidad (electrones) en energía química mediante el proceso llamado transferencia de electrones. El estudio de los mecanismos de transferencia de electrones (en inglés EET) en los BES puede ayudar a entender las interacciones que se dan entre los microorganismos y los electrodos, y determinar la participación de moléculas intermediarias como el H_2 , como mecanismo opuesto a la transferencia directa de electrones en la electrosíntesis. Para el estudio de los genes posiblemente implicados en los eventos de EET se usó un reactor electrometanogénico en el que se promovía la reducción del CO_2 a metano (CH_4). El objetivo fue determinar cambios a corto plazo en la expresión génica de [NiFe]-hidrogenasas (Eha, Ehb y Mvh), heterodisulfuro reductasa (Hdr), coenzima F_{420} [NiFe]-hidrogenasa (Frh) y la proteína de maduración HypD según el flujo de electrones (circuito eléctrico abierto o cerrado). En el análisis de la composición de la comunidad microbiana usando como aproximaciones el ADN y el ADN complementario se destacó *Methanobacterium* sp. como la principal arquea presente en el sistema. Los resultados obtenidos por RT-PCR sugerían que los mecanismos implicados en la transferencia de electrones no estaban regulados a nivel transcripcional, una vez las células de *Methanobacterium* sp. se exponían a periodos cortos de circuitos eléctricos abiertos/cerrados.

Teniendo en cuenta que el H_2 se destaca como una molécula dadora de electrones en el metabolismo microbiano, los potenciales catódicos usados para el reciclaje del CO_2 aseguran que el H_2 no sea un factor limitante. No obstante, algunos microorganismos pueden ser usados como potenciales bio-productores de H_2 en los biocátodos. En este trabajo se ha estudiado la producción biológica de H_2 en biocátodos operados a $-1.0 \text{ V vs. Ag/AgCl}$, usando una metodología comparable y CO_2 como fuente de carbono. Se escogieron diez cepas bacterianas de los géneros *Rhodobacter*, *Rhodospseudomonas*, *Rhodocyclus*, *Desulfovibrio* y

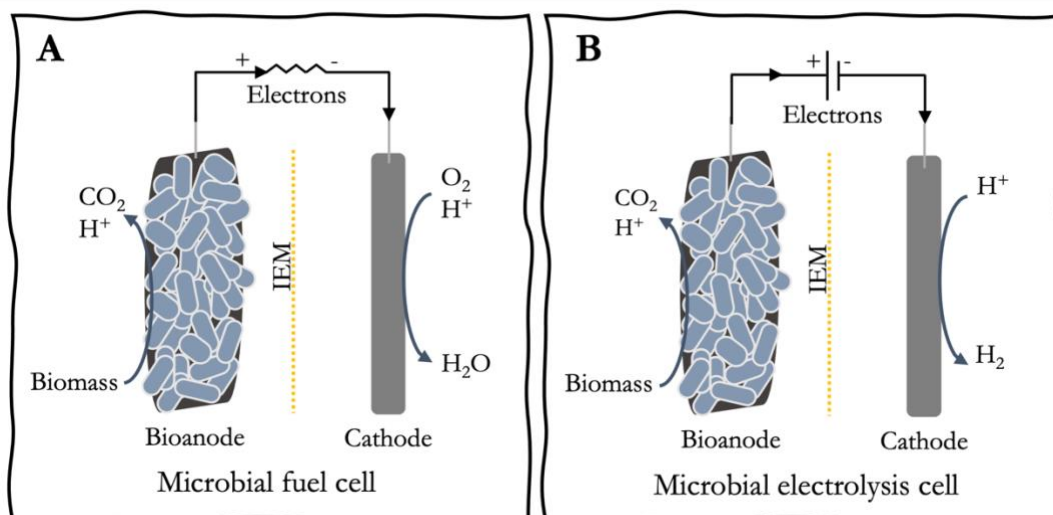
Sporomusa, todos ellos descritos como potenciales candidatos para la producción de H₂. Se generaron biofilms mono-específicos sobre la superficie de los cátodos y la evolución de H₂ se monitoreó constantemente usando un microsensar. Ocho de las diez cepas testadas mostraron electroactividad y las tasas de producción de H₂ fueron significativamente superiores respecto a las condiciones abióticas (de 2 a 8 veces) en dos de ellas (*Desulfovibrio paquesii* DSM 16681 y *Desulfovibrio desulfuricans* DSM 642). *D. paquesii* exhibió la mayor tasa de producción de H₂. No obstante, las tasas de producción específicas (por unidad de biomasa) resultaron ser muy similares entre las cepas testadas. Los resultados demostraban que, aunque muchos microorganismos han sido propuestos por su directa implicación en la producción neta de H₂, existen diferencias inherentes entre ellas. Estas, deben ser consideradas para el futuro desarrollo de biofilms estables en cátodos para la producción eficiente de H₂ durante la electrosíntesis microbiana.

La aplicación de biocátodos para la producción sostenida de H₂ puede no ser suficientemente eficiente para el mantenimiento de los requerimientos que deben permitir incentivar el metabolismo de otras cepas microbianas. Por esto, hemos aplicado métodos de ingeniería genética para incrementar la habilidad de *D. paquesii* para la producción de H₂. Los genes seleccionados para ser sobre-expresados fueron la [Fe]-hidrogenasa y el citocromo *c3* en dos cepas, *D. vulgaris* DSM 644 y *D. paquesii* DSM 16681. Se testaron varias condiciones y protocolos experimentales para la implementación de los mecanismos adecuados que asegurasen la sobreexpresión de los genes seleccionados, pero no se obtuvieron los resultados deseados. No obstante, se ha podido realizar una revisión crítica y exhaustiva de los factores que se deben controlar y las limitaciones del proceso.

Siguiendo una analogía arquitectónica, el estudio de la producción de H₂ en los BES es la piedra angular de esta Tesis, y los procesos modelo (como la metanogénesis, la bio-producción de H₂ y la homoacetogénesis) las bóvedas de crucería necesarias para completar la estructura deseada. En el proceso de finalización de la cúpula, las aproximaciones presentadas han contribuido a entender mejor el papel clave del H₂ durante la electrosíntesis microbiana y han derivado en varias conclusiones. La primera, ampliar el conocimiento sobre los mecanismos de transferencia de electrones debe permitir un mayor control de los sistemas bioelectroquímicos. La segunda, el requerimiento de H₂ que permite operar los procesos bioelectroquímicos de manera sostenida, puede suministrarse usando microorganismos con la capacidad de producir H₂. Y, por último, la aplicación de la biología sintética, así como de los co-cultivos definidos, deben ser consideradas dos contribuciones prometedoras en el campo de las tecnologías electroquímicas.

INTRODUCTION

Microbial electrochemical technologies (MET) are defined as ‘*technologies or applications that utilize the electrochemical interaction of microbes and electrodes*’ (Schröder et al., 2015). METs are conducted in bioelectrochemical systems (BES) consisting of two electrodes, a cathode, and an anode, that can be housed in two separated compartments divided by an ionic exchange membrane, or in a single compartment in which electrodes are set apart from each other. Surrounding the electrodes, there is the electrolyte (usually an aqueous solution) which provides stable conditions for the electrodes to operate and allow bacteria to grow (Rabaey & Rozendal, 2010). BES exploit the capacity of some microorganisms to transfer electrons from the cell to a solid electrode, or vice versa. These microorganisms are known as electroactive bacteria (Lovley, 2012), and have the ability to transform electrons into soluble energy-containing compounds (Logan et al., 2019). Electroactive bacteria have contributed to the development of practical applications in environmental and industrial biotechnologies (Sánchez et al., 2020). The first proposed application of BES was microbial fuel cells (MFC) where microorganisms present in the anode compartment could be exploited to produce electrical energy at expenses of waste or biodegradable organic substances (*i.e.*, industrial, domestic, or agricultural wastewater) (Logan & Rabaey, 2012; Schröder et al., 2015). In other systems, the energy provided by an MFC reaction, or externally, employing a potentiostat or power source, can be used for hydrogen (H_2) or methane (CH_4) production in microbial electrolysis cells (MEC), to remediate contaminants in microbial remediation cells (MRC), to drive desalination processes in microbial desalination cells (MDC) or to synthesize organic compounds in microbial electrosynthesis (MES) (Figure 1) (Sánchez et al., 2020; Wang & Ren, 2013).



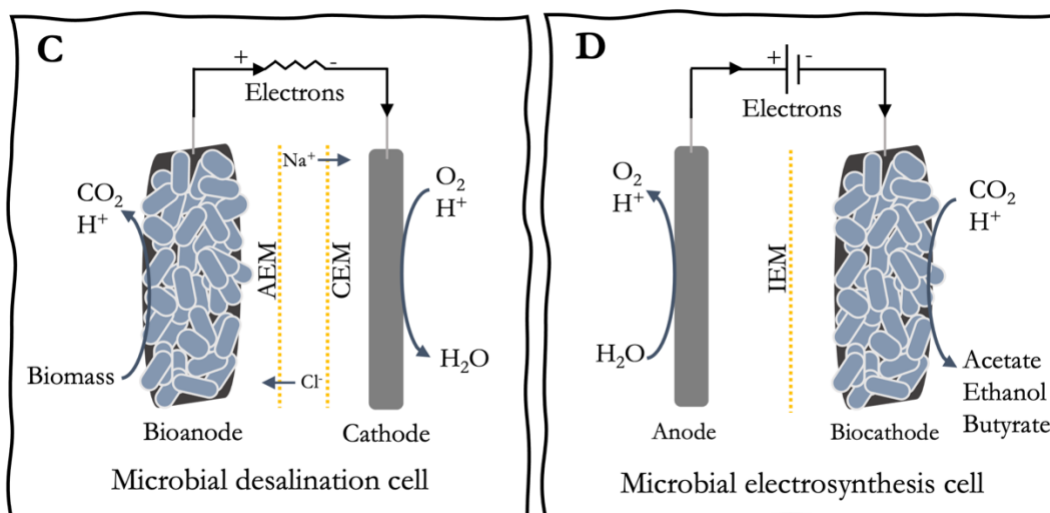


Figure 1. Basic applications of microbial electrochemical technologies. A. Electricity generation from wastes with microbial fuel cell (MFC). B. Hydrogen production in a microbial electrochemical cell (MEC). C. Middle chamber in microbial desalination cell enables migration of salts between selective membranes. D. Reduction of CO₂ into C-based molecules with microbial electrosynthesis cell. MEC and MES require external energy supply (potentiostat). IEM: Ionic exchange membrane. AEM: Anionic exchange membrane. CEM: Cationic exchange membrane. Adapted from (Wang & Ren, 2013).

MES was initially defined as *‘the microbially catalysed synthesis of chemical compounds in an electrochemical cell’* (Rabaey & Rozendal, 2010). MES is engineered to use electric power and carbon dioxide (CO₂) as the only energy and carbon sources in reductive bioelectrochemical processes for biosynthesis (Nevin et al., 2010). It enables the storage of energy (electricity) into commodity chemicals and the usage of CO₂ that is fully available in the atmosphere, oceans, and soils. Among potential uses of MES, the production of alternative fuels copes for most of the scientific attention and deserves an intense research activity (Choi & Sang, 2016; Lovley & Nevin, 2013). However, CO₂ fixation into desired organic multi carbon compounds requires a significant amount of energy (electrons) that hampers the scale-up of reactors (Tremblay & Zhang, 2015). Under laboratory conditions, CO₂ has been converted using electricity into CH₄ (Batlle-Vilanova et al., 2015; Cheng et al., 2009; Marshall et al., 2012), acetate (Nevin et al., 2011; Jourdin et al., 2015; Batlle-Vilanova et al., 2016), formate (Marshall et al., 2013; Rotaru et al., 2012; Yu et al., 2017), ethanol (Blasco-Gómez et al., 2019), butyrate, isobutanol, 3-methyl-1 butanol, and others (Batlle-Vilanova et al., 2017; Ganigué et al., 2015; H. Li et al., 2012).

The use of microorganisms in MES takes advantage of self-regeneration, flexibility in substrate usage, and adaptability to environmental conditions, mainly due to the wide diversity of enzymatic possibilities these organisms have. The limitations of BES

development are non-selective product spectrum, low production rates, and titers, high cell voltage, low energy conversion efficiency, consumption of a part of the substrate and/or energy for microbial growth and division, and not complete energy conservation (PrévotEAU et al., 2020; Rabaey & Rozendal, 2010). In addition to this constraint, BES processes are much affected by the rate at which microbial catalysts acquire electrons from a poised electrode (Kracke et al., 2015). Consequently, optimization of microbial catalysts and metabolic processes of microbe-electrode interactions are among the largest challenges to drive microbial electrochemical technologies (METs) beyond fundamental studies.

1. Complex microbial populations and pure cultures for microbial electrosynthesis

Several studies have demonstrated acetate production during MES utilizing pure cultures of *Sporomusa ovata*, *Sporomusa sphaeroides*, *Clostridium aceticum*, *Clostridium ljungdahlii*, *Moorella thermoacetica*, and *Moorella thermoautotrophica* (Bajracharya et al., 2015; Faraghiparapari & Zengler, 2017; Nevin et al., 2011, 2010) and methane with the archaeon *Methanococcus marispludis* (Lohner et al., 2014). The use of pure cultures for MES processes has the advantage to control growth and product spectrum, which is conditioned by the metabolic capacities of the used microorganism. Nevertheless, severe limitations due to correct maintenance of reactors during long runs and to prevent contaminations with unwanted microorganisms must be considered and may impact severely on large-scale MES performance. On the other hand, the utilization of undefined mixed cultures can be more easily maintained in the long-term, sterilization can be neglected, and the overall process may benefit from syntrophy (May, Evans, & Labelle, 2016). Inoculum sources of mixed cultures of unknown composition for MES are wastewater treatment sludge, anaerobic sediments and soils, or the effluent of previously operated BES reactors. Therefore, inoculums adapt to the operation conditions, and only those species able to survive are enriched and constitute a stable microbiome. However, since the composition of the microbial community is changing continuously as conditions in the reactor evolve, undesired activities may appear as the availability of carbon compounds (mainly short carbon molecules such as CH₄ and acetate) increases. For example, Batlle-Vilanova and co-workers detected higher relative abundances of *Methylocystis* sp. (20% of the total bacterial community, according to 16S rRNA gene sequence reads) when conducting electromethanogenesis. *Methylocystis* sp. have a methylotrophic metabolism favoured in highly abundant CH₄ environments and under microaerophilic conditions (Batlle-Vilanova et al., 2015). Similar results were found when

conducting long-term operation of electroacetogenic systems. Fermentative strains (*i.e.*, *Cellulomonas* and *Rhodocyclaceae*) were found at higher relative abundances in older biofilms compared with newly formed biofilms (results not published). This evolution of the microbial communities may be caused by non-controlled operation and/or poor sterility conditions during the manipulation of BES. The interaction of the different members in a microbial community may lead to positive (*i.e.*, syntrophy) or negative (*i.e.*, competition) interactions, that can be completely avoided with the use of pure cultures. Bajracharya and co-workers compared the performance of an undefined mixed culture and a pure culture (*C. ljungdahlü*) during MES indicating that production profiles were more consistent in pure culture biocathodes. Mainly acetate and methane were produced with mixed culture and only acetate was detected with the pure culture. Specifically, they observed differences in maximum production rates of acetate and current efficiencies (CE), being higher when utilizing pure cultures ($1.3 \text{ mM}\cdot\text{d}^{-1}$ - 50% CE and $2.4 \text{ mM}\cdot\text{d}^{-1}$ - 89% CE, respectively). Probably, competitive reactions were also taking place when using complex communities making the process less efficient compared to pure cultures (Bajracharya et al., 2015). Nevertheless, knowledge acquired from the use of non-defined mixed communities in METs might enable the use of pure cultures and consortia applications. For that purpose, it is essential the characterization of the active members in the community being directly involved in the processes of interest (Sun et al., 2012).

Acetogenic and methanogenic microorganisms described during MES can reduce CO_2 utilizing hydrogen (H_2) as electron donor, and produce acetate and methane, respectively. In acetogenic bacteria, CO_2 fixation proceeds via the reductive acetyl-CoA pathway, also known as the Wood-Ljungdahl pathway (WLP) (Ragsdale & Pierce, 2008) ([Figure 2A](#)). WLP is hypothesized to be the most ancient biological CO_2 fixation pathway (Martin, 2012). Acetyl-CoA is used as an intermediate to produce a variety of molecules, being acetate the most common. Acetyl-CoA can be further converted to ethanol, 2,3-butanediol, lactate, butyrate, butanol, and others, providing specific conditions are given (Lovley & Nevin, 2013). Hydrogenotrophic methanogens can reduce CO_2 through the Wolfe cycle (Thauer, 2012) ([Figure 2B](#)). Therefore, H_2 has a relevant role to exploit the potential of BES for commodity chemicals production (Blanchet et al., 2015). Remarkably, methanogens are the dominant hydrogenotrophs in many environments and, they conserve more energy by the conversion of H_2 and CO_2 into CH_4 in contrast with the conversion to acetate done by acetogens but utilizing the same amount of reducing power as H_2 (Equations 1 and 2, respectively) (Ragsdale & Pierce, 2008).

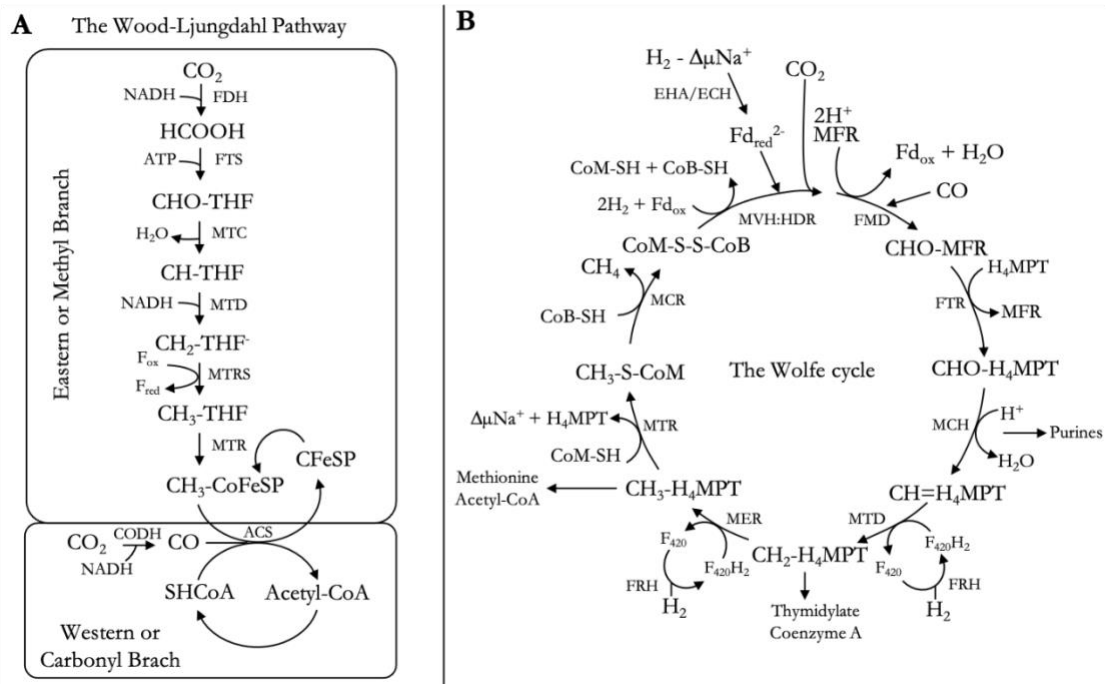
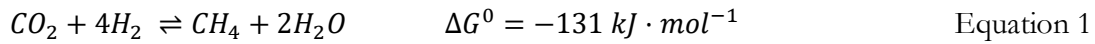


Figure 2. Wood-Ljungdahl pathway (A) and Wolfe cycle (B) for the reduction of CO_2 . Enzymes in the Wood-Ljungdahl pathway: FDH, formate dehydrogenase; FTS, formyl-THF synthase, MTC, methenyl-THF; MTD, methylene-THF; MTRs, methylene-THF reductase; MTR, methyl transferase; ACS, acetyl-CoA synthase and CODH, CO hydrogenase. Enzymes in the Wolfe cycle: FMD, formylmethanofuran dehydrogenase; FTR, formylmethanofuran/ H_4MPT formyltransferase; MCH, methenyl- H_4MPT cyclohydrolase; MTD, methylene- H_4MPT dehydrogenase; MER, methylene- H_4MPT reductase; MTR, methyl- H_4MPT /coenzyme M methyltransferase; MCR, methyl-coenzyme M reductase; MVH:HDR, electron-bifurcating hydrogenase-heterodisulfide reductase complex; FRH, F_{420} -reducing hydrogenase; and EHA/ECH, energy-converting hydrogenase catalysing a sodium motive force-driven reduction of ferredoxin with H_2 . Adapted from (Ragsdale & Pierce, 2008) and (Thauer, 2012).

2. Extracellular electron transfer mechanisms

Some microorganisms can transport electrons out of their cell walls and directly interact (electrically) with the near environment (Kracke et al., 2015; Logan et al., 2019; Rosenbaum et al., 2011). This characteristic has allowed the classification of several microorganisms (*i.e.*, *Geobacter sulfurreducens*, *Geobacter metallireducens*, *Shewanella oneidensis*, *Desulfovibrio* spp.) as electroactive bacteria (EAB) (Koch & Harnisch, 2016). Depending on their ability to transfer or uptake electrons, bacteria can be classified as electrogenic or as electrotrophic, respectively. Both are defined as being able to perform extracellular electron transfer (EET) during anaerobic respiration (Logan et al., 2019). While electrogens have been widely studied

and characterized, the pool of available electrotroths is extremely restricted, and information about their ability to use EET mechanisms scarce (Logan et al., 2019). Therefore, a better understanding of how both bacteria and archaea interact with the solid electrodes could lead to breakthroughs in the effort to optimize MES.

Extracellular electron transfer (EET) can occur after direct (dET), mediated (mET) and indirect (iET) events (Sydow et al., 2014) ([Figure 3](#)). Direct ET is considered a mechanism in which no diffusible molecule is required for the electrons to be transported (Rabaey & Rozendal, 2010). For dET a close contact between the microorganisms and the electrode surface is needed to maintain its native enzymes involved in electron transport near to the electrode surface. The mechanism is well studied for *Geobacter* and *Shewanella* (considered both as electrogens and electrotroths) where cytochrome c-type has a key role in the e-transfer (Rosenbaum et al., 2011). Also for this genera, cellular appendages known as protein nanowires (composed by multi-heme c-type cytochrome) have been described for being enabling EET, connecting microorganisms with conductive surfaces (Lovley & Holmes, 2020; Lovley & Walker, 2019; Subramanian et al., 2018). However, both direct and indirect mechanisms of EET have been suggested for acetogenic (*S. ovata*, *C. ljungdablii*, *M. thermoacetica*) and methanogenic (*M. maripaludis*) microorganisms identified as EAB in reductive BES and molecular mechanisms are poorly understood (Lohner et al., 2014; Nevin et al., 2011, 2010). The use of metatranscriptomics (methods for a deep analysis of highly expressed or repressed genes in bacteria) enables the analysis of expression patterns of genes related to EET if gene expression profiles are compared at different conditions. Molecular methods have been used for different purposes. On the one hand, Ishii and co-workers elucidated the relationship between the physiological function of specific microbes (mainly *Geobacter*) and genes in EET-active anodic microbial communities exposed to increasing and decreasing EET rates (Ishii et al., 2013; 2018; 2015). On the other hand, Marshall and colleagues suggested that soluble hydrogenases, ferredoxins, formate dehydrogenase, and cytochromes actively participated in the initial steps of MES in an enriched biofilm containing mainly *Acetobacterium* sp. and *Desulfovibrio* sp. (Marshall et al., 2017). Moreover, in both approaches, metabolic interactions between microbes could be established.

Mediated ET requires the production or presence of shuttle molecules (natural or artificial molecules). Some of the well-described natural shuttles are flavins produced by *Shewanella oneidensis* and phenazines by *Pseudomonas aeruginosa* being important vehicles for electron transfer mainly between bacteria and from bacteria to anodes (Light et al., 2018; Pham et al., 2008). In addition to those naturally produced electron shuttles, other compounds can be

added to the culture to promote electron transfer. One such compound that has been used thoroughly is methyl viologen, which in combination with *Desulfovibrio vulgaris* (strain Hildenborough) significantly increased the catalysis of H_2 at a low redox potential using a graphite electrode as electron donor (Lojou et al., 2002).

Indirect ET consists of the production of H_2 and formate that can be utilized by microorganisms. The majority of acetogens, methanogens as well as, sulphate-reducing bacteria are described as hydrogenotrophic bacteria (can use H_2 as electron donor) (Gupta et al., 2020). Although METs take advantage of that unique feature (EET) of some microorganisms, it is still not clear if coexistence of dET and iET or prevalence of iET (mainly H_2 -mediated) mechanisms has been occurring in the developed approaches until now. Especially this seems a possibility when using mixed cultures or H_2 -evolving cathode potentials, knowing that H_2 gas is electrochemically produced at a theoretical potential more negative than $-0.61\text{ V vs. Ag/AgCl}$ under standard conditions and neutral pH (Logan et al., 2008). Additionally, it has been described that when conducting reductive BES with some microorganisms adhered to cathodes (*i.e.*, *Sporomusa sphaeroides*, *Sporomusa ovata*, and *Methanococcus maripaludis*), electrode surface modifications via metal deposition (nickel and cobalt) and/or free extracellular enzymes (hydrogenases and formate dehydrogenases) led to an increased H_2 production only when cells in suspension were removed and the cell-free exhausted medium was used, indicating that cathode modifications via enzyme and/or metals had a direct effect on H_2 evolution only in absence of active microorganisms (Deutzmann et al., 2015; Lienemann et al., 2018; Tremblay et al., 2019).

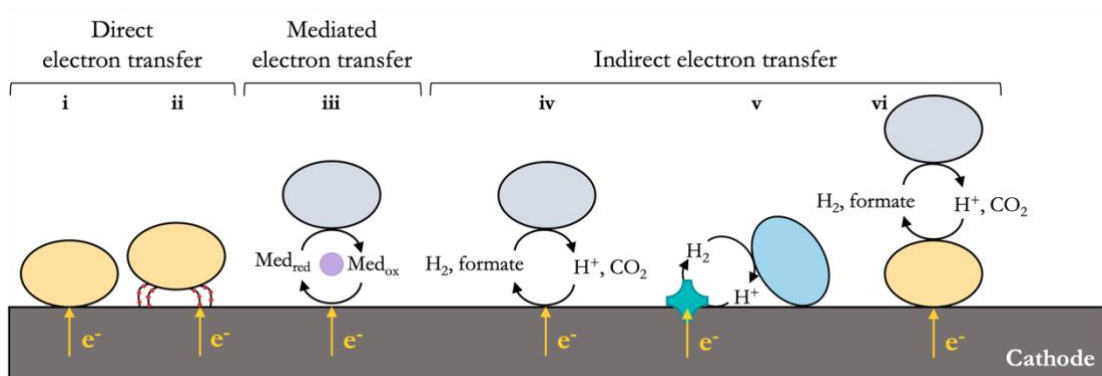


Figure 3. Extracellular electron transfer mechanisms in biocathodes: (i) direct electron transfer via direct contact between microorganisms and the cathode, (ii) direct electron transfer via conductive pili or nanowires, (iii) mediated electron transfer via endogenous and exogenous electron shuttles, (iv) indirect electron transfer via hydrogen or formate electrochemically produced, (v) indirect electron transfer via H_2 enzymatically produced by extracellular hydrogenases and (vi) indirect electron transfer via H_2 or formate produced by a syntrophic

interaction with a microorganism able to direct uptake electrons. Adapted from (Philips, 2020).

3. Better together: synergistic consortia

In both natural or synthetic environments, microbes interact between them, and these interactions led to different consequences for microbial fitness, population dynamics, and functional capacities within a microbiome. Interactions are not restricted to the same species since could occur at any taxonomic level. In general, interactions can be positive (mutualism, synergism, or commensalism), negative (predation, parasitism, antagonism, or competition), or neutral that do not have any effect on the interacting microbes (Berg et al., 2020). Syntrophy is defined as the relationship between two (or more) organisms in which one member of the consortium utilizes molecules produced by a second member. Therefore, syntrophy is considered a beneficial relationship between microorganisms but can be also described as a tight dependence between species being unable to survive as separate populations (Morris et al., 2013). This positive interaction is present in METs (Dolfing, 2014) demonstrating that, although a lower number of species can be selected as active electrode-cell energy converters, they can feed a plethora of additional bacteria by producing intermediate compounds that can be used as substrates for electrosynthesis (Escapa et al., 2016; Moscoviz et al., 2016; Tremblay & Zhang, 2015).

The development of synergistic consortia (via co-cultures or defined mixed cultures) enabling an improved performance is now under intensive development in METs. The use of defined cultures (synthetic consortia) could be an intermediate strategy between pure and non-defined mixed cultures to ensure proper target products (possibly, more complex ones) and better performance (production rates and product selectivity) during MES. However, advancement with this strategy is both time and resources demanding to understand in detail genetic characteristics and metabolic processes of the consortium members to boost biotechnological applications beyond the use of pure cultures. Co-cultures potentially present a whole range of desirable characteristics over pure cultures such as modularity, robustness, predictability, scalability, and stability, and at the same time, these are the main challenges to be solved (Goers et al., 2014). Controlled environments are required with both pure and defined co-cultures. Strict control to prevent contamination is essential mainly with pure cultures but consortia seem to be more stable against contaminations, reducing the need for extreme sterile conditions (Schievano et al., 2016). Interactions between population members are not always predictable or stable and might change the system's performance over time with either pure or co-cultures (Goers et al., 2014). However, the occurring

interactions especially between consortium members may be limited and might need to be adjusted using additional methods, such as synthetic biology directed to genetic engineering of biocatalysts to promote dependency of consortium members, new approaches or product spectrum (more specific and/or complex target products) in METs (Song et al., 2014). However, it is needed to understand how functions can be partitioned across a microbial population in productive compartments to achieve a desirable population behaviour (Johns et al., 2016).

As an example, the co-cultivation of ethanol-oxidizing *Geobacter metallireducens* with fumarate-reducing *Geobacter sulfurreducens* enabled the discovery of direct interspecies electron transfer (DIET) (Summers et al., 2010). DIET is defined as ‘a syntrophic metabolism in which free electron flow from one cell to another without being shuttled by reduced molecules such as H₂ or formate’ (Dubé & Guiot, 2015). The artificial consortium was metabolically dependent since none of the bacterial strains could use ethanol or fumarate as energy sources alone (Summers et al., 2010). The participation of H₂ or formate as interspecies exchange molecules was discarded using co-cultures with mutant strains of *G. sulfurreducens* unable to metabolize H₂ or formate. Instead, extracellular electron exchange was taking place through electrically conductive pili (e-pili) in *G. metallireducens* (electron release) and outer-membrane c-type cytochromes in *G. sulfurreducens* (electron uptake) (Rotaru et al., 2012; Shrestha et al., 2013; Summers et al., 2010). Interspecies electron communication studies beyond typical electroactive species, demonstrated the applicability of co-cultures to enhance methane production, reducing start-up times, and promoting stability in anaerobic digestion systems (Lovley, 2011, 2017). DIET together with conductive particles such as iron-oxide minerals (magnetite) or carbon-based materials can be suitable applications to facilitate MES. For instance, during methanogenesis, the addition of granular activated carbon or magnetite increased the methane accumulation and reduced the start-up time (Kato et al., 2012; LaBarge et al., 2017; Vu et al., 2020).

Setting a synergic consortium in MES requires an electron uptake step (cells forming the biofilm) separated from biosynthesis (planktonic cells), defining a compartmentalized system with unique roles for each strain involved in the process. Therefore, one of the aspects conditioning the strategy is the selection of the appropriate bacterial strains. For instance, co-cultivation of strain IS4 (*Desulfopila corrodens* DSM 15630) together with the methanogen *Methanococcus maripaludis* or with the acetogen *Acetobacterium woodii* increased overall production rates of methane and acetate, respectively. Furthermore, the ability of strain IS4 to directly uptake electrons from the poised cathode and to produce H₂ bioelectrochemically, was determined. The co-culture allowed to use less negative cathode potentials (-0.6 and -0.5

INTRODUCTION

V *vs.* Ag/AgCl) in comparison with the usually used for H₂ evolution (-0.8 to -1 V *vs.* Ag/AgCl) getting an energetic benefit (Deutzmann & Spormann, 2017).

OBJECTIVES

The aim of this Ph.D. Thesis was twofold. First, to improve the knowledge on microbial electrosynthesis focusing especially in direct and H₂-mediated electron transfer mechanisms by elucidating which enzymes can directly uptake electrons from a poised electrode. Second, to develop a resilient platform to produce H₂ electrochemically as a first step to establish defined co-cultures for MES improvement and move towards scaling up the technology.

Specific objectives were:

1. To identify archaeal and bacterial enzymes potentially involved in direct electron transfer in enriched biocathodes.
2. To analyse the electrochemical behaviour of several model bacterial strains (*Rhodobacter* sp., *Rhodospseudomonas* sp., *Rhodocyclus*, *Sporomusa*, and *Desulfovibrio*) and their ability to improve H₂ evolution into biocathodes.
3. To define a strategy towards genetically modify *Desulfovibrio* sp. to achieve higher H₂ titers in BES.

MATERIALS AND METHODS

1. Bacterial strains and maintenance conditions

Bacterial strains were obtained from Leibniz Institute DSMZ – German Collection of Microorganisms and Cell Cultures, except for isolates C2T108.3 and C1S119.2 obtained from a denitrifying biocathode and tentatively identified as *Rhodopseudomonas* sp. (Vilar-Sanz et al., 2018). *Rhodobacter* sp. DSM 5864, *Rhodobacter capsulatus* DSM 152, *Rhodopseudomonas pseudopalustris* DSM 123, *Rhodocyclus tenuis* DSM 112 and isolates C2T108.3 and C1S119.2 were cultured using DSM 27 medium ([Table 1](#)). *Sporomusa ovata* DSM 2662 was routinely cultured on DSM 311 ([Table 2](#)) medium and *Desulfovibrio paquesii* DSM 16681, *Desulfovibrio vulgaris* DSM 644, *Desulfovibrio desulfuricans* DSM 642 using DSM 63 medium ([Table 3](#)). All cultures were grown at recommended culturing conditions following the instructions provided by the DSMZ. Incubations were done with constant light and at 25 °C in an incubator (Sanyo, MIR-253) for *Rhodobacter*, *Rhodopseudomonas*, and *Rhodocyclus* strains. The other strains were incubated at 30 or 37 °C as recommended.

[Table 1](#). Medium DSM 27 was used for *Rhodobacter* sp., *Rhodopseudomonas* sp., and *Rhodocyclus* sp. cultivation.

Component	Amount
Yeast extract	0.30 g
Na ₂ -succinate	1.00 g
(NH ₄)-acetate	0.50 g
Fe (III) citrate solution (0.1% in H ₂ O)	5.00 mL
KH ₂ PO ₄	0.50 g
MgSO ₄ ·7H ₂ O	0.40 g
NaCl	0.40 g
NH ₄ Cl	0.40 g
CaCl ₂ ·2H ₂ O	0.05 g
Vitamin B ₁₂ solution	0.40 mL
*Trace element solution SL-6	1.00 mL
L-Cysteine-HCl·H ₂ O	0.30 g
Na-resazurin solution (0.1% w/v)	0.50 mL
Distilled water	1,000 mL

*Trace element solution composition is detailed in [Table 5](#)

Table 2. Medium DSM 311 used for *Sporomusa ovata* cultivation.

Component	Amount
NH ₄ Cl	0.50 g
MgSO ₄ ·7H ₂ O	0.50 g
CaCl ₂ ·7H ₂ O	0.25 g
NaCl	2.25 g
FeSO ₄ ·7H ₂ O solution	2.00 mL
*Trace element solution SL-10	1.00 mL
Selenite-tungstate solution	1.00 mL
Yeast extract	2.00 g
Casitone	2.00 g
Betaine·H ₂ O	6.70 g
Na-resazurin solution (0.1% w/v)	0.50 mL
K ₂ HPO ₄	0.35 g
KH ₂ PO ₄	0.23 g
Na ₂ CO ₃	1.00 g
*Vitamin solution	10.00 mL
L-Cysteine-HCl·H ₂ O	0.30 g
Na ₂ S·9H ₂ O	0.30 g
Distilled water	1,000 mL

*Trace element solution and vitamin solution compositions are detailed in [Table 4](#) and [Table 5](#), respectively.

Table 3. Medium DSM 63 used for *Desulfovibrio* sp. cultivation.

Component	Amount
K ₂ HPO ₄	0.50 g
NH ₄ Cl	1.00 g
Na ₂ SO ₄	1.00 g
CaCl ₂ ·H ₂ O	0.10 g
MgSO ₄ ·7H ₂ O	2.00 g
Na-D-Lactate	2.00 g
Yeast extract	1.00 g
Na-resazurin solution (0.1% w/v)	0.50 mL
FeSO ₄ ·7H ₂ O	0.50 g
Na-thioglycolate	0.10 g
Ascorbic acid	0.10 g
Distilled water	1,000 mL

Table 4. Composition of trace element solutions.

Trace element solution SL-6		Trace element solution SL-10	
ZnSO ₄ ·7H ₂ O	0.10	HCl (25%; 7.7M)	10.00 mL
MnCl ₂ ·4H ₂ O	0.03	FeCl ₂ ·4H ₂ O	1.50 g
H ₃ BO ₃	0.30	ZnCl ₂	0.07 g
CoCl ₂ ·6H ₂ O	0.20	MnCl ₂ ·4H ₂ O	0.10 g
CuCl ₂ ·2H ₂ O	0.01	H ₃ BO ₃	0.006 g
NiCl ₂ ·6H ₂ O	0.02	CoCl ₂ ·6H ₂ O	0.19 g
Na ₂ MoO ₄ ·2H ₂ O	0.03	CuCl ₂ ·2 H ₂ O	0.002 g
Distilled water	1,000 mL	NiCl ₂ ·6H ₂ O	0.24 g
		Na ₂ MoO ₄ ·2H ₂ O	0.36 g
		Distilled water	990 mL

Table 5. Composition of vitamins solution.

Component	Amount
Biotin	2.00 mg
Folic acid	2.00 mg
Pyridoxine hydrochloride	10.00 mg
Thiamine-HCl	5.00 mg
Riboflavin	5.00 mg
Nicotinic acid	5.00 mg
Calcium D-(+)-pantothenate	5.00 mg
Vitamin B12	0.10 mg
p-Aminobenzoic acid	5.00 mg
Thioctic acid	5.00 mg
Distilled water	1,000 mL

All bacteria were inoculated and maintained in serum bottles with butyl rubber septa under anaerobic conditions. All manipulations were carried out in an anaerobic chamber (gas mixture N₂:H₂:CO₂ [90:5:5], COY Laboratory Products, INC, USA).

Bacterial strains used in each Chapter of this Ph.D. Thesis:

- Chapter 2. *Rhodobacter* spp., *Rhodopseudomonas* spp., *Rhodocyclus tenuis*, *Sporomusa ovata*, and *Desulfovibrio* spp.
- Chapter 3. *Desulfovibrio* spp.

2. Configuration of bioelectrochemical systems

For this Ph.D. Thesis, two different configurations were used to conduct BES experiments: (i) three-neck flask and (ii) H-type reactors.

2.1. Three-neck flask BES

Three-neck round bottom flask (Duran-Group, Germany) had a nominal capacity of 1 L. Anodic and cathodic chambers were set at working volumes of 15 and 940 mL, respectively. Anodic and cathodic chambers were separated by a cationic exchange membrane (CMI-7000, Membranes International Inc, USA). The BES contained four cathodes made of carbon cloth (NuVant's ELAT LT2400W, FuelCellsEtc, USA) each one with a 42 cm² surface area. Cathodes were independently connected to a potentiostat through a stainless-steel wire (Figure 4). Biocathodes were used as working electrodes operated chronoamperometrically at -1.0 V *vs.* Ag/AgCl to guarantee hydrogen production (Batlle-Vilanova et al., 2015). A carbon rod (5x250 mm, MERSEN IBERICA, Spain) was used as a sacrificial anode. An Ag/AgCl reference electrode (+197 mV *vs.* SHE, sat KCl, SE11 Sentechniek Meinsberg, Germany) was placed in the cathode chamber. Precision rubber septa tightly closed the

reactor compartments. Before usage, carbon cloth pieces meant to be used as electrodes were cleaned with 0.5 M HCl, 0.5 M NaOH, and Mili-Q water for 12 hours each solution to remove impurities.

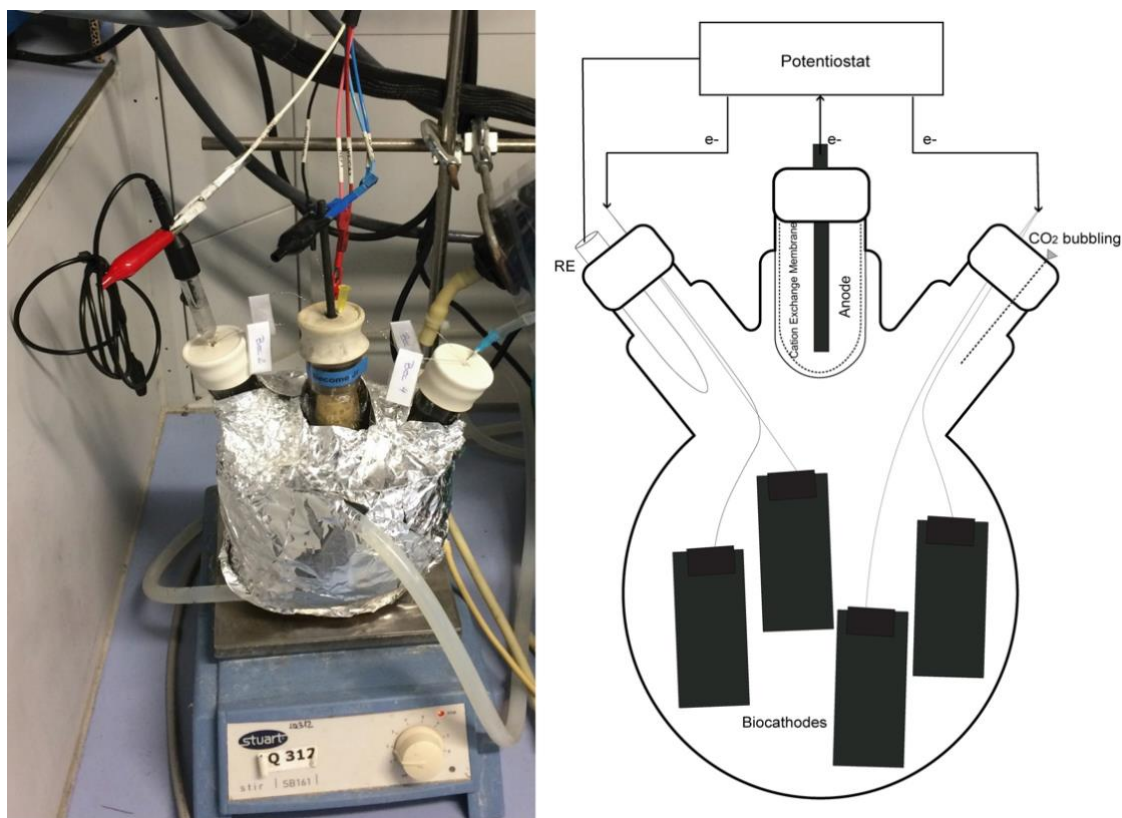


Figure 4. Three-neck round flask BES configuration. RE: reference electrode.

2.2. H-type reactors

H-type bioelectrochemical systems (BES) reactors with a nominal capacity of 150 mL (Adams & Chittenden Scientific Glass, Berkeley CA – USA) were used. Each one consisted of two chambers, anodic and cathodic, separated by a cation exchange membrane (21.2 cm² surface area; CMI-7000, Membranes International Inc, USA). Carbon cloth (NuVant's ELAT® LT2400W, FuelCellsEtc USA) with 24 cm² surface area connected directly to a stainless-steel wire (AISI 304 Grade, 20 cm length and 1 mm thickness) was used as cathode electrode (working electrode). An Ag/AgCl reference electrode (+197 mV *vs.* SHE, sat KCl, SE11 Sensortechnik Meinsberg, Germany) was placed into the cathodic chamber. A graphite rod (5x250 mm, MERSEN IBERICA, Spain) was used as anode (counter electrode) ([Figure 5](#)). Before usage, carbon cloth pieces were conditioned (see [section 2.1](#) for details).

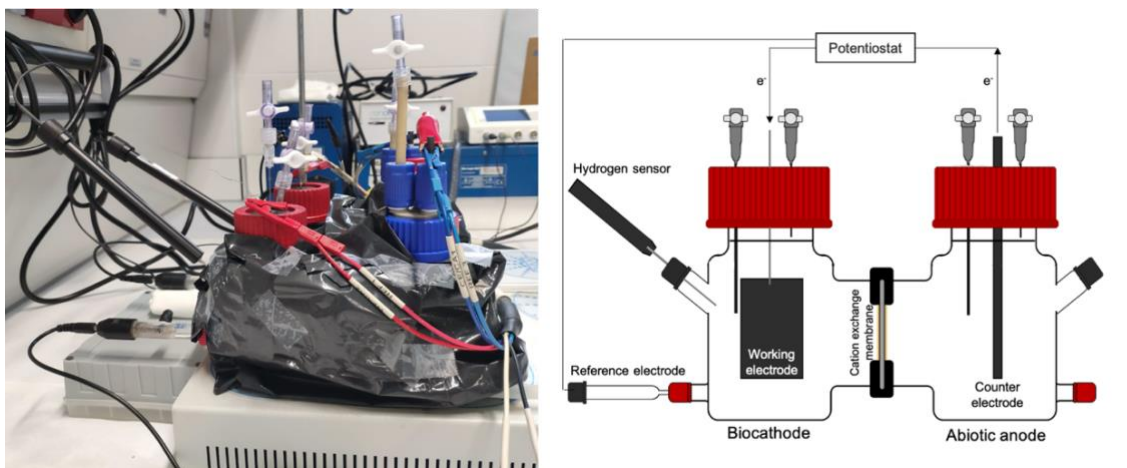


Figure 5. H-type BES configuration. A simplified scheme of the experimental setup is shown (right).

The three-neck flask was used to conduct the experiments in *Chapter 1* while, H-type reactors were used in *Chapter 2*.

3. Operation of bioelectrochemical systems

3.1. Electromethanogenesis

A three-neck round bottom flask was inoculated with the effluent of a parent electromethanogenic reactor operated according to Battle-Vilanova et al. (Battle-Vilanova et al., 2015). The parent reactor exhibited a constant methane production at the time of effluent sample collection. Two samples were collected at different positions in the reactor and mixed at equal volumes to inoculate the BES used here. Inoculation was done at a 1:10 volume ratio. Cathode and anode chambers were filled with mineral medium ([Table 6 and 7](#)). Before the inoculation of the system, cathodic and anodic chambers were bubbled with pure CO₂ (<99.95%, Praxair, Spain) for at least 10 minutes. The BES was kept at constant stirring, temperature 37±1 °C, atmospheric pressure, and was wrapped in aluminium foil to restrict phototrophic activity. The BES was operated chronoamperometrically (closed electric circuit) for 53 days until methane production rates and current demand were maintained constant for at least one week. Once these conditions were achieved, two of the electrodes were disconnected (open electric circuit; named as Cat1 and Cat2) and maintained for up to six hours to test for changes in gene expression. The other two electrodes remained connected to the electric circuit (closed electric circuit). Six hours incubation was chosen to detect sudden changes in gene expression levels in the event of a restriction on the electron availability and to minimize potential side effects due to H₂ production (biotically or

abiotically) in the biofilm. After this period the four electrodes were removed, biofilm and bulk samples were collected for molecular analyses. Unfortunately, experiments could not be repeated for longer incubation times due to the sacrificial sampling strategy of the cathode.

Table 6. Modified ATCC 1754 PETC medium used in BES.

Component	Amount
KH ₂ PO ₄	0.1 g
NaCl	0.8 g
NH ₄ Cl	1.0 g
MgCl ₂ ·6H ₂ O	0.2 g
KCl	0.1 g
CaCl ₂ ·2H ₂ O	0.02 g
MES	1.95 g
Cysteine HCl	0.4 g
Distilled water	1,000 mL

Table 7. Modified trace element solution and vitamin solution based on ATCC 1754 PETC medium.

Trace metal solution		Vitamin solution	
Nitrilotriacetic acid	2.0 g	Biotin	20.0 mg
MnSO ₄ ·H ₂ O	1.0 g	Folic acid	20.0 mg
Fe(SO ₄) ₂ (NH ₄) ₂ ·6H ₂ O	0.8 g	Pyridoxine hydrochloride	100.0 mg
CoCl ₂ ·6H ₂ O	0.2 g	Thiamine hydrochloride	50.0 mg
ZnSO ₄ ·7H ₂ O	0.0002 g	Riboflavin	50.0 mg
CuCl ₂ ·2H ₂ O	0.02 g	Nicotinic acid	50.0 mg
NiCl ₂ ·2H ₂ O	0.02 g	DL- calcium pantothenate	50.0 mg
Na ₂ MoO ₄ ·2H ₂ O	0.02 g	Vitamin B12	1.0 mg
Distilled water	1,000 mL	Distilled water	1,000 mL

Trace metal and vitamin solution were added at a concentration of 1 mL·L⁻¹.

3.2. Electromicrobiology towards hydrogen evolution

Slight modifications of culture conditions were applied to stimulate the formation of monospecific biofilms on carbon cloth (Tables 8-10). The addition of a sole source of organic matter was done as a step adaptation for fully autotrophic conditions that were used during BES operation. Modifications of DSM 27 included: substitution of NH₄-acetate for Na-acetate (0.53 g·L⁻¹) and exclusion of yeast extract, Na-succinate, Na-resazurin solution, and NH₄Cl. pH was set to 6.8, and the medium was degasified with helium (He) to reduce the presence of N₂ in the medium. All modifications were carried out to avoid product inhibition of the nitrogenase activity, and force bacteria to get rid of the excess energy and reducing power through H₂ production. Modifications of DSM 311 medium included:

exclusion of casitone, betaine, L-cysteine-HCl, Na₂S, and Na-resazurin, the solution was set at pH 7 and degasified with nitrogen (N₂). Modified medium specially designed was used for *Desulfovibrio* species (Aulenta et al., 2012). For all strains and isolates, brand-new treated carbon cloth electrodes were immersed in freshly prepared media modified to enhance bacterial growth and biofilm formation. Incubations were performed in 100 mL serum bottles. *Rhodobacter*, *Rhodospseudomonas* (including isolates C2T108.3 and C1S119.2), and *Rhodocyclus* species were incubated under constant light at 25 °C, while *Sporomusa ovata* and *Desulfovibrio* sp. were maintained in the dark and 30 °C. As for bacterial strains maintenance, all manipulations were carried out under anaerobic conditions. Biofilms were allowed to grow on the surface of electrodes for a minimum of 10 days.

Table 8. Modifications of basal medium DSM 27 composition (Table 1) applied during biofilm formation and BES operation.

	Biofilm formation	BES operation
(Na)-acetate	0.53 g	----
KH ₂ PO ₄	0.50 g	0.50 g
MgSO ₄ ·7H ₂ O	0.40 g	0.40 g
NaCl	0.40 g	0.40 g
CaCl ₂ ·2H ₂ O	0.05 g	0.05 g
Vitamin B ₁₂ solution	0.40 mL	0.40 mL
Trace element solution SL-6	1.00 mL	1.00 mL
L-Cysteine-HCl·H ₂ O	0.30 g	0.30 g
Distilled water	1,000 mL	1,000 mL

Table 9. Modifications of basal medium DSM 311 composition (Table 2) applied during biofilm formation and BES operation.

	Biofilm formation	BES operation
Yeast extract	2.00 g	----
NH ₄ Cl	0.50 g	0.50 g
MgSO ₄ ·7H ₂ O	0.50 g	0.50 g
CaCl ₂ ·7H ₂ O	0.25 g	0.25 g
NaCl	2.25 g	2.25 g
FeSO ₄ ·7H ₂ O solution	2.00 mL	2.00 mL
Trace element solution SL-10	1.00 mL	1.00 mL
Selenite-tungstate solution	1.00 mL	1.00 mL
K ₂ HPO ₄	0.35 g	0.35 g
KH ₂ PO ₄	0.23 g	0.23 g
NaHCO ₃	4.00 g	4.00 g
Vitamin solution	10.00 mL	10.00 mL
Distilled water	1,000 mL	1,000 mL

Table 10. Medium based on Aulenta *et al.*, 2012 and modifications during biofilm formation and BES operation (Aulenta *et al.*, 2012).

	Biofilm formation	BES operation
Na-D-Lactate	1.12 g	----
K ₂ HPO ₄	0.40 g	0.40 g
NH ₄ Cl	0.50 g	0.50 g
CaCl ₂ ·H ₂ O	0.05 g	0.05 g
MgCl ₂ ·6H ₂ O	0.10 g	0.10 g
NaHCO ₃	1.50 g	1.50 g
FeSO ₄ ·7H ₂ O	1.39 g	----
Trace element solution	1 mL	1 mL
Vitamin solution	1 mL	1 mL
Distilled water	1,000 mL	1,000 mL

Chronoamperometric experiments were performed in abiotic and biotic conditions at -1.0, -0.8 and -0.6 V *vs.* Ag/AgCl using a potentiostat (BioLogic, Model VSP, France). H-type cells were maintained at 30 ± 2 °C, with constant stirring utilizing a magnetic bar at 200 rpm (MultiMix D9 P V1, OVAN, Spain) and in the dark. Anodic and cathodic chambers were filled with the corresponding modified inorganic media (Tables 8-10). Abiotic (cell-free) cathodes poised at -1.0 V *vs.* Ag/AgCl were used to test the BES set-up. After five-six hours of operation, H₂ saturation was reached (~800 μM, given the media composition and reactor temperature). Slight increases from saturation value were recorded over time if overpressure was allowed to the system. The presence of leaks in the reactor were tested after disconnecting the potentiostat and recording the H₂ concentration decrease. Measured leaks did not exceed 3.5 μM·h⁻¹.

After abiotic tests were performed, the same electrode was incubated in the presence of bacteria in an independent culture bottle until a biofilm was formed and was visible at naked eye. Carbon cloth electrodes with a monospecific biofilm formed on its surface were placed directly into the cathodic chamber. Remaining cells into the supernatants (90 mL) were harvested in the late exponential phase at an optical density (OD₆₀₀) of 0.3-0.4, pelleted by centrifugation (4,400 rpm, 15 min, 4 °C), resuspended into 1 mL of inorganic modified medium and added into the cathodic chamber. Headspace was saturated with filter-sterilized pure CO₂ at the beginning of the operation. Biotic experiments lasted 5 days. Once set-up was completed, H₂ production rates were evaluated and compared to abiotic tests using the same operational conditions (cathodic voltage -1.0 V *vs.* Ag/AgCl) and maintained for 3 days. After this, reactor headspace was flushed with a filter-sterilized pure CO₂ stream, and

production was re-evaluated for two additional days (second CO₂ feeding). Flushing was repeated on day 5 to ensure inorganic carbon source availability before cyclic voltammetries were done.

On-line hydrogen concentration measurements were performed using an H₂ NP-500 microsensor (Unisense, Denmark) directly placed in the liquid compartment close to the cathode surface. Microsensors were regularly calibrated using a saturated water solution using a CO₂:H₂ gas mixture (80:20 % v/v) following the specifications of the manufacturer. H₂ production rates in all conditions and strains were calculated as a linear response covering the first 25 minutes of operation according to Tremblay and co-workers (Tremblay et al., 2019). Linear regressions were calculated for this time-period using SigmaPlot 11.0 (Systat Software Inc., USA) and H₂ production rates were obtained from the slope. Unpaired t-tests were used to evaluate statistical significance between biotic and abiotic H₂ production rates, current demand, or energy consumption.

4. Chemical analyses

Gas and liquid samples were taken periodically (on average, twice per week) from the cathode compartment to monitor pH and gas- and liquid-phase composition. Pressure in the headspace of the reactors was measured using a digital pressure sensor (differential pressure gauge, Testo 512, Spain) and gas samples were analysed by gas chromatography. A 490 Micro GC system (Agilent Technologies, USA) was used to analyse other gases. The gas chromatograph was equipped with two columns: a CP-molesive 5A for methane (CH₄), carbon monoxide (CO), H₂, oxygen (O₂), and nitrogen (N₂) analysis, and a CP-Poraplot U for CO₂ analysis. Both columns were connected to a thermal conductivity detector (TCD). Isobutene was analysed using a gas chromatograph Agilent 7890A (Agilent Technologies, USA) equipped with a GS-alumina column and flame ionization detector (FID). Liquid-phase samples containing volatile fatty acids (*i.e.*, acetate) and alcohols (*i.e.*, ethanol) were analysed using a gas chromatograph Agilent 7890A (Agilent Technologies, US) equipped with a DB-FFAP column and a FID. pH was measured with a pH meter (pH meter Basic 20, Crison Instruments, Spain). After each liquid sample extraction, withdrawn volumes were replaced with freshly prepared medium and CO₂ was bubbled for over ten minutes to ensure substrate availability.

5. Calculations

During chronoamperometrical operation, power (P , Equation 1) and energy requirements (E , Equation 2) were calculated as shown in Equations 1 and 2,

$$P = I \cdot V \quad \text{Equation 1}$$

$$E = P \cdot t \quad \text{Equation 2}$$

being I intensity, and V voltage.

Coulombic efficiency (CE) was calculated according to Patil *et al.* (Patil et al., 2015) (Equation 3). C_i is the compound i concentration in the liquid phase (mol C_i L⁻¹), n_i is the molar conversion factor (2 and 8 eq. mol⁻¹ for H₂ and acetate, respectively), F is Faraday's constant (96485 C mol e⁻¹), V (L) is the net liquid volume of the cathode compartment, and I is the intensity demand of the system (A).

$$\text{CE}(\%) = \frac{C_i \cdot \sum_i n_i \cdot F \cdot V}{\int_0^t I \cdot dt} \times 100 \quad \text{Equation 3}$$

6. Electrochemical characterization

Cyclic voltammetries (CV) were performed to confirm electrochemical activity. The technique allowed the characterization of electroactive biofilms analysing changes in the slope of current *vs.* cathode potential curves, and estimate cathode potentials at which redox reactions are taking place (Harnisch & Freguía, 2012). CVs were performed using EC-Lab v10.37 software (Bio-Logic Science Instruments, France). Four cycles were done within a range of 0.2 V to -1.0 V and at a scan rate of 1.0 mV·s⁻¹. The obtained CV signals in biotic conditions were compared to abiotic ones. Raw CV data were used for oxidative-reductive peak detection by calculating the first derivative. Analyses were performed using the free-software QSoas (Fourmond, 2016). The mid-point potential (E_f) of redox couples was calculated as the mean value of the oxidative and reductive potential.

7. Nucleic acids (DNA and RNA) extractions

Nucleic acids were extracted using different methodologies.

7.1. Electromethanogenesis

Electrodes were cut into small pieces using RNase free forceps and scissors. Samples for RNA extraction (approximately, 30 cm²) were immediately frozen in liquid nitrogen. Samples for DNA extraction (approximately, 8 cm²) were maintained at -20 °C. The rest of the

cathode material was preserved to analyse the biofilm structure by scanning electron microscopy.

DNA was extracted from bulk liquid and biofilm samples. For the bulk liquid samples, cells were pelleted by centrifugation before DNA extraction, whereas carbon cloth samples were used directly for biofilm DNA extraction. DNA was extracted using the FastDNA SPIN kit for Soils (MP Biomedicals, USA) following the manufacturer's instructions. The extracts were distributed in aliquots and stored at -20 °C. DNA concentration was measured using a Nanodrop 1,000 spectrophotometer (Thermo Fisher Scientific, USA). RNA was extracted from biocathodes using TRIzol Max Bacterial RNA Isolation Kit (Ambion, USA). Lysis of cells was performed in a bead-beater. Carbon cloth samples were placed in bead tubes (0.3 g zirconia beads, 0.1 mm diameter) followed by the addition of 200 µL of MAX Bacterial Enhancer (Ambion, USA). Tubes were incubated at 95 °C for 4 minutes. After this incubation Trizol (1 mL) was added and samples were incubated for 5 minutes at room temperature, before being shaken at maximum speed using a Mo-Bio Vortex-Genie 2 (Mo-Bio Laboratories, Inc., USA) for 15 minutes. RNA extracts were quantified using the Agilent 2100 Bioanalyzer (Agilent Technologies, USA). Co-extracted DNA was cleaned up from RNA extracts by using the DNase digestion and RNA Clean-up protocols of RNeasy Mini Kit (QIAGEN, Germany). cDNA was synthesized with the High Capacity cDNA Reverse Transcription kit (Applied Biosystems, USA) according to the manufacturer's instructions. 10 µL of digested RNA extracts at a minimum concentration of 5 ng/µL were used in all cases. Quality of DNA and cDNA extracts for downstream molecular applications were checked after PCR detection of 16S rRNA using universal bacterial primers 357F and 907R.

7.2. Electromicrobiology towards hydrogen evolution

Samples from both biofilm and bulk liquid were collected under anaerobic conditions during the growth of bacteria and under BES operation. For biofilm measurements, pieces of carbon cloth electrode (1.5 cm² each) were taken directly using sterile forceps and scissors. For bulk measurements, 10 mL samples were centrifuged (4,400 rpm, 15 min, 4 °C) and supernatants were discarded. Both electrode and pelleted cells were stored at -20 °C until DNA extraction was performed. DNA was extracted using a cetyltrimethylammonium bromide (cTAB) based protocol (Llirós, Casamayor, & Borrego, 2008). DNA concentrations were measured using Qubit 2.0 Fluorometer (Thermo Fisher Scientific, USA).

8. Microbial community structure determination

The hypervariable V4 region of the 16S rRNA gene for both DNA and cDNA samples was amplified using the primers 515F - 806R and method described by Kozich and Schloss adapted to produce a dual-indexed Illumina compatible libraries in a single PCR step (Kozich et al., 2013). Primary PCR was performed using fusion primers with target-specific portions (Stoeck et al., 2010), and Fluidigm CS oligos at their 5' ends. Secondary, PCR targeting the CS oligos was used to add sequences necessary for Illumina sequencing and unique indexes. PCR products were normalized using Invitrogen SequelPrep DNA normalization plates. The pooled samples were sequenced using an Illumina MiSeq flow cell (v2) using a 500-cycle reagent kit (2x250bp paired-end reads). Sequencing was done at the RTSF Core facilities at the Michigan State University USA (<https://rtsf.natsci.msu.edu/>).

Paired-end sequences were merged, quality filtered, and clustered into OTUs (Operational Taxonomic Units) using USEARCH v9.1.13 (Edgar & Flyvbjerg, 2015). Sequences were filtered for minimum length (>250 nt) and maximum expected errors (<0.25). OTUs were clustered at the 97% identity using UCLUST (Edgar, 2010), and checked for the presence of chimeras. OTUs containing only one sequence (singletons) were removed. The subsequent analyses were performed with QIIME v1.9.1 (Caporaso et al., 2010). Representative OTUs sequences were aligned using PyNAST with default parameters against Silva 128 release (February 2017). The same reference database was used to taxonomically classify the representative sequences using UCLUST. Direct BLASTn searches at the NCBI of selected sequences were used when poor identifications with the Silva database were obtained.

Richness indicators (*i.e.*, the number of different species in the sample) were calculated as the observed (Sobs) and maximum estimates thus showing the number of species at 100% coverage (Chao1). Diversity indicators (*i.e.*, a measure of the relative abundance and composition of microbial species in the sample) were calculated as Shannon and Phylo-diversity indices. These indicators were calculated only for DNA samples using randomly collected subsets of 61,000 sequences per sample. Ten iterations were performed, and mean values were calculated. Beta diversity was only calculated for biofilm samples (DNA and cDNA-based analyses) using randomly collected subsets of 21,000 sequences. Unweighted and weighted UniFrac distances were calculated to compare the microbial community structure between samples (Lozupone & Knight, 2005). Weighted UniFrac distances were used for the jack-knife-resampling analysis. Differences in the community structure were visualized either as a dendrogram or a Principal Coordinates plot. Dendrogram of sample

distributions generated in QIIME was visualized in the Interactive Tree of Life software (Letunic & Bork, 2016). Groups of samples were statistically compared using ANOSIM.

Significant differences in OTU abundance between groups (DNA *vs.* cDNA-based communities or open *vs.* closed electric circuits) were analysed using non-parametric t-tests with QIIME and based on rarefied OTU tables for each sample. The sequences presented in this study have been submitted to the GenBank database within the SRA accession number SRP153784 (BioProject ID PRJNA481232).

9. qPCR analyses

Quantitative PCR (qPCR) assays targeting the 16S rRNA gene were used as a proxy for cell abundance in the biofilm and bulk liquid of reactors. Before qPCR amplification, samples with 10 ng· μL^{-1} or higher were diluted to avoid inhibition due to excess DNA. qPCR was used to quantify DNA gene copies targeting 16S rRNA in each sample using 341F and 534R primer pair following the conditions described by López-Gutiérrez and co-workers (López-Gutiérrez et al., 2004). The reaction was performed using the LightCycler® 480 SYBR Green I Master Mix (Roche Life Science, Switzerland) and a Lightcycler 96 Real-Time PCR instrument. In all cases, 2 μL in a 20 μL total volume were used. A 10-fold dilutions series (10^2 - 10^8 copies/mL) of a linearized plasmid containing a 16S rRNA gene sequence was used as a standard curve. qPCR efficiency was above 90%.

qPCR targeting 16S rRNA gene was used in *Chapter 2*.

10. Gene selection, primer design, and RT-PCR analyses

Sequences of the genes of interests (GOIs) coding for subunits of hydrogenase complexes or maturation proteins (*ebaB*, *ebbL*, *mvhA*, *bdrA*, *frhA*, and *hypD*), formyl-methanofuran dehydrogenase (*fydD*), formate dehydrogenase (*fdhB*) and, housekeeping genes (HKG) cell division protein FtsZ (*ftsZ*) and 16S rRNA of members of the genus *Methanobacterium*, were retrieved from the NCBI database. Representative sequences for each gene were aligned using Bioedit (Biological sequence alignment editor v7.2.6), and conserved regions were primarily searched for suitable specific degenerated PCR primers. Primers were designed using the Primer-BLAST design tool (Ye et al., 2012). The following parameters were used: amplicon size was limited to 300 bp and predicted melting temperatures were set between 57 °C and 65 °C. *In silico* predictions of primer specificity were performed against the nr database of the NCBI, and the organism of choice was restricted to *Methanobacterium*

(taxid:2160). Primers with the least self-complementarity value and minimum difference between melting temperatures were selected ([Table 10](#)). Primer specificity towards *Methanobacterium* was checked using DNA extracts of other microorganisms, *Archaeoglobus fulgidus* DSM 4304, *Halobacterium salinarum* DSM 3754, *Thermoplasma acidophilum* DSM 1728, *Methanobacterium alcaliphilum* DSM 3387, *Sulfolobus solfataricus* DSM 1616, *Methylobacterium extorquens* DSM 1337, and *Methylomonas methanica* NCIMB 1130. Changes in annealing temperature and MgCl₂ concentrations were applied, when necessary, for PCR optimization. No product specificity towards *fwdD* and *fdhB* resulted with the designed primers for *Methanobacterium* sp. PCR reactions were run at GeneAmp PCR System 2,700 (Applied Biosystems, USA) with Ampli Taq 360 (Applied Biosystems, USA). Optimized reaction conditions were used for semi-quantitative RT-PCR using the LightCycler 480 SYBR Green I Master (Roche Life Science, Switzerland). RT-PCR reactions were run in a Lightcycler 96 Real-Time PCR system. Two sample volumes, 1 and 2 µL in a 20 µL total volume were used to ensure no inhibition occurred. In all cases, conventional and quantitative RT-PCR, amplicons were visualized in agarose (2%) gel. Additionally, melting curves were also recorded for quantitative RT-PCR amplification.

Standard curves for each set of primers were calculated using sequential dilutions from a DNA sample (1:10 to 1:50000). Quantitative efficiencies were slightly high, specifically at the low concentration range ([Table 11](#)). The number of copies per gene was estimated from calibration curves. To facilitate comparison between open and closed conditions, relative gene concentrations were calculated (copies of gene/copies of 16S rRNA). Changes in the relative concentration of each hydrogenase gene were tested for statistical significance using a non-parametric (U Mann-Whitney test).

Table 11. Designed primers for *Methanobacterium* sp. Target gene, primer name, sequence, and annealing temperature are shown. Underlined degenerated positions. (ND. Not determined).

Gene	Primer	Sequence (5'-3')	Annealing temperature (°C)	Expected amplicon size (bp)	Primer efficiencies (%)	Reference
Heterodisulfide reductase associated [NiFe]-hydrogenase subunit A <i>mvhA</i>	mvhA-F	AGGAAA <u>Y</u> GT <u>Y</u> SAGGACACCAA	57	263	204.09	This study
	mvhA-R	AGTAGAAGT <u>G</u> V <u>A</u> G <u>W</u> GCGTGG				
Heterodisulfide reductase subunit A <i>hdrA</i>	hdrA-F	CATCCCAT <u>T</u> CCCAC <u>A</u> R <u>G</u> CA	57	183	164.73	This study
	hdrA-R	GTTGGG <u>T</u> YGTATGGG <u>T</u> CGT				
Coenzyme F ₄₂₀ -reducing [NiFe]-hydrogenase subunit A <i>frhA</i>	frhA-F	TAGTATH <u>A</u> GT <u>C</u> CTGTTAGAGGTT	57	204	189.83	This study
	frhA-R	ATGG <u>T</u> R <u>T</u> GGGCAGCAAGAGT				
Energy-converting hydrogenase A subunit B <i>ehaB</i>	ehaB-F	CTTTGGTAA <u>Y</u> MGGCTGTGCG	60	151	167.12	This study
	ehaB-R	GCCCTGGATGGTAAGGATGG				
Energy-converting hydrogenase B subunit L <i>ehbL</i>	ehbL-F	ATTGGCTGCGG <u>R</u> GG <u>W</u> TGCAG	62	200	125.90	This study
	ehbL-R	GGGTGTATGGTT <u>C</u> CTGCCTG				
Hydrogenase expression-formation protein HypD	hypD-F	GTCTGCGGAT <u>C</u> M <u>C</u> ATGAACA	60	109	147.26	This study
	hypD-R	CGGGTACACAGC <u>A</u> B <u>A</u> CH <u>G</u> GGA				
Formyl-methanofuran dehydrogenase subunit D <i>fwdD</i>	fwdD-F	AAAGGT <u>A</u> K <u>G</u> TGGAGTTGCTT	ND	207	ND	This study
	fwdD-R	CAGCAGCAGTAGGTT <u>T</u> CGTG				
Formate dehydrogenase subunit B <i>fdhB</i>	fdhB-F	C <u>T</u> Y <u>G</u> TCTTCCCAAT <u>C</u> K <u>T</u> TACCTT	ND	160	ND	This study
	fdhB-R	TGTTCC <u>C</u> CTAAAGGT <u>G</u> Y <u>T</u> GAA				
rRNA subunit 16S	Arc915f	AGGAATGGCGGGGGAGCAC	63	283	156.30	(Raskin et al., 1994)
	MB1174	TACCGTCGTCCACTCCTTCCTC				(Cheng et al., 2009)
Cell division protein FtsZ	ftsZ-F	CTGGGAAGGGC <u>W</u> GT <u>D</u> AAGGG	60	122	172	This study
	ftsZ-R	TCACCAT <u>T</u> CC <u>K</u> ATCAT <u>K</u> GC				

11. Scanning electron microscopy (SEM)

Samples were immersed in a 0.1 M cacodylate buffer solution at pH 7.4 with 2.5% (w/v) glutaraldehyde for 4 hours. After immersion, they were washed twice with cacodylate buffer and water, and dehydrated in an ethanol series. Dehydration with graded ethanol followed temperature steps of 50, 75, 80, 90, 95, and 3 times of 100 °C in periods of 20 min. The fixed samples were dried with a critical point dryer (model K-850 CPD, Emitech, Germany) and sputtered-coated with a 40 nm gold layer. The coated samples were examined with SEM (model DSM-960; Zeiss, Germany) at 20 kV. Images were captured digitally by ESPRIT 1.9 BRUKER software (AXS Micro-analysis GmbH, Germany). All analyses were performed in the Serveis Tècnics de Recerca (STR) at the University of Girona (www.udg.edu/str).

This technique was only used in *Chapter 1*.

12. Plasmid construction for *Desulfovibrio* strains

Four available plasmids for *Desulfovibrio* strains (pSC27, pMO719, pMO746, and pMO9075) (Keller et al., 2009; Parks et al., 2013) were obtained from Addgene (#117478, #117479, #117480 and #117481, respectively). Upon reception of *Escherichia coli* DH5 α transformants, the four plasmids were propagated using conventional methods. Plasmid purification was performed using Monarch Plasmid MiniPrep kit (New England BioLabs, USA) from 2 mL of liquid culture, and DNA concentrations were measured using NanoDrop™ One/One^C (ThermoScientific™, USA). Plasmids were checked by single and double digestion using restriction enzymes EcoRI and ApaI (FastDigest, ThermoScientific™, USA). pMO9075 plasmid was selected to be used for new vector construction since it was described as the most stable in different sulphate-reducing bacteria and contains the suitable expression promoter (Keller et al., 2009).

Sequences for the genes of interest (GOIs) were retrieved from both *D. vulgaris* DSM 644 and *D. paquesii* DSM 16681 according to the information available in the whole genome sequences (NCBI NC_002937 and JGI-IMG ID 2571042346, respectively). Primers ([Table 12](#)) for the selected genes (Fe-only hydrogenase and cytochrome *c3*) were designed using the first 50 nucleotides (nt) in both 5' and 3' ends. With NEB Tm Calculator (<https://tcalculator.neb.com/#!/main>) primers were adjusted to a suitable size (18 to 22 nt) ensuring that the last nucleotide was a G or C alone. Maximum and minimum annealing temperatures were set at 70 and 40 °C, respectively, and maximum temperature difference was restricted at 5 °C. Restriction sites sequences (EcoRI and ApaI) were added in forward

and reverse primers, respectively. Besides the restriction sites, 6 extra Cs were added to ensure restriction enzymes could bind in their targeted sequences. NEBuilder tool (<https://nebuilder.neb.com/>) was used to design the primers needed for overlap extension PCR. As recommended by Keller et al. to ensure proper translation of the gene, a 21-bp ribosomal-binding site sequence was added into the reverse primer (Keller et al., 2011).

Genomic DNA extraction from *Desulfovibrio* spp. was performed using NucleoSpin® Microbial DNA (Macherey-Nagel, Germany) with 2 mL of initial culture volume for both strains. Centrifugations were performed at 10,000 rcf for 1 minute and cell disruption was performed using a bead-beater (MP instruments) at 4 M/s for 2 minutes. Conventional PCR was used to amplify the GOIs using Phusion™ High-Fidelity DNA polymerase (ThermoScientific™, USA). PCR products were visualized using a 1% agarose electrophoresis gel and properly sized bands were cut and purified using MonarchDNA Gel Extraction kit (New England BioLabs, USA). Purified fragments of big and small subunits of Fe-only hydrogenase for both strains were joined using overlap extension PCR. For that, equivalent molar ratio of the fragments was calculated using NEBioCalculator (<https://nebiocalculator.neb.com/#!/ligation>). Digestion of both plasmid and GOIs obtained from purified PCR products was done using EcoRI and ApaI restriction enzymes (FastDigest, ThermoScientific™, USA). Extended digestion time was used (20 minutes) to ensure proper results. To avoid plasmid re-ligation, 1 µL of Thermosensitive Alkaline Phosphatase (FastAP, ThermoScientific™, USA) was added after 10 minutes of reaction. Desired fragments were purified from an agarose gel using MonarchDNA Gel Extraction kit (New England BioLabs, USA). Ligation was performed using Thermo Scientific T4 DNA Ligase (ThermoScientific™, USA) maintaining a molar ratio insert:vector of 3:1. NEBioCalculator was used to calculate the required volumes of both insert and vector in each reaction. Right after ligation was completed, 5 µL of the reaction was added to a tube containing 50 µL of chemically competent *E. coli* DH5α cells, and transformation was performed by heat shock. Clone screening was performed by selecting and transferring 16 isolated colonies to LB medium containing the required antibiotic (50 µg/mL spectinomycin) and incubating them overnight at 37 °C. Plasmid purification for each of the selected clones was performed from 2 mL of liquid culture using Monarch Plasmid MiniPrep kit (New England BioLabs, USA) and plasmid size was checked by single digestion using EcoRI. Vectors were checked by sequencing using the common sequencing primer M13 reverse-29 (5'-CAGGAAACAGCTATGAC-3').

MATERIAL AND METHODS

Table 12. Primer design for *Desulfovibrio* spp. vectors construction. Blue-coloured nucleotides indicate the overlapping sequence, underlined nucleotides are the restriction sites and **BOLD** upper-case nucleotides are the ribosomal-binding site sequence.

Strain	Gene	Primer	Sequence (5'-3')	Expected amplicon size (bp)	Annealing temperature (°C)
<i>Desulfovibrio vulgaris</i>	Fe-only hydrogenase big subunit (DVU1769)	fw-Febig-vulgaris-gDNA	ctacgaatag ATGAGCCGTACCGTCATG	1276	64
		rev-Febig-vulgaris-gDNA	CTATGCCITTGTGGCGCTC		
	Fe-only hydrogenase small subunit (DVU 1770)	fw-Fesmall-vulgaris-gDNA	ATGCAGATAGCCAGCATC	382	59
		rev-Fesmall-vulgaris-gDNA	tacggctcat CTATTCGTAGGGGTACGG		
	Fe-only hydrogenase	fw-Fe-vulgaris-plasmid	ccccccgggccc CTATGCCITTGTGGCGCTC	1276	63
		rev-Fe-vulgaris-plasmid	ccccccgaattc TGCAGTCCCAGGAGGTACCAT ATGCAGATAGCCAGCATCAC		
Tetraheme cytochrome <i>c3</i> (DVU3171)	fw-cytc3-vulgaris-gDNA	ccccccgggccc CTATTCGTGGCACTTGGAC	424	57	
	rev-cytc3-vulgaris-gDNA	ccccccgaattc TGCAGTCCCAGGAGGTACCAT ATGAGGAAA CTGTTTTTCTG			
<i>Desulfovibrio paquesii</i>	Fe-only hydrogenase big subunit	fw-Febig-paquesii-gDNA	tggtgtcat ATGAAAAAGCAGATCGAGATGGAAG	828	64
		rev-Febig-paquesii-gDNA	TCAGATCAATGCCGGCCTG		
	Fe-only hydrogenase small subunit	fw-Fesmall-paquesii-gDNA	ATGAACACCATCGCGTATG	378	57
		rev-Fesmall-paquesii-gDNA	attgatctga CTATTCGTACGGATAGGTG		
	Fe-only hydrogenase	fw-Fe-paquesii-plasmid	ccccccgggccc TCAGATCAATGCCGGCC	1240	61
		rev-Fe-paquesii-plasmid	ccccccgaattc TGCAGTCCCAGGAGGTACCAT ATGAACAC CATCGCGTATG		
Tetraheme cytochrome <i>c3</i>	fw-cytc3-paquesii-gDNA	ccccccgaattc TGCAGTCCCAGGAGGTACCAT ATGAAACG TACTGTCTGGCCAC	448	68	
	rev-cytc3-paquesii-gDNA	ccccccgggccc CTAGCTGTGGCAGGCGGAG			

13. Transformation of *Desulfovibrio* strains

Previously described protocols were followed to transform *Desulfovibrio* strains (Keller et al., 2011; Keller et al., 2009). Briefly, *Desulfovibrio* cells were grown until an OD₆₀₀ of 0.4-0.6 AU was achieved using DSM 63 medium (Table 3) and incubating the cells at 37 °C. Cells were harvested by centrifugation at 14,000 rcf for 12 minutes at 4 °C and, pellets were washed with ice-cold 30 mM Tris-HCl buffer (pH 7.2, anaerobic). Subsequently, washed cells were resuspended in 50 µL ice-cold Tris-HCl buffer, 1 µg of plasmid DNA was added, and the mixture was directly transferred into a precooled electroporation cuvette with a gap-size of 0.1 cm. Electroporation was performed at the following conditions: 1,75 kV, 250 Ω and 25 µF. Directly after electroporation, the cells were transferred into 1 mL of DSM 63 medium and incubated for 24 h at 37 °C. After this non-selective outgrowth step, 50 µL, 250 µL, and 700 µL of culture were plated using the pour-plating method. The plates were incubated at 37 °C until colonies were obtained (4 to 7 days). All the procedure was performed in an anaerobic glove box (Coylab, USA) under a gas atmosphere of about 5% H₂, 20% CO₂ and 75% N₂. Also, other transformation protocols described for other strains such as *Geobacter sulfurreducens* and *Clostridium ljungdablii* were adapted and tried with *Desulfovibrio* spp. (Coppi et al., 2001; Molitor et al., 2016). Colony PCR was used to check the presence of the plasmid. Each isolated colony was resuspended in 50 µL of sterile Mili-Q water and 0.2 µL was used as the template. PCR was performed using primers L4440 (5'-AGCGAGTCAGTGAGCGAG-3') and M13-rev29 (5'-CAGGAAACAGCTATGAC-3') with an expected amplicon size of ~3,000 bp and DreamTaq DNA Polymerase (ThermoScientific™, USA). Plasmid extraction from *Desulfovibrio* spp. was performed using Monarch Plasmid MiniPrep kit (New England BioLabs, USA) and extracts were transformed back to *E. coli* DH5α (section 12) to determine if plasmids were present in *Desulfovibrio* cells.

CHAPTER 1

[NiFe]-hydrogenases are constitutively expressed in an enriched *Methanobacterium* sp. population during electromethanogenesis

Published as: **Perona-Vico, E.**, Blasco-Gómez, R., Colprim, J., Puig S., Bañeras, L. (2019) [NiFe]-hydrogenases are constitutively expressed in an enriched *Methanobacterium* sp. population during electromethanogenesis. PLoS One 14(4): e0215029. Public Library of Science. ISSN 1932-6203 <https://doi.org/10.1371/journal.pone.0215029>

1. Background

The term electromethanogenesis was first coined by Cheng and co-workers to indicate the reduction of CO₂ to CH₄ mediated by *Methanobacterium palustre* using an electrode as electron donor (Cheng et al., 2009). Indeed, it was suggested that methane was directly produced from the electrical current as the sole source of energy and reducing equivalents. However, this may not be the general rule for electromethanogenesis since hydrogen-mediated CO₂ reduction has also been observed in bioelectrochemical systems (BES), suggesting that the two processes may coexist (Batlle-Vilanova et al., 2015; Van Eerten-Jansen et al., 2013).

Recently, researchers have focused on the detection of proteins likely involved in electron transfer mechanisms to elucidate biological mechanisms for the electrode-to-cell or cell-to-cell electron flow (Deutzmann et al., 2015; Rowe et al., 2018). The participation in electron uptake of the heterodisulfide reductase supercomplex (Hdr-SC) and, also, formate dehydrogenase (Fdh) has been confirmed in the methanogenic archaeon *Methanococcus maripaludis*. Although the two enzymes are initially located in the cytoplasm, they can be exported to the outside of the cell coming in close contact with the electrode in which electron harvesting would occur (Deutzmann et al., 2015; Lienemann et al., 2018).

Soluble hydrogenases, ferredoxins, formate dehydrogenase, and cytochromes have been suggested to actively participate in the initial steps of microbial electrosynthesis in BES containing biofilms enriched with *Acetobacterium* sp. and *Desulfovibrio* sp. (Marshall et al., 2017). Hydrogenases catalyse the reversible reduction of ferredoxin with hydrogen (H₂) driven by a proton or sodium ion motive force ($\text{Fd}_{\text{ox}} + \text{H}_2 + \Delta\mu\text{H}^+/\text{Na}^+ \Leftrightarrow \text{Fd}_{\text{red}}^{2-} + 2\text{H}^+$) and are ubiquitously distributed among methanogenic archaea (Thauer et al., 2010). Hydrogen is used by hydrogenotrophic methanogens as the primary energy source for catabolism (Thauer et al., 2010), but also fuels CO₂ fixation during anabolism (Major et al., 2010), and different anaplerotic functions (Lie et al., 2012), being the major energy source.

Different [NiFe]-hydrogenase subtypes are found in methanogens (Thauer et al., 2010), and are likely to participate in energy conversion. Specifically, *Methanobacterium* sp. contains [NiFe] group 3, subgroups 3a (F₄₂₀-coupled) and 3c (heterodisulfide reductase-linked) and 4, subgroups 4h (Eha) and 4i (Ehb) (Søndergaard et al., 2016). Eha and Ehb are the only enzyme complexes of the methanogenic electron transport chain to have membrane integral subunits (Tersteegen & Hedderich, 1999). Operons (ehaA-T and ehbA-Q) encode for several integral membrane proteins, hydrophilic subunits, two polyferredoxin subunits, and [NiFe] small and large subunits (Tersteegen & Hedderich, 1999). Ehb is specifically linked to CO₂

fixation providing anabolic electrons for carbon assimilation (Major et al., 2010) and, it is highly expressed in comparison to Eha (directly involved in the methanogenic pathway), at least in *M. thermoautotrophicus* (Tersteegen & Hedderich, 1999).

Heterodisulfide reductase complex (Hdr) involves the participation of the mentioned cytoplasmic [NiFe]-hydrogenases and two dehydrogenases, formyl-methanofuran dehydrogenase (FwdABD) and formate dehydrogenase (FdhAB). The complex is involved in the methanogenic pathway from CO₂ where H₂ or formate donates electrons to it via Hdr-associated hydrogenase (Mvh) or formate dehydrogenase (Fdh). Also, coenzyme F₄₂₀ (Frh) participates in the pathway as an electron donor (Costa et al., 2013; Thauer et al., 2010). In addition, a series of cytoplasmic proteins (known as expression formation proteins HypA-F) participate in the maturation of hydrogenases (Thauer et al., 2010). One of these proteins, HypD, is highly conserved and essential for the maturation of hydrogenases. HypD contributes to the insertion of the Fe(CN)₂(CO) moiety in the correct oxidation state into the active site of different [NiFe]-hydrogenases (Beimgraben et al., 2014). Due to this tight relationship, HypD is a good candidate to measure the expression of different soluble [NiFe]-hydrogenases.

Increasing the current knowledge on the mechanisms involved in electrode-to-cell electron transfer at the molecular level is crucial for stepping forward in electromethanogenesis through genetic engineering of methanogenic archaea (Blasco-Gómez et al., 2017). In the present section, we aimed at studying changes in the expression of genes coding for selected subunits of membrane-bound Eha and Ehb hydrogenases, cytoplasmic Hdr complex, and hydrogenase maturation protein HypD, in naturally enriched cultures of methanogenic archaea. Experiments were conducted in electromethanogenic reactors built *ad hoc* for the present experiments. *Methanobacterium* sp. was the main responsible archaeon for electromethanogenesis in our system. Changes from closed and open electric circuits were used to analyse the relative expression of the selected genes.

EXPERIMENTAL DESIGN IN BRIEF

Three-neck flasks with four carbon cloth cathodes were used during this experiment (Figure 4). Biocathodes used as working electrodes were operated at -1.0 V vs. Ag/AgCl. Once stable methane production was achieved, two electrodes were disconnected (named as open electric circuit) from the current and the other two remained connected (named as closed electric circuit) for six hours. After that, the operation was stopped to collect biofilm and bulk samples for downstream DNA and RNA extraction. Microbial community structures for DNA and cDNA were analysed and expression of the selected

genes of interest (*ehaB*, *ehbL*, *mvhA*, *hdrA*, *frhA*, and *hypD*, *fwdD*, and *fdhB*) was done by RT-PCR.

2. Results and Discussion

2.1. Bioelectrochemical performance and methane production

The electromethanogenic system was operated for 53 days feeding CO₂ as the sole carbon source. Hydrogen was only recorded at the beginning of the experiment, 1.78 mmol (73.5% v/v in the headspace) and 1.33 mmol (54.8% v/v) at days 3 and 5, respectively, and remained below detection limits (< 2% v/v) for most of the time ([Figure 6](#)). Low hydrogen concentration indicated a high consumption rate for methanogenesis. The volumetric concentration of methane remained from 70 to 90% (v/v), reaching its maximum at day 17 where the concentration was 2.77 mmol (98.8% v/v in the headspace). Invariably, at the time gas samples were collected CO₂ was detected at a 10 to 30% (v/v) in the headspace, indicating that CO₂ was not limiting for methanogenesis in the used conditions. Oxygen was detected occasionally (<5%) in the cathode and was most likely due to diffusion from the anode compartment. To avoid this accumulation, extended CO₂ bubbling times were used. As previously shown, oxygen is an effective methanogenesis inhibitor at rather low concentrations (Botheju, 2011). Acetate presence was minimal (maximum concentration of 1.0 mM on day 10).

Cyclic voltammeteries (CV) were performed before inoculation of the system and on day 34 for the four biocathodes independently ([Figure 7](#)). A redox pair was clearly identified at -0.7 ± 0.25 V *vs.* Ag/AgCl at 37°C, which is within the range of redox potential values generally assigned to the activity of hydrogenases (Guiral-Brugna et al., 2001). This redox pair was also observed in H₂-producing biocathodes, in which an active biofilm was suspected to catalyse biotic hydrogen evolution, decreasing the important energy losses associated with catalytic hydrogen production (Batlle-Vilanova et al., 2015; Puig et al., 2017). This decrease in the redox pair implies that reduction is kinetically favoured and accordingly, hydrogen could be produced more energy efficiently. In other studies, is shown that microorganisms can act as catalysts producing hydrogen but consuming almost half of the energy when compared with an abiotic cathode (Batlle-Vilanova et al., 2015)

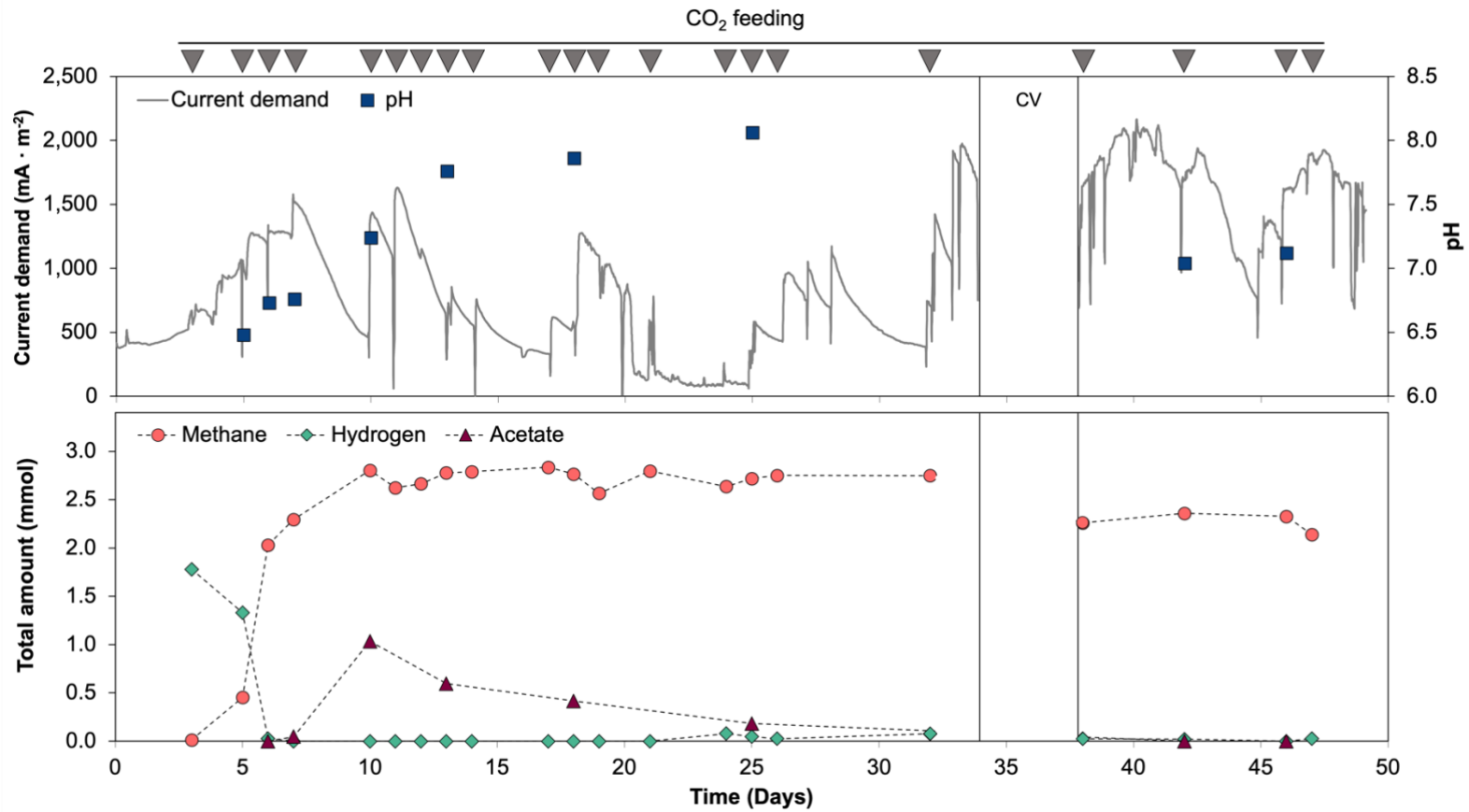


Figure 6. Time course of state variables during the operation time of the BES reactor (53 days). Upper plot – Current density and pH variation. Lower plot – Methane, hydrogen, and acetate amounts (mmol). Methane and hydrogen were calculated as added amounts considering the liquid and gas phases. CO₂ flushes are indicated with grey triangles on top of the graph.

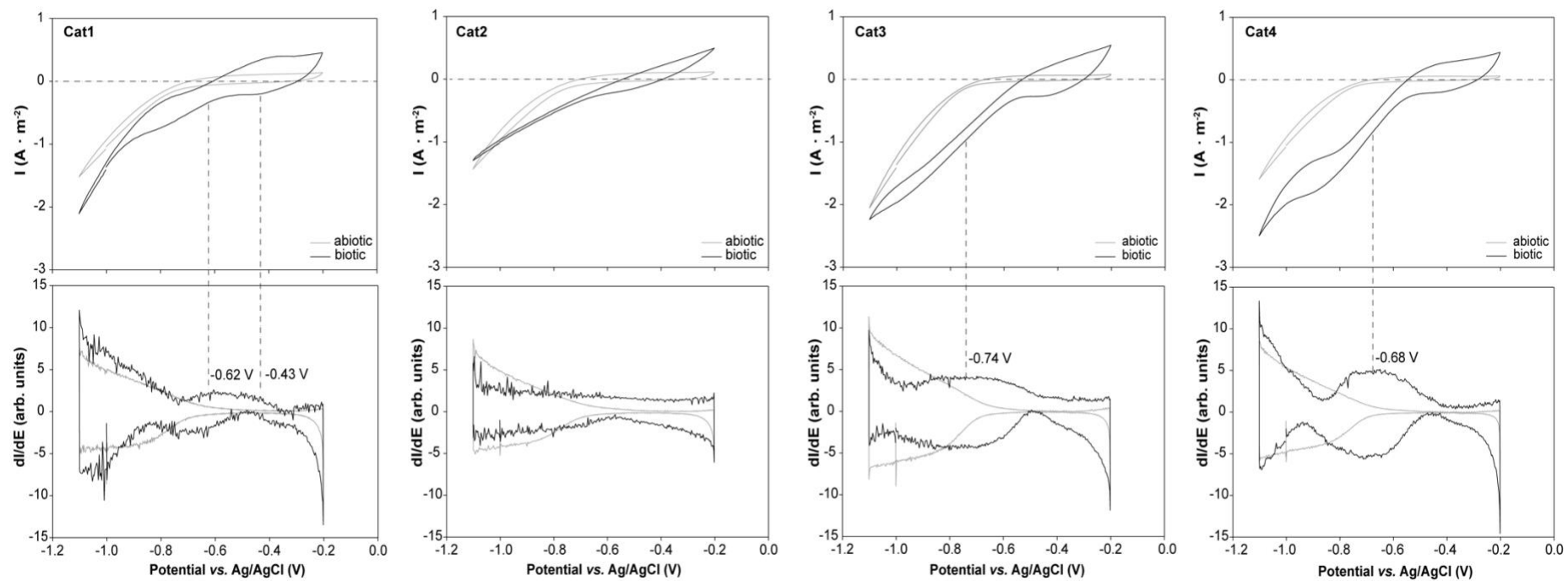


Figure 7. Electrochemical performance of each cathode was assayed independently using CV after 34 days of operation. Cyclic voltammetry (CV) tests for each electrode (above) and first derivative of the respective CVs (below) under abiotic (grey) and biotic (black) conditions.

2.2. DNA based microbial community structure

The presence of a dense biofilm attached to the electrode surface was visualized by SEM observations. Most microbes attached to the carbon cloth were rod-shaped and thin appendage-like structures, between cells and cathode surface were sporadically observed ([Figure 8](#)).

The microbial community structure was analysed by sequencing a 250 bp fragment of the V4 region in 16S rRNA gene. A total of 854,427 valid sequences were obtained. The average number of sequences per sample was 71,202 (from 63,505 to 144,017). One of the bulk liquid samples was removed due to a limited sequencing depth. Sequences were clustered in 443 OTUs at a similarity level of 97%. Each sample was rarefied at 61,000 sequences to analyse changes in the composition of the microbial community. For all samples, coverage was higher than 99%. Richness and diversity indicators were invariably lower in the BES compared to the sample used as inoculum ([Table 13](#)), showing a selective enrichment of species in the cathode biofilms (lower number of species).

Table 13. Richness and diversity indicators according to sample type.

	Inoculum (n=2)	Biofilm (n=4)	Bulk liquid (n=1)
Observed Richness (Sobs)	201.2 ± 9.6	117.5 ± 27.1	158.7
Maximum richness (Chao1)	205.6 ± 10.9	134.9 ± 28.7	172.7
Shannon diversity (H')	4.5 ± 0.5	2.8 ± 0.7	3.9
Phylodiversity (PD)	11.4 ± 0.4	7.9 ± 1.1	9.9

BES biofilms resulted in a highly enriched population of methanogenic archaea (75.7% of sequences in the biofilm) compared to bulk liquid (56.7%) ([Figure 9](#)). *Proteobacteria* showed an opposite trend and were more abundant in the bulk liquid (8.9% and 25.7% of the sequences in biofilm and bulk liquid samples, respectively). Despite the higher enrichment of methanogenic organisms in the biofilm, no significant differences in overall community structure were detected ($R = 0.92$, $p > 0.05$).



Figure 8. Scanning electron micrograph of the biofilm attached to the cathodes. (A) Colonized carbon cloth fiber. (B) Detail of rod-shaped microbes. (C) Thin appendage-like structures (white arrows) between microorganisms and carbon cloth surface were observed.

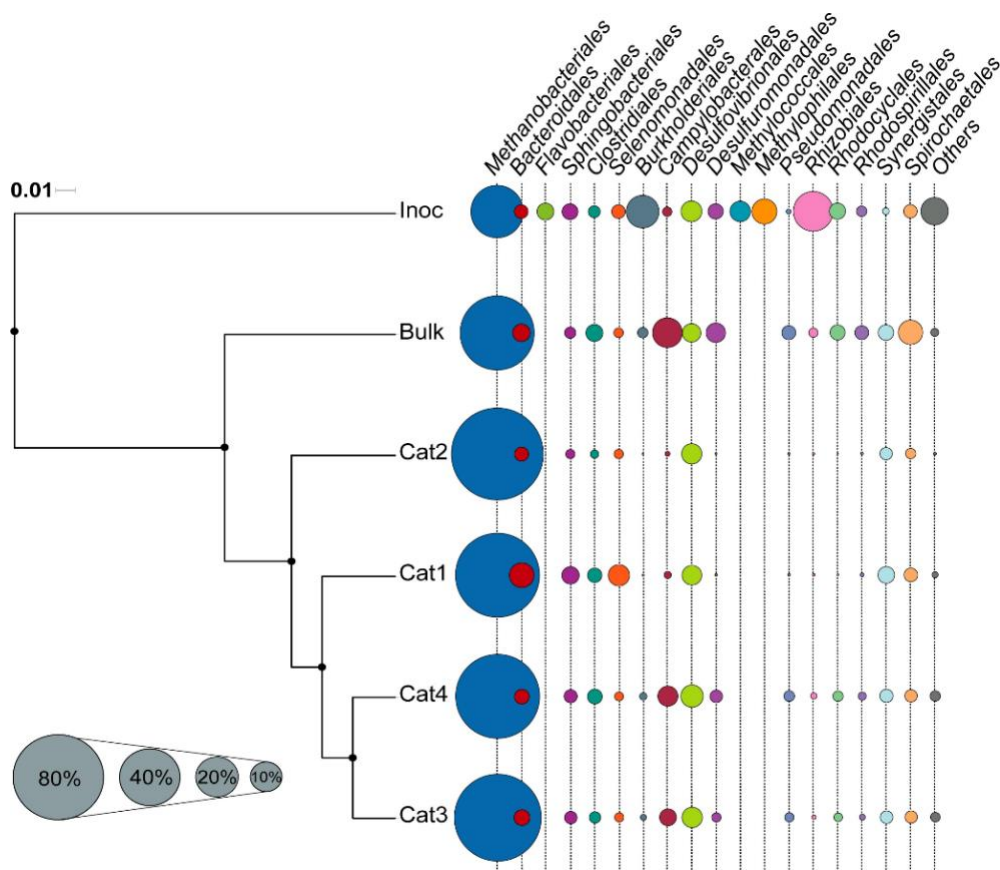


Figure 9. Microbial community composition in inoculum, bulk, and biofilm samples. Dendrogram based on weighted Unifrac measures of the microbial community rarefied at 61,000 sequences per sample. Black dots in nodes indicated bootstrap supported levels above 90%. Bubble chart shows the relative abundance of main archaeal and bacterial orders in each sample. Phyla accounting for less than 0.01% of all the sequences have been grouped as Others. Cat1, Cat2, Cat3, and Cat4, are samples from the biofilm of the four carbon cloth

cathodes.

At the genus level, BES was dominated by *Methanobacterium* spp. BLASTn searches of the most abundant OTUs resulted in the presence of sequences highly similar to *M. congolense* and *M. formicicum* (Table 14). Other methanogens, such as *Methanobrevibacter* sp., were represented at lower relative abundances (<2% considering all sequences).

Table 14. Most probable identification (BLAST, RefSeq RNA database), and relative abundance of the two most abundant archaeal 16S rRNA sequences in the electromethanogenic reactor.

Most probable identification	Similarity (%)	Relative number of sequences (%)		
		Inoculum	Biofilm	Bulk liquid
<i>Methanobacterium congolense</i> strain C NR_028175.1	99	2.9 ± 2.2	49.6 ± 19.3	31.4
<i>Methanobacterium formicicum</i> strain MF NR_115168.1	100	25.6 ± 18.3	12.6 ± 7.8	15

Bacterial members of the microbial community were distributed in different abundances between biofilm and bulk liquid communities (Figure 9). Interestingly, members with an active sulphur related metabolism, like *Desulfovibrio* and *Sulfurospirillum*, were detected in all the analysed samples in which the former was present at relatively higher densities. *Desulfovibrio* sp. could be contributing to the bioelectrically mediated production of H₂, as an intermediate step to methanogenesis, like previously reported (Marshall et al., 2012; Van Eerten-Jansen et al., 2013). Biotic H₂ production has been demonstrated in biocathodes when these sulphate-reducing bacteria are present (Aulenta et al., 2012; Croese et al., 2011).

2.3. Determination of active members of the microbial community by RNA analysis

Dominance of *Methanobacterium* in BES has been previously reported in studies conducting electromethanogenesis where both H₂-mediated and direct electromethanogenesis were supposed to occur (Batlle-Vilanova et al., 2015; Cheng et al., 2009; Marshall et al., 2012; Van Eerten-Jansen et al., 2013). All *Methanobacterium* spp. have been considered as hydrogenotrophic methanogens (Kotelnikova et al., 1998), and more specifically *Methanobacterium palustre* has been suggested as being responsible for direct electron transfer in a cathode (Cheng et al., 2009). However, the applied potentials in Cheng et al. work (from -0.5 to -1.2 V *vs.* Ag/AgCl) did not guarantee that H₂-mediated methanogenesis was not taking place simultaneously. Abiotic hydrogen production in graphite electrodes has been studied at cathodic voltages ranging -0.6 to -2.0 V *vs.* Ag/AgCl and it was only detected at potentials below -1.1 V *vs.* Ag/AgCl (Batlle-Vilanova et al., 2014). Similar voltage ranges (below -1.0 V *vs.* Ag/AgCl) were recorded as the threshold for significant abiotic hydrogen

evolution for carbon cloth cathodes (Selembo et al., 2010). These values have been confirmed experimentally with the same systems used here (unpublished results). Although abiotic H₂ evolution cannot be overridden in the present system, it should have remained at low rates. Moreover, H₂ was not detected above the detection limit in any of the gas samples analysed, suggesting a high consumption rate, and limiting H₂ availability at the used conditions.

cDNA analysis was used as a proxy to identify the active members in the biofilm community, in both open and closed electric circuit cathodes. *Methanobacterium* sp. related sequences (70.0% to 87.0% of sequences) were dominant in the active community (Figure 10).

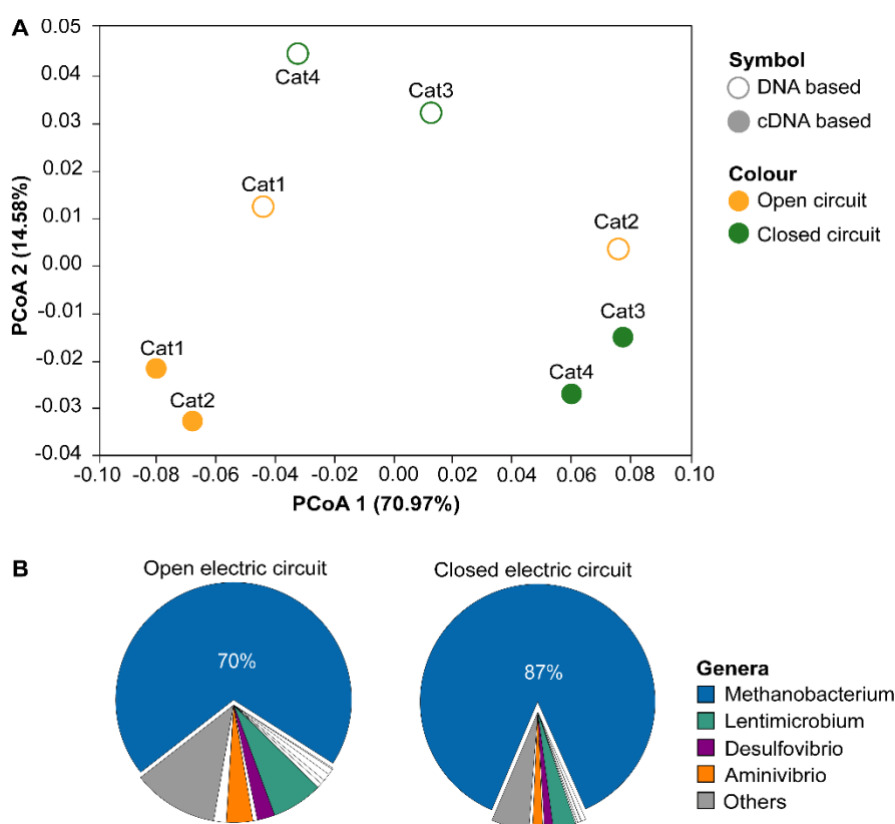


Figure 10. Changes in the DNA and cDNA-based microbial community structures of cathodes. (A) Distribution of samples in a Principal Coordinates Analysis (PCoA) according to weighted Unifrac dissimilarity index using 21,000 sequences per sample (see text for details). The variance (%) explained by each axis is indicated. (B) Pie charts of the average microbial composition (relative number of sequences) for the cDNA-based community of open and closed circuits.

As described before, the sensitivity of electromethanogenic biofilms to the electrode-to-cell flow showed a negative effect in methane production rates when reactors were exposed to an open electric circuit (cathode was disconnected from the potentiostat), suggesting that current was the unique energy source for methanogenesis (Batlle-Vilanova et al., 2015).

Methanobacterium was the main responsible archaeon conducting electromethanogenesis in the studied set-up. This archaeon, being the most abundant, and in an active state, was used as a model to study if cathode poisoning was a key factor in the expression of *Methanobacterium* membrane-bound and soluble [NiFe]-hydrogenases involved in the electron transfer chain during methanogenesis.

2.4. Changes in the expression of *Methanobacterium* sp. [NiFe]-hydrogenases

[NiFe]-hydrogenases were tested as proteins putatively implicated in electron transfer mechanism in *Methanobacterium* sp. We designed specific primers for key components of the enzyme complexes and tested for changes in their relative abundance using quantitative RT-PCR. Primers were directed to subunits containing [NiFe] or [Fe-S] clusters. Unfortunately, no reliable primer pairs could be obtained for the active subunit of Eha and we considered using primers for subunit *ebaB* being representative of hydrogenase expression since they are transcribed as a single operon (Tersteegen & Hedderich, 1999). Albeit not significant (non-parametric U Mann-Whitney test, p-value > 0.05), the observed relative expression of hydrogenases pointed to an increase of the relative expression of four of the genes, *ebaB*, *ebbL*, *hdrA*, and *hyyD*, accounting for increases up to 1.5-fold when electrodes were disconnected. Similar results were obtained when the relative expression was calculated according to *ftsZ* as the housekeeping gene for normalization (Figure 11).

We hypothesized a change in the relative expression levels of genes coding for enzymes participating in direct electron capturing would occur after disconnection of the electric circuit if the process was regulated at the transcriptomic level. With the used BES configuration, H₂-mediated and direct electromethanogenesis were supposed to occur concomitantly, therefore at open circuit conditions, availability of reducing equivalents would have been reduced immediately, and a change in the expression of selected hydrogenases would be expected in the event of their participation in direct electron capturing. The observed increase in the relative number of transcripts of the selected genes at disconnected conditions pointed to a more severe hydrogen limitation.

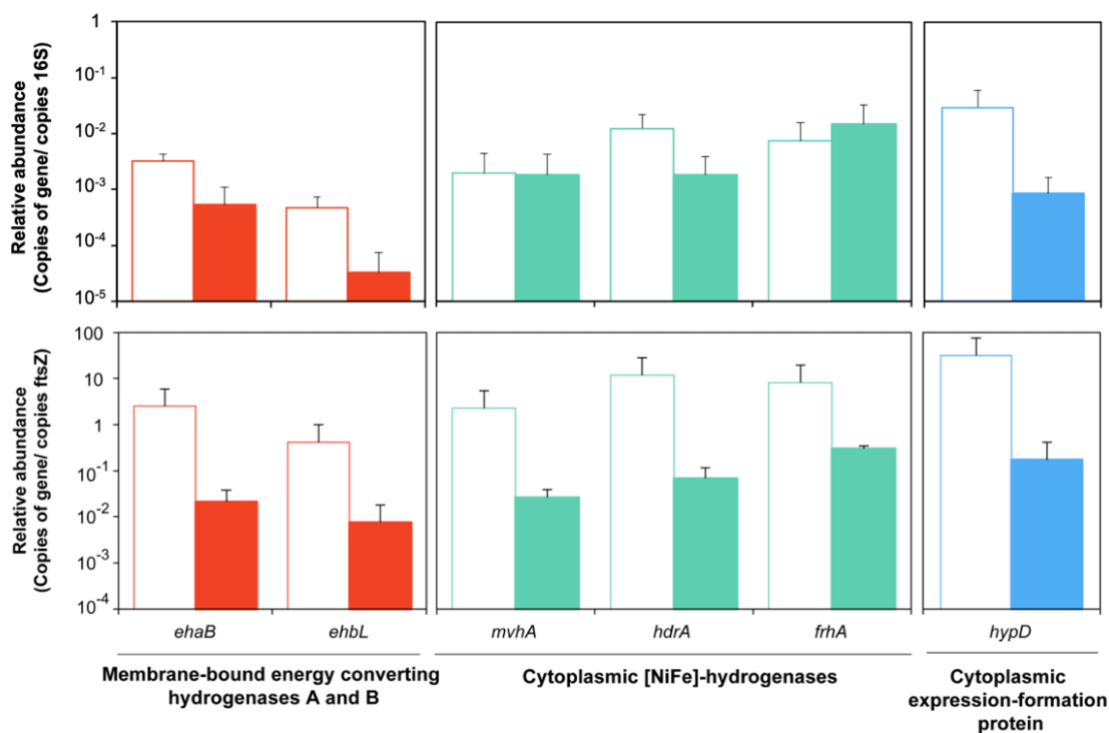


Figure 11. Relative content, number of target gene copies/number of copies of 16S rRNA or *ftsZ* gene of *Methanobacterium* sp. hydrogenases related genes (above and below, respectively). Open (empty bars) and closed (filled bars) electric circuit conditions were analysed. Mean values and standard deviations are represented in the bar chart. Relative abundance is expressed using a logarithmic scale. *ehaB* – energy-converting hydrogenase A subunit B. *ehbL* – energy-converting hydrogenase B subunit L. *mvhA* - heterodisulfide reductase associated [NiFe]-hydrogenase subunit A. *hdrA* - heterodisulfide reductase subunit A. *frhA* - Coenzyme F₄₂₀-reducing [NiFe]-hydrogenase subunit A. *hypD* – hydrogenase formation protein hypD. *ftsZ* – cell division protein FtsZ.

The bioavailability of H₂ affects several physiological and regulatory processes, altering the expression of some of the key genes for methanogenesis (Costa et al., 2013). For instance, H₂ limiting conditions in *M. maripaludis*, resulted in a higher expression of coenzyme F₄₂₀ [NiFe]-hydrogenase (Frh), a moderately up-regulation of Ehb, whereas no significant effect was detected in the expression of Eha and heterodisulfide reductases (Hdr) (Hendrickson et al., 2007). In the event of electrons causing a similar effect as H₂ limitation in cells, we expected an up-regulation of Ehb and Frh. In contrast, we did not observe any significant expression differences analysing *ehbL* and *frhA* in *Methanobacterium* sp. Any of the other analysed genes (*ehaB*, *mvhA*, *hdrA*, and *hypD*) presented significant expression differences.

The reduced changes of the relative expression of *Methanobacterium* sp. hydrogenases when shifted from closed to open circuits can be due to a combination of different aspects. First, the hydrogen produced at the electrodes that remained connected to the current (located in the same reactor) would maintain minimum levels of available reducing equivalents

preventing significant changes in the gene expression. Second, six-hour exposure to the open electric circuit was not sufficient to trigger significant changes in expression levels of the target genes, which would have been facilitated in the presence of an H₂ sensory apparatus. Regulating H₂-sensors are absent in *M. marburgensis* and *M. thermoautotrophicus* genomes (Kaster et al., 2011), suggesting that longer exposure times to open electric circuits should be tested to confirm changes in the relative expression of hydrogenase genes. Third, the tested enzymes were not participating in electron capture in *Methanobacterium* sp., or they were not sensitive to changes in electron availability.

In a previous report, Lohner and co-workers suggested the presence of a hydrogenase-independent mechanism of electron catabolism with the archaeon *Methanococcus maripaludis* MM1284. MM1284 is a mutant strain, carrying deletions of six hydrogenase genes, and is unable to perform methanogenesis from CO₂ and H₂. Bioelectrochemical mediated methane production of MM1284 was observed at cathode potentials of -0.8 V and -0.9 V vs. Ag/AgCl, suggesting the existence of a hydrogenase-independent electron uptake mechanism later shown to be involving formate by Deutzmann and co-workers (Deutzmann et al., 2015; Lohner et al., 2014). According to our results, participation of *Methanobacterium* sp. hydrogenases (Ehb and Eha) in electron capture could not be confirmed. More recently, the participation of heterodisulfide reductase complex has also been reported as a facilitator for electromethanogenesis in *M. maripaludis* (Lienemann et al., 2018). We analysed three *Methanobacterium* sp. proteins forming heterodisulfide complexes. Transcripts of *hdrA*, *mvhA*, and *frhA* (in proportion to 16S rRNA gene) seemed to be unaffected when cells were shifted from connected to disconnected conditions. Unfortunately, formate dehydrogenase (Fdh) and formyl-methanofuran dehydrogenase (Fwd) could not be analysed due to the lack of specificity of the primers for *Methanobacterium* sp.

Most genes coding for proteins highlighted as putative electron harvesting proteins have been investigated in this work, and changes in their relative expression analysed in a highly enriched *Methanobacterium* population. Our results point to a slight increase in the relative expression of four of these genes (*ehaB*, *ehbL*, *hdrA*, and *hypD*) although differences were not conclusive with the conditions used here. Additional tests need to be performed to confirm the observed tendency and to incorporate other proteins, such as ferredoxins (Choi & Sang, 2016), or pili proteins (Rotaru et al., 2014) that are likely to be involved in electron capturing and deserve further investigation in electromethanogenesis.

CHAPTER 2

Bacteria coated cathodes as an *in-situ* hydrogen evolving platform for microbial electrosynthesis

Published as: **Perona-Vico, E.**, Feliu-Paradedda, L., Puig, S, Bañeras, L. (2020) Bacteria coated cathodes as an *in-situ* hydrogen evolving platform for microbial electrosynthesis. Scientific Reports. 10 – 19852. Nature Publishing Group. ISSN 2045-2322. DOI: <https://doi.org/10.1038/s41598-020-76694-y>

1. Background

A major limitation in BES processes is the rate at which microorganisms acquire electrons from solid-state electrodes for CO₂ reduction (Kracke et al., 2015). Several studies have proposed hydrogen (H₂) as the principal electron donor intermediary in the production of commodity chemicals from carbon dioxide and electricity (Batlle-Vilanova et al., 2014; Jourdin et al., 2015; Puig et al., 2017). Molecules such as H₂, carbon monoxide (CO), and formate are the most preferable for microbial catalysts (Liu et al., 2020). Microbial electrosynthesis will be reinforced by the integration of proper H₂-producing microbial catalysts.

Metabolically, surplus hydrogen production for most anaerobic microorganisms is an induced response to avoid the accumulation of reduced cofactors (NAD, NADP, FAD, ferredoxins, and others) so that metabolic processes can continue (Ergal et al., 2018). Hydrogenases and nitrogenases are among the most widespread enzymes involved in proton reduction for hydrogen production. Hydrogenases are responsible for the reversible reaction to convert protons and electrons into hydrogen ($2\text{H}^+ + 2\text{e}^- \leftrightarrow \text{H}_2$). Contrarily, nitrogenases naturally produce H₂ as a by-product of nitrogen fixation ($\text{N}_2 + 8\text{e}^- + 8\text{H}^+ + 16\text{ATP} \leftrightarrow 2\text{NH}_3 + \text{H}_2 + 16\text{ADP} + 16\text{P}_i$). Under nitrogen limitation, nitrogenases function as a hydrogenase and only produce H₂ by proton reduction to molecular hydrogen ($2\text{H}^+ + 2\text{e}^- + 4\text{ATP} \leftrightarrow \text{H}_2 + 4\text{ADP} + 4\text{P}_i$) (Ergal et al., 2018; Koku et al., 2002).

In biocathodes, H₂ is produced either abiotically (pure electrocatalytic process) or biotically, with the participation of living microorganisms or isolated enzymes. Abiotic or electrocatalytic H₂ is produced when using carbon-based materials (*i.e.*, graphite cathodes) at cathode potentials below -1.0 V *vs.* Ag/AgCl (Batlle-Vilanova et al., 2014). Biologically produced H₂ (BioH₂) have been proven in biocathodes by using both pure and mixed microbial cultures. *Geobacter sulfurreducens*, *Rhodobacter capsulatus*, and *Desulfovibrio* spp. catalyse hydrogen production at cathode potentials below -0.8 V *vs.* Ag/AgCl (Aulenta et al., 2012; Geelhoed & Stams, 2011; Puig et al., 2017; Yu et al., 2011). Microbial community characterizations demonstrated that highly H₂ producing biocathodes were enriched mainly by *Proteobacteria* (Croese et al., 2011; Jourdin et al., 2015; Puig et al., 2017). Croese and co-workers described a cathodic microbial community mainly composed of *Deltaproteobacteria* in which *Desulfovibrio* spp. were the most abundant (Croese et al., 2011). *Alpha*- and *Betaproteobacteria* (*Rhodocyclaceae*) have also been highlighted to be mediating H₂ production in cathodes (Jourdin et al., 2015; Puig et al., 2017). In addition, increased H₂ production rates

in the presence of cell-free exhausted medium from cultures of *Sporomusa sphaerodites*, *Sporomusa ovata*, and *Methanococcus maripaludis* have also been confirmed (Deutzmann et al., 2015; Lienemann et al., 2018; Tremblay et al., 2019). The authors demonstrated that the former presence of microorganisms in the reactor had changed the electrode surface via metal deposition (nickel and cobalt) leading to increased H₂ production (Tremblay et al., 2019). Alternatively, free enzymes (hydrogenases and formate dehydrogenases) previously released by microorganisms (Deutzmann et al., 2015; Lienemann et al., 2018) could also be deposited in the electrode surface reinforcing H₂ production yields.

Another feasible strategy aiming to improve H₂ production in biocathodes is the integration of low-cost metal-based cathode materials such as cobalt phosphide, molybdenum disulphide, and nickel-molybdenum with putatively electroactive microorganisms. Although its integration with the required conditions for microbial growth might cause toxicity towards microorganisms (Kundu et al., 2013), some of these materials have been demonstrated as a promising and biocompatible electrocatalytic H₂-producing platform, while combining with CO₂-reducing and H₂-utilizing bacteria (like *S. ovata* and *M. maripaludis*) ensuring higher value-added chemicals production (Kracke et al., 2019).

In the present section, we aimed at assessing the capacity of ten strains of *Rhodobacter*, *Rhodopseudomonas*, *Rhodocyclus*, *Desulfovibrio*, and *Sporomusa* previously reported as potential cathodic H₂ producers. This approach may allow selecting potential candidates to establish resilient co-cultures, ideally composed of an H₂ producing strain in combination with a homoacetogen, for microbial electrosynthesis processes and electro-fermentation. We used an optimized experimental protocol which could facilitate the comparison among strains thus limiting the effect of heterogeneous reactor designs and analytical tools which are found in the literature. H₂ evolution was continuously monitored using an H₂ microsensor placed directly in contact with the liquid medium and close to the cathode surface. H₂ production efficiencies in monospecific biofilms of each strain were analysed repeatedly and compared to abiotic conditions.

EXPERIMENTAL DESIGN IN BRIEF

H-type cells were inoculated with pure cultures of *Rhodobacter* sp., *Rhodopseudomonas* sp., *Rhodocyclus tenuis*, *Sporomusa ovata*, and *Desulfovibrio* sp., and operated for five days at -1 V vs. Ag/AgCl to test bio-H₂ production. Previously to the characterization of the strains, the same carbon cloth electrodes were tested for abiotically H₂ produced. Online monitoring of the H₂ was performed using an NP-500 Unisense H₂ sensor and

production rates were calculated as a linear response covering the first 25 minutes of operation.

2. Results and Discussion

2.1. Electrocatalytic H₂ production at carbon cloth electrodes

Accurate choice of control conditions in reactor set-ups (as abiotic controls) is mandatory to avoid data deviation and facilitate interpretation (Deutzmann et al., 2015). Several tests were carried out to determine the electrocatalytic (or abiotic) H₂ production in carbon cloth electrodes. The use of a fixed methodology and an exhaustive analysis of control experiments facilitated comparison among strains and detection of relevant biotic effects. Carbon cloth electrodes were operated at different potentials (-0.6, -0.8, and -1.0 V *vs.* Ag/AgCl) and H₂ evolution was monitored. Under these conditions, catalytic H₂ was only detected when cathodes were poised at -0.8 and -1.0 V *vs.* Ag/AgCl (Table 15). Independently on the used medium, higher H₂ production rates (8.4 ± 3.0 , 6.4 ± 1.8 and $5.1 \pm 0.8 \mu\text{M}\cdot\text{min}^{-1}$, respectively) were achieved at -1.0 V.

Table 15. Hydrogen production rates, current demand, and energy consumption in abiotic conditions at different cathode potentials with the three used inorganic media modified for BES operation.

Medium	Cathode potential (V <i>vs.</i> Ag/AgCl)	H ₂ production rate ($\mu\text{M}\cdot\text{min}^{-1}$)	Current demand ($\text{mA}\cdot\text{m}^{-2}$)	Energy (kWh)
Modified DSM 27	-0.6	n.d.	-	-
	-0.8	2.3 ± 0.8	689.6 ± 387.1	$6.0 \cdot 10^{-6} \pm 4.5 \cdot 10^{-6}$
	-1.0	8.4 ± 3.0	1749.2 ± 894.4	$1.2 \cdot 10^{-5} \pm 6.0 \cdot 10^{-6}$
Modified DSM 311	-0.6	n.d.	-	-
	-0.8	2.1 ± 0.7	644.9 ± 75.6	$5.1 \cdot 10^{-6} \pm 2.4 \cdot 10^{-6}$
	-1.0	6.4 ± 1.8	1626.2 ± 125.9	$3.8 \cdot 10^{-5} \pm 1.0 \cdot 10^{-5}$
Modified medium based on Aulenta <i>et al.</i>	-0.6	n.d.	-	-
	-0.8	1.9 ± 0.6	781.0 ± 213.2	$4.6 \cdot 10^{-5} \pm 3.3 \cdot 10^{-6}$
	-1.0	5.1 ± 0.8	1534.7 ± 105.2	$2.7 \cdot 10^{-5} \pm 1.3 \cdot 10^{-5}$

n.d. Hydrogen was not detected.

Electrocatalytic H₂ production is conditioned by several factors, such as liquid medium composition, temperature, overpressure, electrode material, reactor designs, and/or operating modes (Call & Logan, 2008; Kracke et al., 2019; Kundu et al., 2013; Selembo et al., 2010). To estimate if the medium composition was affecting hydrogen production, ionic losses were calculated (Table 16) for each medium used. The ionic loss (mV) is related to the electrolyte resistance of the anolyte and catholyte and was estimated according to Ter Heijne

et al. (Ter Heijne et al., 2006). Differences in medium composition result in certain ionic losses due to its electrical conductivity. Similar ionic losses were found for DSM 311 and Aulenta *et al.* modified media (+85 and +89 mV, respectively) but, slightly higher ionic loss (+184 mV) was estimated for modified DSM 27. These differences were related to the different salinities. However, they should not have a significant effect on catalytic hydrogen productions.

Despite special care was applied to minimize effects in cathode sizes and qualities, differences in H₂ production rates were detected between carbon cloth electrodes, suggesting that parameters such as material integrity or the presence of impurities, could be affecting H₂ production. Consequently, it was necessary to measure abiotic H₂ concentrations for each carbon cloth electrode later used for monospecific biofilm formation to ensure proper results interpretation.

Table 16. Ionic losses (mV) for each of the three used media modified for BES operation.

Media	I _{ions} (A·m ⁻²)	d _{an} (m)	d _{cat} (m)	A _{an} (m ²)	A _{cat} (m ²)	Cond _{an} (S·cm ⁻¹)	Cond _{cat} (S·cm ⁻¹)	Ionic loss (mV)
Modified DSM 27	1.078	0.0375	0.045	0.0014	0.0024	0.22	0.22	+184
Modified DSM 311	1.545	0.0375	0.045	0.0014	0.0024	0.68	0.68	+85
Modified medium based on Aulenta <i>et al.</i>	1.050	0.0375	0.045	0.0014	0.0024	0.44	0.44	+89

I_{ions}: Current density.

d_{an}, d_{cat}: Distance between the anode/cathode and the membrane.

A_{an}, A_{cat}: Surface area.

Cond_{an}, Cond_{cat}: Conductivity.

2.2. Formation of monospecific biofilms and stability

The abundance of the 16S rRNA gene was used as a proxy for bacterial density in BES. Although 16S rRNA gene copies could be translated into cell abundance given 16S rRNA copies per unit genome (Acinas et al., 2004), no such transformation was performed since differences were only analysed in terms of biofilm stability of individual strains during experiments. As expected, the presence of bacteria from the beginning of the BES operation was confirmed. 16S rRNA gene copies ranged from 3.7·10⁶ to 4.5·10⁵ gene copies/cm² in biofilm samples, and 1.5·10⁸ to 9.7·10⁴ gene copies/mL in the bulk liquid.

Proportions between abundances measured before and after BES operation were used to assess the short-term stability of the biofilm. Except for *Rhodospseudomonas pseudopalustris* DSM 123 and isolate C2T108.3, all bacterial strains tended to remain attached to the cathode during the operation, or even grow as a biofilm, since an increase in gene copies

concentrations was found (more than 10-fold increase for *Rhodobacter capsulatus* DSM 152; [Figure 12](#)). Total 16S rRNA gene copies in BES (*i.e.*, bulk liquid + biofilm cells) remained almost invariable during operation, except for strains DSM123 and C2T108.3 which experienced a significant decrease, confirming no growth occurred. Collectively, abundance data indicates that monospecific biofilms could be effectively formed and maintained stable for the duration of the experiment.

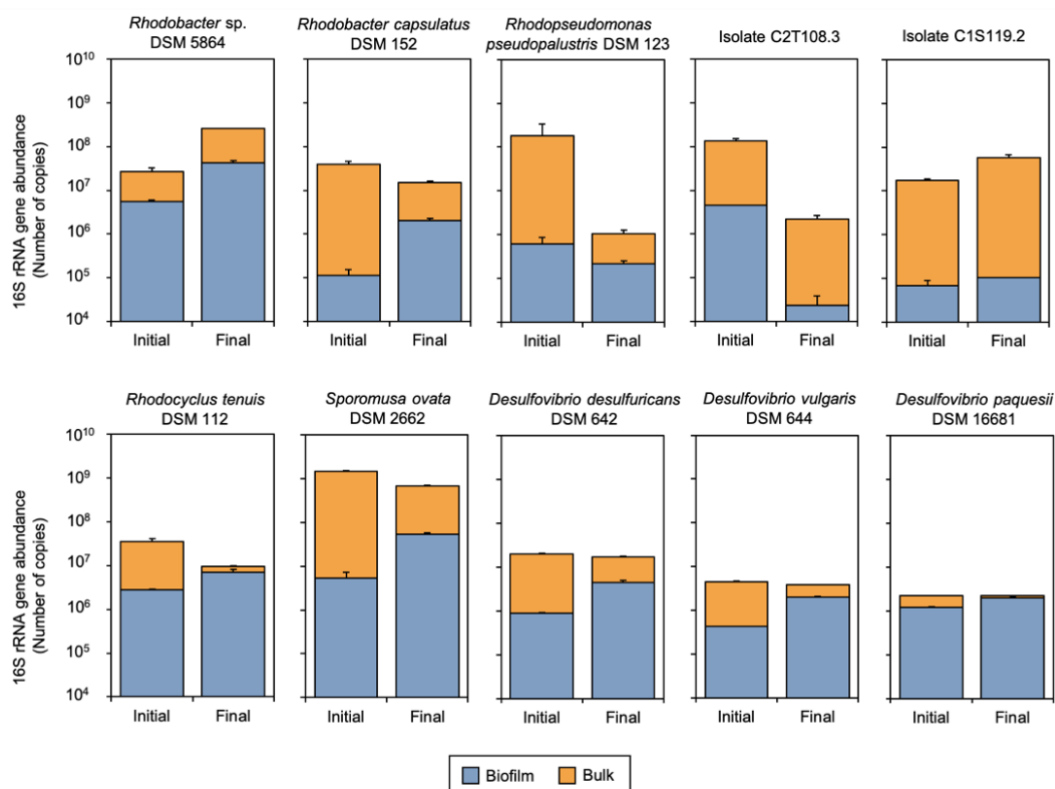


[Figure 12](#). Abundance of 16S rRNA genes into biofilm and bulk samples. Logarithmic scale is used to show the number of copies from samples taken at the beginning (Initial) and the end of BES operation (Final).

2.3. Bioelectrochemical production of H₂ in purple non-sulphur (PNS) bacteria

Inoculation and growth experimental procedures were optimized to enable monospecific biofilm formation on the cathode surface and short-term evaluation of H₂ production. As stated above, pure electrocatalytic H₂ production was estimated for every cathode and used as a threshold to determine the effect of the bacterial presence.

For all tested PNS strains, H₂ production started immediately after feeding reactors with CO₂ and accounted for higher productions (1.2 to 2.2-fold) compared to abiotic conditions ([Figure 13](#)). Specific net productivities (per unit biomass) ranged from 3.6 to 283.3 (μM·min⁻¹

$1 \cdot 10^7$ copy⁻¹ 16S rRNA). In addition, higher current demands and lower energy consumptions were recorded ([Table 19](#)). Strain-specific differences were observed after the two CO₂ feedings. In particular, H₂ production rates for the two *Rhodobacter* sp. (DSM 5864 and DSM 152) decreased to values similar to abiotic conditions (6.7 ± 0.6 and 5.9 ± 1.8 $\mu\text{M} \cdot \text{min}^{-1}$, respectively). In contrast, for *Rhodopseudomonas* sp. (DSM 123 and isolates C2T108.3 and C1S119.2) and *Rhodocyclus tenuis* biofilms, successive CO₂ feedings caused a severe decrease of H₂ production rates (from 2 to 7-fold compared to maximum production). Differences in current demand and energy consumption occurred accordingly ([Table 19](#)). Decreasing H₂ production rates with *R. pseudopalustris* DSM 123 and isolate C2T108.3 could be explained due to the large decrease (from 1 to 3 magnitude orders) observed in cell densities attached to the cathode over experimental time ([Figure 12](#)). Coulombic efficiencies (CE) to produce H₂ remained similar as the found in abiotic conditions when using the two *Rhodobacter* sp., except after the second CO₂ feeding for DSM 5864 with a lower CE (67.8%). Also, when testing *R. tenuis* DSM 112 CE remained similar to abiotic conditions after the second CO₂ feeding (76.4% and 83.5%, respectively). Contrarily, coulombic efficiencies were severely lower when using *Rhodopseudomonas* sp. in comparison with abiotic conditions ([Table 19](#)).

pH has a great impact on electrochemical performance. According to the Nernst equation and typical solution conditions, an overpotential of -59 mV is expected per pH unit increase (Clauwaert et al., 2008). For that, pH was measured several times during the BES operation ([Table 17](#)). For all the tested bacteria starting pH was between 6.8-7.0. pH plummeted to 5.4-5.7 immediately after sparging pure CO₂ for over 10 minutes and increase continuously afterwards. From a thermodynamic point of view, such acidic pH reinforced the production of hydrogen. During the experimental period pH followed different trends for each strain. pH decreased to around 5.7-5.8 in the two *Rhodobacter* sp. (DSM 5864 and DSM 152), while for isolate C1S119.1 went up to 7.4 after five days of operation. Similar pHs were measured for the other PNS strains (around 6.6-6.9 at the end of the operation). Differences were linked to the rate of bioelectrochemical H₂ production of each strain and the buffer capacity of each medium ([Table 18](#)).

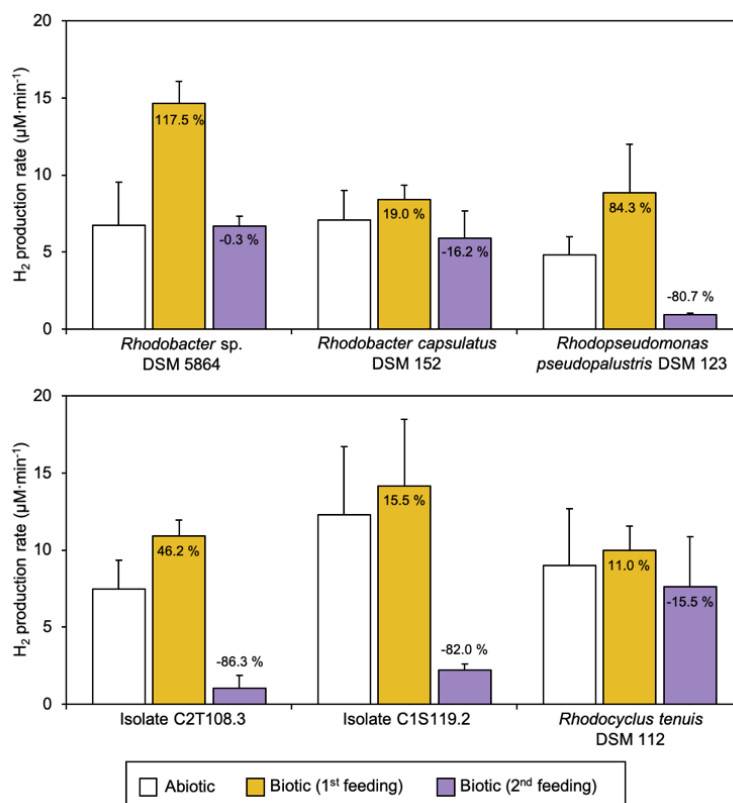


Figure 13. Hydrogen production rates ($\mu\text{M}\cdot\text{min}^{-1}$) of monospecific biofilms of purple non sulphur (PNS) bacteria after successive CO_2 feeding in BES reactors. Rates are compared to values obtained for the same electrode in abiotic conditions (white bar) and percentages indicate production rates increase or decrease (negative values).

Table 17. pH during BES operation. Measurements were performed before CO_2 feeding procedure.

Bacterial strain	Day of operation		
	0	3	5
<i>Rhodobacter</i> sp. DSM 5864	6.79	5.79	5.65
<i>Rhodobacter capsulatus</i> DSM 152	6.80	6.08	5.75
<i>Rhodopseudomonas pseudopalustris</i> DSM 123	6.91	6.33	6.55
Isolate C2T108.3	6.86	7.30	6.73
Isolate C1S119.2	6.80	7.48	7.41
<i>Rhodocyclus tenuis</i> DSM 112	6.99	7.11	6.91
<i>Sporomusa ovata</i> DSM 2662	7.41	6.54	6.51
<i>Desulfovibrio desulfuricans</i> DSM 642	7.66	7.68	7.18
<i>Desulfovibrio vulgaris</i> DSM 644	7.67	6.92	6.77
<i>Desulfovibrio paquesii</i> DSM 16681	7.70	7.38	6.17

Table 18. pH values recorded after ten minutes of CO_2 bubbling for each medium used for BES operation.

	Inorganic DSM 27	Inorganic DSM 311	Inorganic Aulenta <i>et al.</i> , 2012
Initial	6.8	7.0	7.0
After CO_2 bubbling	5.7	5.4	5.7

Hydrogen production by PNS occurs under photoheterotrophic metabolism (Koku et al., 2002). Although several studies have highlighted the metabolic versatility of PNS, focusing mainly on the *in-situ* bioH₂ production under different substrates, reactor designs, and environmental conditions (Carlozzi & Lambardi, 2009; Ergal et al., 2018; Gebicki et al., 2010; Koku et al., 2002), few studies have been conducted using pure cultures in BES (Guzman et al., 2019; Puig et al., 2017; Vilar-Sanz et al., 2018). Observed changes in H₂ production rates after different CO₂ flushes in the reactor, when operated with PNS, could be due to two opposite effects. First, the possibility that H₂ was being produced as a residual activity from photo-fermentative growth. This could explain the higher production rates when starting BES operation, but only if some intracellular carbon reservoir had been accumulated during the preparation of biofilms. Both *Rhodobacter* and *Rhodospseudomonas* species can accumulate polyhydroxy butyrate (PHB) under nutrient starvation (*i.e.*, nitrogen, phosphor, sulphur) and excess organic carbon source. Larger amounts of PHB are accumulated under nitrogen limitation and especially when acetate is used as carbon source. These are also suitable conditions for H₂ production via photo-fermentation. In the event of exposure of cells to non-optimal conditions, PHB can be mobilized and used as energy and carbon source (Kim et al., 2012; Wu et al., 2012). Second, an enhanced H₂ consumption after completed adaptation of cells to the new reactor environment. Although *Rhodobacter* sp. and *Rhodospseudomonas* sp. have been proposed as H₂-producing bacteria in biocathodes by other authors (Puig et al., 2017; Vilar-Sanz et al., 2018), in the tested conditions these strains did not show such a capacity in the long-term, *i.e.*, H₂ consumption surpassed production after CO₂ replenishment. However, current demands increased in three of the tested PNS strains (*R. pseudopalustris* DSM 123; isolate C2T108.3 and *R. tenuis* DSM 112) after the second CO₂ feeding (Table 19). This may be indicative of H₂ being produced and rapidly consumed by the cells. Unfortunately, due to the technical limitation for sampling the gas phase no data for CO₂ consumption is available to confirm this hypothesis. An alternative would be a direct electron transfer without H₂ accumulation. In this sense, Bose and co-workers tested *Rhodospseudomonas palustris* strain TIE-1 in cathodes poised at -0.1 V *vs.* Ag/AgCl elucidating that this strain was able to accept electrons from the poised electrode (Bose et al., 2014). Derived electrons from the cathode surface were entering the photosynthetic electron transport chain, leading to a highly reduced cellular environment. Further transcriptomic analysis on the expression levels of *ruBisCO* forms I and II using wild-type strain and a *ruBisCO* double mutant, determined that electron uptake was connected to CO₂ fixation (Guzman et al., 2019).

2.4. Bioelectrochemical production of H₂ in *Sporomusa ovata*

For the system inoculated with *S. ovata* DSM 2662, the H₂ production rate was 4-fold lower after the first CO₂ feeding. Remarkably, after the second feeding no H₂ production could be detected (Figure 14). Coulombic efficiency to produce H₂ was lower in biotic than in abiotic conditions (46.1% and 80.7%, respectively). Volatile fatty acids and alcohols were measured during BES operation in all the experimental conditions and tested strains, however only when using *S. ovata* acetate was detected. Acetate concentrations increased over time reaching 6.4 mM at the end of the operation. Coulombic efficiencies for acetate production increased over the operation from 57.2% to 70.3%. Mainly due to acetate production, pH decreased from 7.4 to 6.5 during operation. *Sporomusa* spp. have been widely used in MES (Aryal et al., 2017; Deutzmann et al., 2015; Nevin et al., 2011), taking advantage of its homoacetogenic metabolism. Therefore, recorded decreasing H₂ concentrations in our system could be explained by a quick consumption of H₂ for acetate biosynthesis. In terms of H₂ production, Deutzmann and co-workers found higher productions when using cell-free exhausted medium from *Sporomusa sphaeroides* cultures, probably due to the presence of enzymes (such as hydrogenases) into the culture supernatants (Deutzmann et al., 2015). More recently, high H₂ evolving BES at different cathode potentials (from -0.5 to -0.9 V *vs.* Ag/AgCl) have been demonstrated by using *S. ovata* cell-free medium due to nickel and cobalt deposition into the electrode surface (Tremblay et al., 2019). Despite being a frequently studied candidate for bioelectrosynthesis development, and considering our main objective, *Sporomusa* strains seem not to be good candidates for a stable H₂ producing platform using modified biocathodes. It seems clear that net H₂ production is only observed in the absence of active microorganisms.

2.5. Bioelectrochemical production of H₂ in sulphate-reducing bacteria

Sulphate-reducing bacteria can use H₂ as electron donor while reducing sulphate in anaerobic conditions (Lojou et al., 2002). But some of them, specially *Desulfovibrio* spp., have been postulated as potentially H₂ producing microorganisms in BES using pure and mixed cultures (Aulenta et al., 2012; Jourdin, Freguia, et al., 2015; Lojou et al., 2002). Here, three different *Desulfovibrio* species were selected as potential candidates to test and compare this process with other phylogenetically distinct bacteria. H₂ production rates at -1.0 V (Figure 14) were consistent over time for the three studied species, in agreement with Aulenta and co-workers with *D. paquesii* DSM 16681 (Aulenta et al., 2012). H₂ production rates in *D. desulfuricans* remained significantly higher compared to abiotic conditions ($p \leq 0.01$) after successive CO₂ feeding (13 ± 2.9 and 5.7 ± 1.0 $\mu\text{M} \cdot \text{min}^{-1}$, respectively; Table 19), but a decrease in

production rate was observed. While energy consumptions remained similar between feedings ($1.3 \cdot 10^{-5}$ to $1.6 \cdot 10^{-5}$ kWh), higher current demands were recorded in comparison to abiotic conditions. Coulombic efficiencies to produce H_2 remained above 70% being lower than the abiotic (Table 19). At the same potential, *D. vulgaris* did not increase production rates when compared to abiotic conditions (3.3 ± 0.9 and $3.2 \pm 0.4 - 4.1 \pm 0.6 \mu\text{M} \cdot \text{min}^{-1}$, respectively) although a higher current demand was measured (Table 19). The highest increase in H_2 production was observed for *D. paquesii* after two CO_2 flushes in the system operated at -1.0 V. A significant 8-fold increase ($p=0.02$) in H_2 production rate compared to abiotic conditions (5.5 ± 0.6 and $45.6 \pm 18.8 \mu\text{M} \cdot \text{min}^{-1}$, respectively) was observed, leading to increased current demand but slightly lower energy consumption. Similarly as exposed by Aulenta and co-workers, coulombic efficiencies (Table 19) remained between 80-100% (Aulenta et al., 2012). For all the tested *Desulfovibrio* starting pH was 7.7 and during BES operation pH decreased to 6.2-7.2 (Table 17).

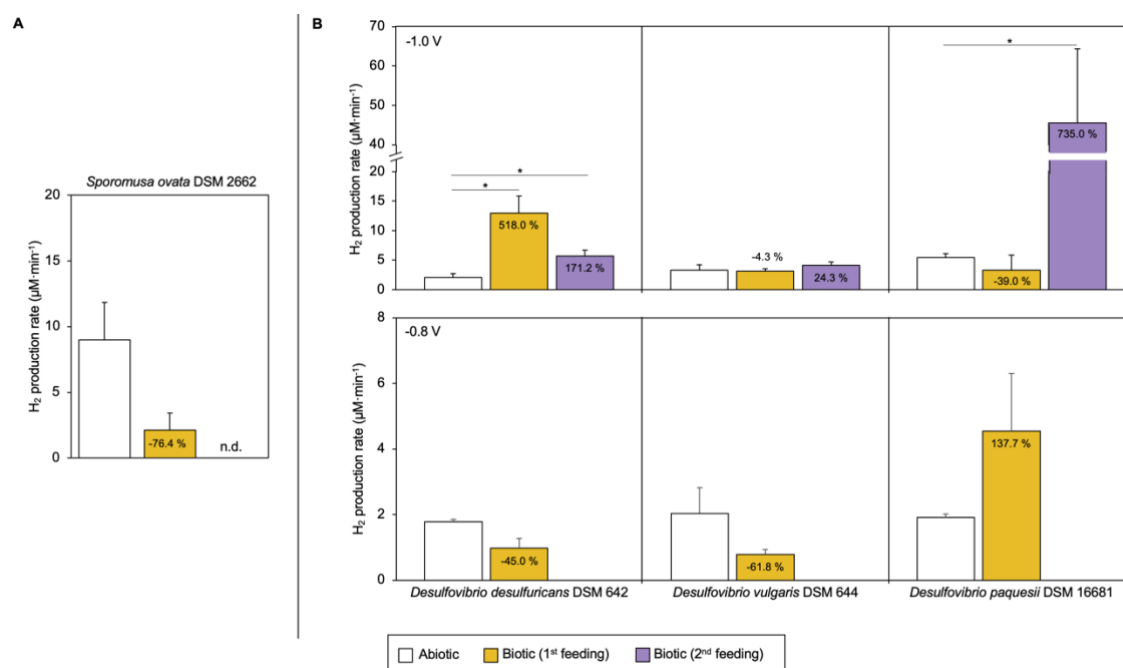


Figure 14. Hydrogen production rates ($\mu\text{M} \cdot \text{min}^{-1}$) using *S. ovata* DSM 2662 (A) and *Desulfovibrio* strains (B) with poised electrodes at -1.0 V (upper plots) and -0.8 V vs. Ag/AgCl (lower plots). Rates are compared to values obtained for the same electrode in abiotic conditions (white bar) and percentages indicate increase or decrease (negative values) in production rates. Statistically significant differences are shown as * ($p < 0.5$).

Since two out of the three *Desulfovibrio* strains showed the highest capacity in net H_2 production among the ten tested strains, experiments at less reducing potentials (-0.8 and -0.6 V vs. Ag/AgCl; Figure 14) were also performed. When biocathodes were poised at -0.8 V, measured current demands increased from abiotic to biotic conditions with all *Desulfovibrio*

strains (Table 19). Similar H₂ production rates were found for *D. desulfuricans* and *D. vulgaris*, being slightly lower than in abiotic conditions. Otherwise, in the presence of *D. paquesii* DSM 16681, higher net H₂ production rate was obtained. H₂ production was not detected either in abiotic or biotic conditions at -0.6 V *vs.* Ag/AgCl. Biocathodes in the presence of *D. paquesii* DSM 16681 had been characterized before at -0.9 and -0.7 V *vs.* Ag/AgCl by Aulenta and co-workers (Aulenta et al., 2012). The authors hypothesized that *Desulfovibrio* could not use efficiently the electrons when cathodes were polarized at potentials above -0.9 V because the recorded current demands in these conditions were very similar to the ones obtained in abiotic conditions. In contrast, our results suggested that at least at -0.8 V *vs.* Ag/AgCl, *D. paquesii* was able to produce H₂ at higher rates, and, regarding the higher current demand, usage of electrons from the cathode was confirmed.

The obtained results demonstrated that at least *D. desulfuricans* and *D. paquesii* were able to increase H₂ production in biocathodes at the used experimental conditions. *D. paquesii* was reported before as an electroactive microorganism able to produce H₂ highly efficiently with production rates from 5 to 10-fold times higher than in abiotic conditions, and coulombic efficiencies nearly to 100% (Aulenta et al., 2012). Also, *D. caledoniensis* has been proved as an H₂ producing catalyst at -0.8 V *vs.* Ag/AgCl (Lin Yu et al., 2011). Conversely, in the tested conditions no conclusive results could be obtained for *D. vulgaris*. However, direct evidence on electrocatalytic H₂ production when using purified *D. vulgaris* [Fe] hydrogenase was obtained when coating cathode electrodes with this enzyme (Guiral-Brugna et al., 2001). Also, stable hydrogen production using whole cells of *D. vulgaris* has been reported (Lojou et al., 2002), confirming electroactivity of the microorganism in the presence of methyl viologen and electrodes poised at -0.7 V *vs.* Ag/AgCl. Although not tested here, the presence of soluble electron shuttles, such as methyl viologen, may impact the H₂ production rate, but of course, the use of these compounds will impose additional parameters to be controlled to develop stable H₂ production platforms for BES.

2.6. Electrochemical characterization

Biofilms were characterized electrochemically using cyclic voltammetries (CV) after 5 days of operation and compared to abiotic CVs (Figure 15). In eight out of the ten tested strains, the current demand of biotic CVs differed significantly from the abiotic control indicating that those biofilms were electroactive. Current demand started to increase around -0.7 to -0.8 V *vs.* Ag/AgCl in abiotic conditions while in the presence of DSM 5864, DSM 152, DSM 123, C1S119.2, and DSM 112 increased current demands were recorded at higher potentials,

from -0.4 to -0.6 V *vs.* Ag/AgCl. This was interpreted as an indication that the biofilm catalysed the reduction reaction of protons (H^+) decreasing energy losses that could be associated with the catalytic hydrogen production. The highest current demands were observed for C1S119.2 and DSM 112 reaching 14.0 and 18.3 mA, respectively. Even though, these results could not be linked to higher net H_2 production rates. It should be considered that CV measurements are highly sensitive and can detect small-induced changes in the redox state of the cell that may not be sustained in the long run.

A redox pair was identified at -0.65 V *vs.* Ag/AgCl for *Rhodobacter* sp. DSM 5864, *R. pseudopalustris* DSM 123, isolate C1S119.2 and *Desulfovibrio* spp., which has been typically observed in H_2 -producing biocathodes (Batlle-Vilanova et al., 2014; Puig et al., 2017) and related to the *D. vulgaris* [Fe] hydrogenase activity (Guiral-Brugna et al., 2001). Similar results as the presented with *Desulfovibrio* species were found by other authors using pure cultures of *D. caledoniensis* and *D. paquesii* (Aulenta et al., 2012; Lin Yu et al., 2011). Redox peaks could not be identified for the experiments with *R. capsulatus* DSM 152, *R. tenuis* DSM 112, and *S. ovata*. An additional reduction peak was found at -0.46 V when using *D. vulgaris*. also found in electrochemical experiments conducted with *D. gigas* [NiFe] hydrogenases in bulk suspension (Cordas et al., 2008). Although electrochemical characterization using CV revealed some electroactivity for almost all the strains, unfortunately, these could not be translated into direct H_2 production, except for *D. desulfuricans* DSM 642 and *D. paquesii* DSM 16681. Defined co-cultures where hydrogenotrophic bacteria could be sustained by an efficient biological hydrogen producer have been highlighted before as an important step forward to improve microbial electrosynthesis (Deutzmann & Spormann, 2017). According to our results, *Desulfovibrio* species are the best candidates, among all tested strains, to further develop the use of biofilm-coated cathodes as a stable H_2 production platform in microbial electrosynthesis.

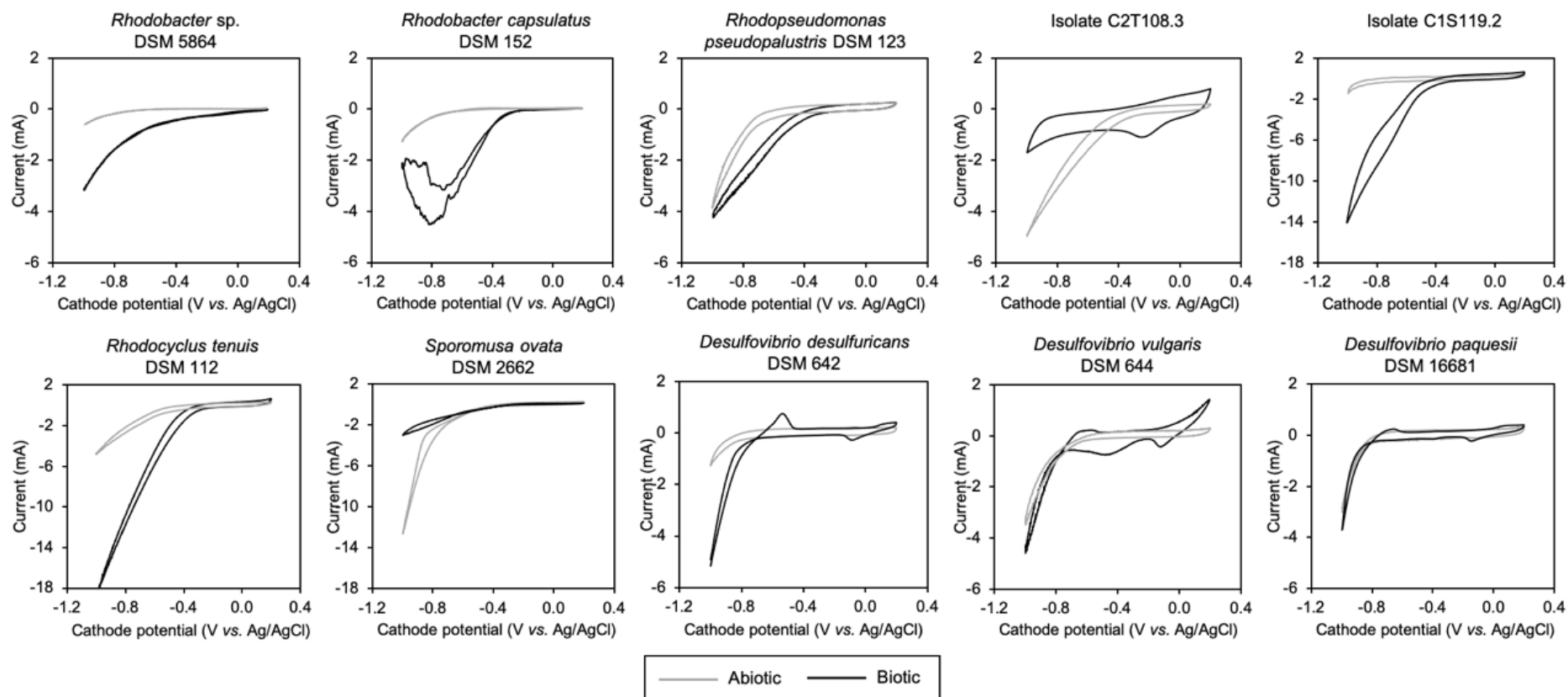


Figure 15. Cyclic voltammeteries (CV) for *Rhodobacter*, *Rhodopseudomonas*, *Rhodocyclus tenuis*, *Sporomusa ovata*, and *Desulfovibrio* strains. Representative voltammograms in abiotic cathode electrodes (grey) and biocathodes (black) are shown.

Table 19. Maximum H₂ accumulated, H₂ production rate, H₂ net production rate, current demand, energy, and coulombic efficiencies (CE%) for the different bacterial strains and experimental conditions. H₂ net production rates have been calculated as: (biotic – abiotic rates) per unit 16S rRNA gene. n.d. Not determined.

Bacterial strain	Potential (vs. Ag/AgCl)	Experimental conditions	Maximum H ₂ accumulated (μM)	H ₂ production rate (μM·min ⁻¹)	Specific net H ₂ production rate (μM·min ⁻¹ ·10 ⁷ copy ⁻¹ 16S rRNA ⁻¹)	Current demand (mA·m ⁻²)	Energy (kWh)	CE (%)
<i>Rhodobacter</i> sp. DSM 5864	-1.0	Abiotic	787.6	6.7 ± 2.8		753.6	2.3·10 ⁻⁶	95.7
		Biotic (1 st feeding)	1897.2	14.6 ± 1.4	14.1 ± 2.5	2397.9	8.0·10 ⁻⁶	94.8
		Biotic (2 nd feeding)	1656.2	6.7 ± 0.6	n.d.	1465.6	5.6·10 ⁻⁶	67.8
<i>Rhodobacter capsulatus</i> DSM 152	-1.0	Abiotic	1355.2	7.1 ± 1.9		962.3	3.3·10 ⁻⁶	82.8
		Biotic (1 st feeding)	2999.0	8.4 ± 0.9	117.2 ± 86.7	817.0	2.4·10 ⁻⁶	93.4
		Biotic (2 nd feeding)	745.9	5.9 ± 1.8	n.d.	647.9	1.8·10 ⁻⁶	83.0
<i>Rhodopseudomonas pseudopalustris</i> DSM 123	-1.0	Abiotic	940.3	4.8 ± 1.2		927.2	2.6·10 ⁻⁶	85.4
		Biotic (1 st feeding)	1173.5	8.9 ± 3.1	66.5 ± 32.1	1675.8	4.5·10 ⁻⁶	42.7
		Biotic (2 nd feeding)	449.8	0.9 ± 0.1	n.d.	2400.9	1.6·10 ⁻⁵	7.9
Isolate C2T108.3	-1.0	Abiotic	816.8	7.5 ± 1.9		2371.2	1.1·10 ⁻⁵	80.6
		Biotic (1 st feeding)	1773.4	10.9 ± 1.0	7.5 ± 1.9	2994.6	9.3·10 ⁻⁶	40.8
		Biotic (2 nd feeding)	655.8	1.0 ± 0.8	n.d.	5603.5	1.8·10 ⁻⁵	11.1
Isolate C1S119.2	-1.0	Abiotic	834.6	12.3 ± 4.5		5019.1	4.1·10 ⁻⁵	83.9
		Biotic (1 st feeding)	1726.9	14.2 ± 4.3	283.3 ± 23.2	5097.2	3.1·10 ⁻⁵	25.5
		Biotic (2 nd feeding)	655.8	2.2 ± 0.4	n.d.	4610.8	2.6·10 ⁻⁵	8.3
<i>Rhodocyclus tenuis</i> DSM 112	-1.0	Abiotic	1511.4	9.0 ± 3.7		2436.8	1.3·10 ⁻⁵	83.5
		Biotic (1 st feeding)	4865.5	10.0 ± 1.6	3.6 ± 7.6	2841.6	2.1·10 ⁻⁶	58.4
		Biotic (2 nd feeding)	3459.0	4.5 ± 1.1	n.d.	5857.9	3.6·10 ⁻⁵	76.4
<i>Sporomusa ovata</i> DSM 2662	-1.0	Abiotic	1454.6	4.0 ± 1.3		1505.6	5.8·10 ⁻⁶	80.7
		Biotic (1 st feeding)	123.9	2.1 ± 1.3	n.d.	820.8	5.5·10 ⁻⁷	46.1
		Biotic (2 nd feeding)	Not detected		n.d.	1228.7	7.8·10 ⁻⁶	n.d.
<i>Desulfovibrio desulfuricans</i> DSM 642	-1.0	Abiotic	938.6	3.5 ± 0.6		1774.6	3.0·10 ⁻⁵	85.9
		Biotic (1 st feeding)	2042.9	13.0 ± 2.9	121.5 ± 25.6	4771.4	1.3·10 ⁻⁵	73.2
		Biotic (2 nd feeding)	1467.3	5.7 ± 1.0	8.0 ± 0.9	4621.9	1.6·10 ⁻⁵	76.6
<i>Desulfovibrio vulgaris</i> DSM 644	-0.8	Abiotic	211.5	1.8 ± 0.1		478.0	1.3·10 ⁻⁵	46.1
		Biotic (1 st feeding)	192.7	1.0 ± 0.3	n.d.	966.8	2.2·10 ⁻⁶	28.4
		Abiotic	1000.0	3.3 ± 0.9		1758.2	3.0·10 ⁻⁵	82.8
<i>Desulfovibrio paquesii</i> DSM 16681	-1.0	Biotic (1 st feeding)	1384.7	3.2 ± 0.4	n.d.	3245.4	8.4·10 ⁻⁶	77.0
		Biotic (2 nd feeding)	1086.6	4.1 ± 0.6	4.1 ± 1.8	4975.4	3.0·10 ⁻⁵	17.4
		Abiotic	213.5	2.0 ± 0.8		1038.0	4.0·10 ⁻⁵	45.8
<i>Desulfovibrio paquesii</i> DSM 16681	-0.8	Biotic (1 st feeding)	124.0	0.8 ± 0.2	n.d.	1805.6	2.0·10 ⁻⁵	15.6
		Abiotic	1435.8	5.5 ± 0.6		1107.6	3.7·10 ⁻⁵	80.8
		Biotic (1 st feeding)	3088.7	3.3 ± 2.6	n.d.	2525.0	6.6·10 ⁻⁶	80.5
<i>Desulfovibrio paquesii</i> DSM 16681	-1.0	Biotic (2 nd feeding)	2826.6	45.6 ± 18.8	202.7 ± 91.9	6872.4	3.0·10 ⁻⁵	91.6
		Abiotic	592.0	1.9 ± 0.1		561.8	1.0·10 ⁻⁶	50.7
		Biotic (1 st feeding)	1232.5	4.5 ± 1.8	13.3 ± 8.3	1241.7	2.6·10 ⁻⁶	68.4

CHAPTER 3

Defining a strategy towards increasing bio-hydrogen production in two *Desulfovibrio* spp. via genetic modification

We performed this part of the Ph.D. Thesis in collaboration with the BioPilot Plant group at Leibniz Institute for Natural Product Research and Infection Biology–Hans Knöll Institute (Germany). Experiments were designed by Lluís Bañeras (L.B.), Sebastià Puig (S.P), Miriam Agler-Rosenbaum (M.A.-R.), Santiago Treceño-Boto (S.T.-B.) and Elisabet Peronavico (E.P.-V.) and performed by E.P.-V. and S.T.-B. Data analysis and writing of these chapter has been done by E.P.-V and reviewed and edited by all the authors.

1. Background

Desulfovibrio spp. belong to the sulphate-reducing bacteria (SRB). These are anaerobic prokaryotes found ubiquitously in nature. They have a relevant role in the biogeochemistry of different environments (*i.e.*, marine, river and lake sediments, mud, and metal surfaces), efficiently linking the sulphur and the carbon cycles. SRB generate energy (ATP) using sulphate as the terminal electron acceptor while oxidizing hydrogen (H₂) or various organic acids and alcohols, resulting in the production of sulphide (Heidelberg et al., 2004). H₂ is intimately involved in the growth of SRB. Key enzymes involved in H₂ metabolism are hydrogenases (H₂ases) which catalyse the reversible reaction $H_2 \leftrightarrow 2H^+ + 2e^-$. Hydrogenases are considered metalloenzymes due to their metal-containing active sites and are present ubiquitously in Archaea and Bacteria (Caffrey et al., 2007). The fully sequenced *Desulfovibrio vulgaris* Hildenborough strain has a total of six hydrogenases, namely: (i) soluble iron-only [Fe]-H₂ase, (ii) membrane-associated nickel-iron [NiFe]-H₂ase isozyme 1, (iii) membrane-associated nickel-iron [NiFe]-H₂ase isozymes 2, (iv) membrane-associated nickel-iron-selenium [NiFeSe]-H₂ase, (v) membrane-bound [NiFe]-H₂ase Ech and (vi) membrane-bound [NiFe]-H₂ase Coo. H₂ases i to iv are located in the cell periplasm and are directly involved in hydrogen oxidation for sulphur reduction whereas, both membrane-bound [NiFe]-H₂ases are involved in H₂ production from lactate (Heidelberg et al., 2004). In addition to H₂ases, periplasmic multiheme c₃-type cytochrome seems to be relevant in the process pursued in this Ph.D. Thesis since its involvement in electron transfer was described before in *Desulfovibrio* (Deng et al., 2018; Marshall et al., 2017). During the sulphate reduction, cytochrome c₃ is responsible for storing the electrons of H₂ oxidation until they are passed through the inner membrane via electron shuttles. Furthermore, the connection between various cytochromes generates a network that serves as a capacitor for the storage of low-potential electrons in the periplasm generated from H₂ or formate oxidation (Heidelberg et al., 2004).

The ability of sulphate-reducing bacteria for extracellular electron transfer (EET) became evident in the past since these bacteria can induce corrosion of metal surfaces utilizing elemental iron granules as the sole electron donor (Gupta et al., 2020). For this reason, SRB could have a relevant role in microbial electrochemical technologies (METs), especially in biocathodes. *Desulfosporosinus orientis*, *Desulfovibrio piger*, *Desulfopila corrodens* strain IS4, *Desulfobacterium autotrophicum* HRM2, and *Desulfovibrio ferrophilus* IS5 were described as directly taken electrons from the cathode and utilizing CO₂ as the sole carbon source since a more positive potential than the H₂ evolution redox potential at neutral conditions ($E_{H^+/H_2}^0 = -$

0.61 V *vs.* Ag/AgCl) was used (Agostino et al., 2018; Beese-vasbender et al., 2015; Deng et al., 2018; Zaybak, et al., 2018). Outer membrane cytochrome of *D. ferrophilus* IS5 was hypothesized as a possible electron conduit for EET (Deng et al., 2018). However, the exact EET mechanisms that are being used by SRB are poorly understood, and both direct ET and indirect ET (mainly H₂-mediated since as stated before SRB possess several periplasmic H₂ases) are possible depending on the used conditions in a BES (Agostino & Rosenbaum, 2018). Despite this lack of knowledge, it seems possible that cytochromes and hydrogenases would take part in the electron-to-hydrogen conversion process to some extent.

Several methodologies such as conjugation, targeted mutagenesis, transduction, transposition, and transformation were reported to serve as tools to genetically modify SRB. Conjugation is the method most extensively used, especially in the past. In conjugation mobilizable plasmids from donors (*Escherichia coli*) were transferred into the host cells (*Desulfovibrio*). This technique allowed for the first time the expression of native *Desulfovibrio vulgaris* Hildenborough cytochrome *c3* in *Desulfovibrio desulfuricans* G20 (Voordouw et al., 1990). Conjugation has been widely explored especially in *D. vulgaris* Hildenborough via overexpression of prismane protein (Stokkermans et al., 1992) or deletion of an oxygen sensor (chemoreceptor protein A, *dcrA*) (Fud & Voordouw, 1997). Electroporation was proven effective for *Desulfovibrio* transformation and successfully used for the first time in *Desulfovibrio fructosovorans* where marker-exchange mutagenesis was achieved by replacing the [NiFe]-H₂ase gene (*hydN*) with a kanamycin resistance cassette using a nonreplicating plasmid (Rousset et al., 1991). Transformation protocols (chemical or by electroporation) were described to be optimal for *D. vulgaris* Hildenborough. Examples of gene insertion (single recombinational events), tag proteins (single and double recombinational events) and marker-exchange deletion mutants (double recombinational events) were obtained (Bender et al., 2007; Keller et al., 2009; Keller et al., 2011; Zane et al., 2010). Although examples for the transformation of heterologous genes in SRB exists, no general protocols are available. In most cases, several conditions have to be tested for a given strain or species. This fact posed extra difficulties in this experimental part of the Ph.D. Thesis.

We aimed to increase the H₂ production capacity of *D. paquesii* via overexpression of genes putatively involved in the process. To achieve this goal, we opted for a classical transformation protocol. Several experimental steps were initially proposed: (i) selection of the genes and vector construction, (ii) defining a workflow to transform *D. paquesii* following the already described protocol optimized with *D. vulgaris*, (iii) confirmation of the

incorporation of the vectors, and (iv) test if the modified strain has the desired behaviour in terms of H₂ evolution.

EXPERIMENTAL DESIGN IN BRIEF

Sequences of the genes of interest (GOIs) were retrieved from the available genomes for both strains *D. vulgaris* Hildenborough (DSM 644) and *D. paquesii* DSM 16681. Modified native plasmids from *D. vulgaris* were obtained from AddGene. Primers and adaptors for an in-frame reading of selected genes were designed using target genes and plasmid sequences. Amplification was performed using conventional PCR. New vectors containing the GOIs were constructed. Different transformation protocols were tested to find proper conditions for the genetic modification of the desired *Desulfovibrio* strains.

2. Results and discussion

2.1. Selection of genes of interest and vector construction

Before starting the construction of the expression vectors, sequences of the available plasmids (named as pSC27, pMO719, pMO746, pMO9075) were analysed *in silico* to test which of them could be more suitable for the present project. Parameters such as size, sequence annotation (if any), and selectable markers included in the plasmids (kanamycin and spectinomycin) were considered in the selection (Table 20). pMO9075 was selected as the first choice since it has a proper size (4,800 bp) and, its stability in *D. vulgaris* has been confirmed (Keller et al., 2011).

Table 20. Characteristics of the available plasmids for SBR strains.

Plasmids	Size (bp)	Description	Selectable markers	Reference
pSC27	8,574	<i>Desulfovibrio</i> shuttle vector containing SRB replicon pBG1; mobilizable	Kanamycin	(Rousset et al., 1998)
pMO719	5,111	<i>Desulfovibrio</i> shuttle vector containing pBG1 and PMB1 replicons	Spectinomycin	(Bender et al., 2007)
pMO746	3,206	Upp in an artificial operon with npt from plasmid pMO9071; ori from pCR4/TOPO	Kanamycin	(Parks et al., 2013)
pMO9075	4,837	<i>Desulfovibrio</i> shuttle vector containing SRB replicon (pBG1) and <i>aph(3')-IIp</i>	Spectinomycin	(Keller et al., 2011; Ray et al., 2014)

SRB species may exhibit a natural resistance to many antimicrobials, therefore preliminary tests of resistance to the contained selection markers are advisable. *D. vulgaris* Hildenborough requires higher kanamycin concentration for effective colony selection in comparison to other species, such as *D. desulfuricans* (Keller et al., 2011). Since no information on possible natural resistance to antibiotics was found for *D. paquesii* and partial kanamycin resistance

was described for other *Desulfovibrio* species, avoiding plasmids containing kanamycin resistance was our best choice at the starting moment.

Enzymes involved in the main metabolism pathway of the strains, H₂ oxidation/sulphate reduction, mainly being hydrogenases and cytochromes were considered as putatively interesting to be our genes of interest (GOIs). Annotated genes in this pathway for the type-strain *D. vulgaris* were used to find homologs in the available *D. paquesii* genome comparing protein sequences with BLASTP and considering a minimum similarity level of 60% (Table 21).

Table 21. Genes of interest in *D. vulgaris* DSM 644 (NCBI accession number NC_002937) and presence of analogues in *D. paquesii* DSM 16681 (IMG Genome ID 2571042346).

Gene	Locus DVU N°	Annotation	Length (bp)	Found in <i>D. paquesii</i> draft genome	
<i>hydA</i>	1769	Fe-only hydrogenase	1,266	✓	
<i>hydB</i>	1770		372	✓	
<i>hynB-1</i>	1921	NiFe hydrogenase isozyme 1	954	✓	
<i>hynA-1</i>	1922		1,701	✓	
<i>hynB-2</i>	2525	NiFe hydrogenase isozyme 2	975	✓	
<i>hynA-2</i>	2526		1,650	✓	
<i>hysB</i>	1917	NiFeSe hydrogenase	954		
<i>hysA</i>	1918		1,533		
<i>cooM</i>	2286	Membrane-bound CooMKLXUHF ortholog	3,762		
<i>cooK</i>	2287*		966		
<i>cooL</i>	2288		435		
<i>cooX</i>	2289		636		
<i>cooU</i>	2290		546		
<i>cooH</i>	2291		1,101		
<i>hypA</i>	2292		363		
<i>cooF</i>	2293		522		
<i>echF</i>	0429		Membrane-bound EchABCDEF ortholog	402	✓
<i>echE</i>	0430			1,077	✓
<i>echD</i>	0431	393		✓	
<i>echC</i>	0432	474		✓	
<i>echB</i>	0433	849		✓	
<i>echA</i>	0434	1,947		✓	
<i>cycA</i>	3171	Predominant tetraheme cytochrome <i>c3</i> (<i>cycA</i>)	390	✓	

* NCBI database annotation indicates that it is a pseudogene.

Although the exact functions of all the described H₂ases for *D. vulgaris* are not completely understood, they are all considered reversible, being able to do both oxidase and produce H₂. To choose a candidate H₂ase gene, those located in the periplasm were considered interesting since they are closer to the extracellular environment. Particularly, [Fe]-only H₂ase were described as probably being more active during H₂ evolution in *D. vulgaris*

Hildenborough under fermentative conditions (Mansure & Hallenbeck, 2008; van den Berg et al., 1993). Therefore, since we found it in the two genomes, [Fe]-only H₂ase (*hydAB*) was selected as a candidate gene. On the other hand, tetraheme cytochrome *c3* (*cycA*) was also selected as interesting for our purpose since it was described as potentially being participating in direct electron transfer (Deng et al., 2018; Marshall et al., 2017). Overall, two pairs of vectors were designed and constructed using plasmid pMO9075 containing each *hydAB* and *cycA* from both, *D. vulgaris* and *D. paquesii* (Figure 16). Confirmation of correct plasmids was done using digestions with restriction enzymes and by sequencing.

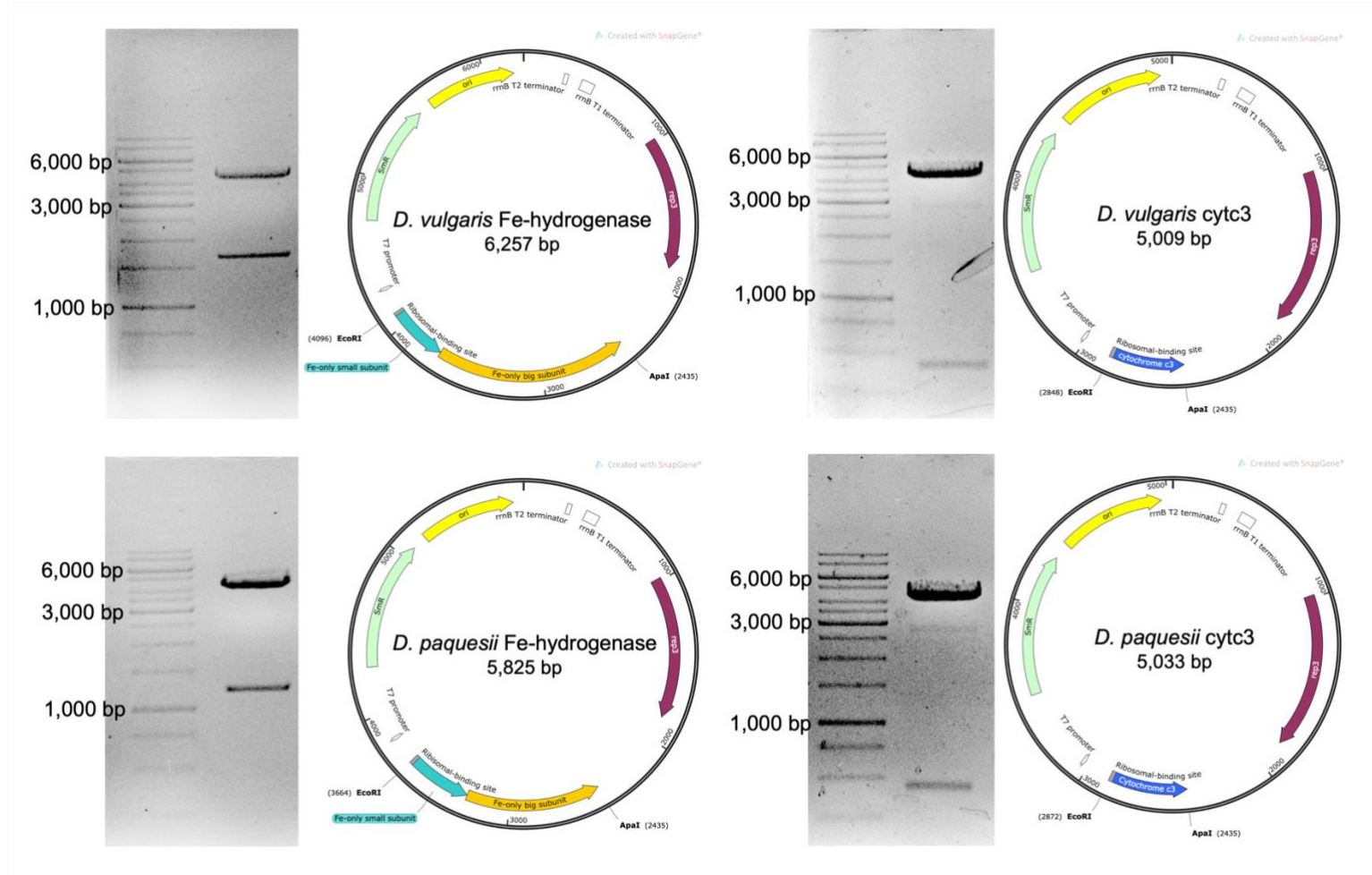


Figure 16. Vector constructions for the two *Desulfovibrio* spp. Fe-only hydrogenase gene (left) containing the two coding subunits (Big and small, marked in yellow and blue, respectively) and tetraheme cytochrome *c3* (right) for both *D. vulgaris* and *D. paquesii* are shown (top and bottom, respectively). Electrophoresis gels show the digested plasmids using *EcoRI* and *ApaI* enzymes as indicated in the plasmid map.

2.2. Protocol assessment to transform the two *Desulfovibrio* spp.

Black iron-sulphide (FeS) was used as an indicative of sulphate reduction and for evidence of bacterial growth. Optical density (OD) was only used before induction of cell competence and electroporation to ensure proper growth of the cells. Optical densities were measured containing and avoiding FeS that was removed by centrifugation (1,000 rpm and 5 min). Removal of FeS prevented the interference of the precipitates for OD measurements, even though cells embedded into them could not be accounted for.

Different transformation protocols were applied to increase the possibility of obtaining positive transformations ([Section 13](#) Material and Methods). Due to the lack of reliable protocols for *Desulfovibrio* with a sufficient tradition and success in transformation, adaptations from other methods used for anaerobic bacteria were also used. Published examples from *D. vulgaris*, *Clostridium* and *Geobacter* were used.

Clostridium-based protocols were optimized by members of the group of Prof. Dr. Miriam Rosenbaum (Molitor et al., 2016). *Geobacter*-based protocols were selected since they were based on a bacterium closely related to *Desulfovibrio*, and electroporation protocols for transformations were available (Coppi, et al., 2001). Modifications of the *Desulfovibrio vulgaris* protocol were made using the method initially described by Keller et al. as a starting point (Keller et al., 2011). The main parameters and conditions changed or modified in each experiment are provided in [Table 22](#). Up to 6 variations were tested in *D. paquesii* since it was the main strain of interest for our objective, and 3 variations were tested in *D. vulgaris* cells.

Different results were obtained for each protocol and strain and are detailed in [Table 23](#). No transformants of *D. paquesii* were observed in agar plates after 7 to 9 days of incubation at optimal conditions when using Molitor et al. (Molitor et al., 2016) and Coppi et al. (Coppi, et al., 2001) protocols ([Table 23](#); tests D-H). Otherwise, colonies were observed at the bottom of the plates when using Keller et al. protocol (Keller et al., 2011) with an initial volume of 9 mL independently on the other parameters used ([Table 23](#); tests C). Isolated colonies were selected and inoculated in new media. However, no growth was detected after several days of incubation on liquid medium at the recommended antibiotic concentration (100 mg·L⁻¹). An increased number of colonies (more than 200) were observed with higher initial culture volume (50 mL) mainly when containing FeS precipitate. A lower number of colonies (less than 50) were visible when FeS was removed before inducing competence into the cells. This should indicate either the presence of cells embedded in the FeS precipitates or a partially decreased effect of the antibiotic in the presence of precipitates. Little growth

was observed for the same transformations in liquid medium (with antibiotic). Colonies were selected from agar plates for all the conditions and were grown on tubes containing decreasing antibiotic concentrations (100, 75, 50, and 25 mg·L⁻¹, respectively). After more than 7 days of incubation, growth was detected in almost all tubes. Although selection pressure via antibiotic was induced, no plasmid was recovered from grown bacteria. Additionally, grown liquid cultures were plated in agar also containing the antibiotic concentrations stated before. Growth was only detected on plates containing 25 mg·L⁻¹ of antibiotic.

When utilizing cell cultures containing FeS precipitate or Tris-HCl wash buffer a visible spark (arc) was detected. This indicated that the mixture of cells and DNA was too conductive (with high ionic strength). Arcing is normally associated with the low efficiency of transformation protocol therefore, Keller and co-workers, indicated that arcing was not visible or at least reduced by reducing the utilized voltage (1,5 kV, 250 Ω and 25 μF) (Keller et al., 2011). Otherwise, in our case, since no transformants could be found in any case this correlation could not be confirmed. Both Keller et al. (Keller et al., 2011) and Molitor et al. (Molitor et al., 2016) protocols were tested with *D. vulgaris* as considered in [Table 22](#). Growth was detected on agar plates using *D. vulgaris* based protocol, independently of the removal or not of FeS precipitates, but the massive presence of FeS precipitates prevented the selection of colonies that could not be isolated and tested for the presence of plasmids. Growth was also observed in tubes, and these were used to streak agar plates with decreasing antibiotic concentrations as done for *D. paquesii*. Growth was detected in all plates, and colonies could be selected to further liquid culture growth. After more than 7 days, growth was observed and new inocula were done. Using the protocol described by Molitor et al. (Molitor et al., 2016), growth was observed in both agar plates and liquid cultures. Plasmid rescue and colony PCR were used to check the presence of the plasmid in *D. vulgaris*. Neither plasmid nor positive PCR amplification was obtained from any of the cultures.

Table 22. Changes on the main parameters of tested protocols to transform *D. paquesii* and *D. vulgaris* cells. Tests were named from A to H.

	Test name								
	A	B	C	D	E		F	G	H
Initial culture volume (mL)	9		50	9		50	10	50	
Presence of FeS precipitate	With and without		With and without	With and without		With	Without	Without	
Centrifugation	12,000 rcf, 12 min, and 4°C			4,000 rcf, 2 min, and 4°C		4,000 rcf, 2 min, and 4°C		4,300 rcf, 8 min, and 4°C	
Wash buffer	Tris-HCl buffer (pH 7.2)			10% glycerol (twice)		10% glycerol (twice)		1 mM HEPES, 1 mM MgCl ₂ and 175 mM sucrose buffer (pH 7.0)	
Final volume (μL)	50			200	50	50		25	
Plasmid	Empty pMO9075					pMO9075+cytochrome <i>c3</i> of <i>D. vulgaris</i>		Empty pMO9075	
Amount of plasmid (μg)	1	0.5	1	2	1		1	1	
Cuvette gap-size (mm)	1 and 2	1	1	2	1 and 2		1	1	
Electroporation parameters (kV, Ω, μF)	1.75 250 25	1.5 250 25	1.75 250 25	2.5 600 10	1.75 250 25	1.5 250 25	1.8 250 25	1.8 250 25	
Over-night incubation volume (mL)	2			5	2		5	1.5	
Reference	(Keller et al., 2011)			(Molitor, et al., 2016)				(Coppi, et al., 2001)	

Table 23. Summary of the results obtained for the different transformations performed with both *D. paquesii* and *D. vulgaris* cells.

Strain	Test name	Initial optical density (AU)		Pulse time (ms)	Colonies on plates	Growth on tubes	Growth after picking a colony	Tested antibiotic concentrations (mg·L ⁻¹)	Plasmid recovery
		With FeS	Without FeS						
<i>D. paquesii</i>	A	0.4 to 0.7	0.1 to 0.3	arc	✓	×	×	100	n.p.
	B	0.4 to 0.7	0.1 to 0.3	arc	✓	×	×	100	n.p.
	C	0.5 to 0.7	0.1 to 0.2	arc	✓	✓	✓	100, 75, 50 and 25	n.p.
	D	0.4 to 0.6	0.1 to 0.4	4.2 to 5.4	×	×	×	100	n.p.
	E	0.4 to 0.7	0.1 to 0.4	6.1 to 6.3	×	×	×	100	n.p.
	H	0.5 to 0.9	0.1 to 0.2	arc	×	×	×	100	n.p.
<i>D. vulgaris</i>	C	0.9	0.1 to 0.2	arc	✓	✓	✓	100, 75, 50 and 25	×
	F	0.7 to 0.9	0.1 to 0.4	4.0 to 5.4*	✓	✓	✓	100, 75, 50 and 25	×
	G	0.3 to 0.5	0.1 to 0.2	4.2 to 5.2*	✓	✓	✓	100, 75, 50 and 25	×
						100			
						Antibiotic concentration (mg·L ⁻¹)			

n.p. Not performed.

(*) pulse times were obtained only when FeS was removed.

2.3. Proposal for improvements and future perspectives

Research activities deserve moments of “deep desperation” which eventually shift to moments of “true hope” when new possibilities are envisioned. Most often, these possibilities come to the surface after a critical and intense analysis of previously obtained results, an action that fuels Science to go on. The efforts devoted to the transformation of *Desulfovibrio* spp. was one such moment. In this section, we critically analysed all data including new information for an effective shift towards hope. Unfortunately, in the moment of the presentation of this Ph.D. Thesis, none of the proposals could be tested effectively.

Several aspects will be considered to further optimize the transformation protocol for *D. vulgaris* and *D. paquesii*. These will include: (i) improvement of medium composition, (ii) enhancing the initial number of cells studying growth phases of the two strains, (iii) decreasing the amount of DNA, (iv) increasing selection pressure through optimal antibiotic concentrations, (v) test other electroporation parameters, (vi) use another mechanism for introducing foreign DNA like conjugation.

Optimization of the medium composition for convenient growth after transformation is an important step. High nutrient-rich media could provide appropriate electron donor(s) and acceptor(s) since mutants might have different nutritional requirements compared to original strains. Here, Postgate medium (DSM 63) was used even though, Keller and co-workers described a modification, named MOYLS4 medium, suitable for difficult experiments (Keller et al., 2011). Medium modifications affect the proportion of lactate: sulphate being higher (60:30) the one used by Keller and co-workers than the described in Postgate medium (Keller et al., 2011). Apart from ensuring the mutant requirements for growth, it is also helpful to have better control of the initial cell amount before inducing competence. Incorporation of data about optimal growth conditions and growth kinetics may lead to knowing exactly at which point the cultures are in a proper OD₆₀₀ described before to be between 0.4-0.7 AU (Keller et al., 2011). However, this value may be strain-dependent, and a systematic evaluation of best conditions (start of growth phase, middle exponential, or late exponential) would be interesting to consider. Therefore, optimized control of the cell growth might enhance the chances to introduce the foreign DNA into the competent cells having an increasing number of initial cells. OD₆₀₀ measurements could be improved utilizing the method described by Wood et al. (Wood et al., 2019). This methodology named acid-amended OD measurements was reported as more accurate and cost-efficient than traditional methods like plate counting or quantitative PCR. Briefly, the method achieves the

complete dissolution of FeS adding concentrated HCl into the growth culture samples not affecting culture turbidity (Wood et al., 2019).

Transformation efficiency is highly dependent on cell and DNA concentrations used for electroporation (Dower et al., 1988). Therefore, apart from controlling the number of cells through better comprehension of strains' growth, it could be also important to optimize the amount of DNA used for electroporation. Although 1 μg of DNA was described as suitable for SBR transformation, the same authors also pointed out the transformation efficiency was higher when using lower amounts of DNA (0.5-0.25 μg) (Keller et al., 2011).

No antibiotic resistance information could be found for *D. paquesii* after reviewing the literature. Otherwise, for *D. vulgaris* it was described that antibiotic G418 also known as geneticin (similar to gentamycin) at a concentration of 400 $\text{mg}\cdot\text{L}^{-1}$ is more effective for kanamycin resistance selection than kanamycin (Keller et al., 2011). Interestingly, for *D. desulfuricans* G20 higher amount of kanamycin and spectinomycin (800 $\text{mg}\cdot\text{L}^{-1}$) had been proposed as effective for transformant selection. Keller and co-workers described different concentrations to be used with *D. vulgaris* and *D. desulfuricans* G20 of the most common antibiotic (Keller et al., 2011). For this reason, antibiotic sensitivity studies might be necessary to determine antibiotic resistances (if any) in *D. paquesii*. Setting a sensitivity range could help to ensure the proper selection of transformants. Obtained results after transformation protocol with *D. paquesii* demonstrated that, since colonies and growth on tubes were visible, the strain is resistant to the concentration of spectinomycin used (100 $\text{mg}\cdot\text{L}^{-1}$). In the case of *D. vulgaris*, even the described spectinomycin concentration was used, no transformants could be detected but colonies were visible in plates, and growth was detected in liquid cultures (Table 23; test C).

Electroporation parameters tested using Keller et al. protocol (Keller et al., 2011) were described before as the optimal for this strain, and several studies were conducted successfully (Johns et al., 2016; Keller et al., 2009; Li et al., 2009; Rajeev et al., 2019; Ray et al., 2014; Zane et al., 2010). However, electroporation efficiency is directly impacted by the voltage drop across each bacterial cell. This considers the size of the cells together with the electric field strength (E) calculated as the proportion between the applied voltage (V) and the distance (in cm) between the electrodes (Sherba et al., 2020). For that reason, testing different voltages might increase the possibilities to achieve our objective and have a suitable protocol for *D. paquesii*. Alternatively, changing from electroporation to conjugation protocols might be a possibility to achieve our objective. Conjugation was the first technique

utilized to introduce foreign DNA into *D. vulgaris* Hildenborough and *D. desulfuricans* G20 (Stokkermans et al., 1992; Voordouw et al., 1990). Different approaches were performed to delete native genes in both *D. vulgaris* Hildenborough and *D. desulfuricans* G20 targeting [Fe]-only H₂ase and chemoreceptor protein A in the former and cytochrome *c3* in the latter (Fud & Voordouw, 1997; Rapp-Giles et al., 2000; Vandenberg et al., 1993). Also, cytochromes *c3* and *c553* from *D. vulgaris* Hildenborough were successfully expressed in *D. desulfuricans* G20 (Blanchard et al., 1993; Voordouw et al., 1990). Although cytochrome *c3* from *D. vulgaris* Hildenborough could be expressed and purified after conjugation in *D. desulfuricans* (Voordouw et al., 1990), it has to be considered that over-expression of [Fe]-H₂ase and cytochrome *c3* may result lethal for the transformant cells.

Overall, this chapter, although resembling a collection of parameters and procedures that led to undesirable results, helped us to set up a solid starting point to further optimizing a transformation protocol for *D. paquesii*. This is a necessary step to elucidate if some of the selected enzymes are directly involved in H₂ evolution during autotrophic growth in a BES. The achievement of this milestone may lead to test the engineered strain at a less reducing potential to avoid the coexistence of abiotically H₂ evolution and reduce the energy demands that are required to operate the BES at such high cathode potential.

GENERAL DISCUSSION

Hydrogen (H₂) as an electron donor plays an important role in microbial metabolism. The ability of bacteria and archaea to interconvert H₂ with the environment is among the most ancient traits in the evolution of microbial metabolism. Approximately, one-third of all known bacterial and archaeal genomes contain hydrogenases, a group of metalloenzymes that can reversibly convert H₂ into electrons and protons (Greening et al., 2016). H₂ is the key element for carbon assimilation during autotrophic growth, being utilized as energy (Schuchmann & Müller, 2014). H₂, as a cornerstone molecule in bacterial metabolism, is also a key element in microbial electrosynthesis and electro-fermentation (Puig et al., 2017). Electrochemical H₂ production in a BES is thermodynamically favoured at cathode potentials below -0.61 V *vs.* Ag/AgCl under standard conditions and neutral pH (Logan et al., 2008). Up to now, most studies conducted in BES have utilized higher negative potentials (from -0.7 to -1.1 V *vs.* Ag/AgCl) to ensure sufficient H₂ production for microorganism growth and maintenance. However, most of the situations do not show favourable conditions for the use of H₂ due to its low solubility in water and its high reactivity in the presence of oxidants. Being H₂ such an important element, this Ph.D. Thesis highlights (i) the importance of understanding deeply the EET mechanisms in biocathodes, (ii) how to enhance H₂ availability utilizing microbes as catalysts, and (iii) the application of synthetic biology to improve BES performance.

1. Understanding EET: a higher ambition race

Microbial electrosynthesis (MES) is considered an environmental-friendly platform to obtain high-energy-containing molecules as an alternative to fossil fuels (PrévotEAU et al., 2020; RabaeY & Rozendal, 2010). The potential of MES relies on the production of carbon-neutral commodity chemicals. (Bio)cathodes are the active core of the technology and unavoidably integrate inorganic surface and bacteria (or archaea) as an active unit. In the biocathode, an intimate contact between the conductive inorganic surface (solid electrode) and cells is mandatory for triggering the desired (bio)chemical reactions. It is essential to fully characterize the microbial community composition when utilizing non-defined mixed cultures (microbial communities left to evolve freely according to conditions) for a better comprehension of bacteria or archaea involved in such reactions.

The utilization of molecular techniques, such as massive parallel sequencing of 16S rRNA gene, are a very common and used technique to have an overview of relative abundances of

the main players in MES. Taxonomic composition and phylogenetic diversity are studied using the 16S rRNA marker, but no information of the community's functional abilities is revealed. Amplicon sequencing suffers from the limitations and bias of the PCR-based method (incomplete primer coverage and copy number differences between microorganisms) but, it is useful since extensive information is found on reference databases allowing identification of microorganisms at genus-level even at low abundances (Kennedy et al., 2014; Langille et al., 2013). The accurate identification of microorganisms at species and strain level could be performed using whole 16S rRNA gene sequencing (Johnson et al., 2019), although this may be a difficult task if complex communities (high richness) are present. Absolute abundances based on the 16S rRNA gene can be also determined using quantitative PCR (qPCR). qPCR is mainly used to estimate “gene” densities in each sample, but conversion into an exact number of cells is sometimes difficult given the variable number of copies of single-gene cells have in their genomes. Corrections of 16S rRNA abundance measured by qPCR could be done only if gene copy numbers of the taxa present in the samples are known (Jian et al., 2020), and this may be accomplished if a good genotypic knowledge of the cells present is available. Deeper analyses are performed using metagenomics since all genes from a community are sequenced (phylogenetic and functional) enabling the construction of metabolic and functional profiles (Langille et al., 2013; Laudadio et al., 2018). However, none of these techniques are suitable for the identification of microorganisms actively participating in a due process, or to gain insight into how they do it. The utilization of RNA as the target molecule can help to further understand the microbial community via 16S rRNA sequencing or metatranscriptomics. The former only provides information about the putatively active community while the latter can reveal expression profiles of selected genes at a given time and conditions, thus enabling the characterization of gene activity within the entire community (Ishii et al., 2015). Metatranscriptomics is pointed out as the most promising molecular technique to further understand how microorganisms are communicating with the electrode surface and to elucidate which EET mechanisms are involved (Ishii et al., 2018; 2015; Marshall et al., 2017).

In the first chapter of this Ph.D. Thesis ([Chapter 1](#)), we aimed at studying transient changes (short-time exposure to open/closed electric circuits) in the expression of genes coding for selected subunits of membrane-bound Eha and Ehb hydrogenases, cytoplasmic Hdr complex (Mvh, Hdr, and Frh), and hydrogenase maturation protein HypD, in naturally enriched cultures of methanogenic archaea conducting the reduction of CO₂ to methane (CH₄). Amplicon massive sequencing was used to characterize an electromethanogenic

community. Analysis revealed the presence of an enriched *Methanobacterium* sp. population (>70% of sequence reads) in the cathode biofilm, which remained in an active state (78% of cDNA reads), tagging this archaeon as the main methane producer in the system. Quantitative RT-PCR determinations of *ebaB*, *ebbL*, *mvhA*, *hdrA*, *frhA*, and *hupD* genes resulted in slight (up to 1.5-fold) changes for four out of six genes analysed when cells were exposed to open (disconnected) or closed (connected) electric circuit events. The results suggested that hydrogenase activity was not regulated at the transcriptional level in *Methanobacterium* sp. for short-time exposures (6 hours) of the cells to open/closed electric circuits. A similar approach has been recently performed in highly enriched biocathodes with *Methanobacterium* sp. strain 34x (Ragab, et al., 2020). In this study metagenomics and metatranscriptomics were used to analyse potential-induced changes (-1.0 and -0.7 V *vs.* Ag/AgCl) in the enriched electromethanogenic communities. At the transcriptional level, no significant differences were found in genes involved in methane production and carbon fixation metabolic pathways, supporting the results on our electromethanogenic systems. The analysis revealed that, although significant differences were not found, (Mcr) and Hdr complex were higher expressed in comparison to the other genes in the metabolic pathway. Especially, higher expression was detected for Mcr (implicated in the final step for CO₂ reduction into CH₄) decreasing over time exposure at -0.7 V compared to operation at -1.0 V explaining why CH₄ could not be detected after 90 min exposure to -0.7 V. In this sense, Ragab and co-workers pointed out that since Mcr isozyme MRI (*mcrABC*) had lower specific activity but higher H₂ affinity may be an indication of H₂-limiting conditions even under -1.0 V operation (Ragab et al., 2020). Similarly, the fact that expression levels of hydrogenases were only slightly changed in the experiment performed in this Ph.D. Thesis, we can conclude that using open or closed electric circuits in the short-term does not cause an effect on the H₂ availability in *Methanobacterium* cells. Recently, Rovira-Alsina et al. performed sequential ON-OFF cycles in a thermophilic BES producing acetate. Interestingly, the overall production was not diminished compared to an “always ON” situation, but slightly increased. Considering possible sources of H₂ in Rovira-Alsina’s work where a combination of pure electrochemical and bioelectrochemical activities, the positive effect of the ON-OFF cycling poses an interesting question on the potential sources of energy and reducing equivalents for the pure autotrophic electrosynthesis (Rovira-Alsina et al., 2021). Nevertheless, H₂ plays a key role in the metabolism of hydrogenotrophic methanogens, how is it generated, and more importantly how is it used in BES is an interesting open question. In most systems where biologically assisted H₂ production is relevant, a first electron-transfer

event has to take place. Our results indicate that reversible hydrogenases may not be participating in the process, at least in *Methanobacterium* as assayed in a transcriptomic approach. It is worth to mention that no direct measurements of activity at the molecular level were performed in our *Methanobacterium* enriched system, and we can speculate of hydrogenases not being a limiting factor in the process, thus not responding to the transient open and closed electric circuit experiment. Overall, more research is needed to further understand, at the biochemical level, EET mechanisms involved during electromethanogenesis with *Methanobacterium* sp. since the occurrence of direct and/or indirect ET mechanisms are not fully elucidated yet.

2. Hydrogen is the key element in microbial electrosynthesis

H₂ has been repeatedly reported as the principal intermediary molecule for the production of desirable chemicals from CO₂ and electricity during MES in both acetogenic and methanogenic microorganisms (Batlle-Vilanova et al., 2014; Jourdin et al., 2015; Puig et al., 2017). However, to what extent production of H₂ is a bottleneck step in BES performance has to be elucidated. We have worked with the hypothesis that an improvement in the performance of MES may require the integration of microbial catalysts able to evolve H₂ efficiently in close contact with the CO₂-transforming bacteria. Interestingly, bio-H₂ production in biocathodes has been described for some bacterial strains (*i.e.*, *Geobacter sulfurreducens*, *Rhodobacter capsulatus*, and *Desulfovibrio* spp.) utilizing potentials below -0.8 V *vs.* Ag/AgCl (Aulenta et al., 2012; Geelhoed & Stams, 2011; Puig et al., 2017; Yu et al., 2011). In these works different set-ups and conditions were used and comparisons of productions efficiency at the species level may be difficult. In the second chapter of this Ph.D. Thesis ([Chapter 2](#)), we developed a method for unifying conditions (despite slight changes in the medium composition) and set-ups to obtain a reliable comparison of the capacity of bioelectro-production.

An evaluation of ten different bacteria (including species of *Rhodobacter*, *Rhodopseudomonas*, *Rhodocyclus*, *Sporomusa*, and *Desulfovibrio*) as a first step in the development of a stable H₂-evolving platform for microbial electrosynthesis was presented. All used strains and isolates were previously proved as H₂ producers in BES by different authors. In this work, we tested all strains using an optimized and identical protocol based on the development of monospecific biofilms, thus facilitating comparisons among them. Cell densities measured by qPCR revealed that cells tended to attach to the electrode surface in BES reactors,

independently of their ability to produce H₂. In all tested strains, except *S. ovata* DSM 2662, hydrogen production rates increased compared to abiotic conditions. In four of them, *R. capsulatus* DSM 152, isolate C1S119.2, *D. desulfuricans* DSM 642, and *D. paquesii* DSM 16681, specific H₂ production rates were markedly higher but only on *Desulfovibrio* strains were sustained in the long-term. This fact, together with a higher stability of the biofilms of these two species, resulted in *D. desulfuricans* DSM 642 and *D. paquesii* DSM 16681 as the most promising candidates to evolve selective biologic H₂-producing cathodes. Despite differences in production rates, eight strains presented electroactivity according to cyclic voltammetry measurements and are considered as potential candidates for additional explorations of their performance in BES under changing conditions (*i.e.*, less reducing potential, production of other relevant chemical compounds, or forming defined co-cultures for other purposes). These results demonstrate that differences among the proposed strains occur in net H₂ production but, at the same time, they represent a significant step forward to further understand H₂-producing bacteria for consortia applications for MES or electro-fermentation.

During MES, C₂ compounds are the main product while C₃-C₆ compounds can be produced at small titers. This is a technological shortcoming in respect to the currently inexpensive C₂ compounds oversupplied by the chemical industry (Harnisch et al., 2015). The application of defined co-cultures (consortia) may address the problem. Rather than direct production of valuable products based on electrical current, defined co-cultures provide the opportunity to couple cathodic electron uptake, C-assimilation, and synthesis reactions separately (two-stage strategy) utilizing intermediary microorganisms for interspecies H₂ transfer or synthesis of initial building blocks (*i.e.*, formate or acetate). The partner microbes could use them to produce higher C-molecules, being more relevant industrially and economically. The production of such molecules is mandatory for MES to be further improved and moved to the industrial sector (PrévotEAU et al., 2020; Rosenbaum & Henrich, 2014). Particularly, an efficient and sustained H₂ production may lead to overcome mass transfer limitations between gas/liquid phases (Blanchet et al., 2015).

The spatial separation of the two (or more) species in the cathodic chamber is an interesting feature of using defined co-cultures for MES. Defined ecological niches in the reactor would be set up, separating the electron uptake reaction carried out by cells conforming a stable biofilm in the surface of the electrodes and, the biosynthesis step being performed by the cells remaining in suspension in the bulk of the reactor (Johns et al., 2016). Puig and co-workers pointed out that due to the higher abundance of homoacetogenic bacteria, such as

Clostridium sp., in the bulk liquid, strains may be directly involved in the autotrophic conversion of CO₂ to organics, whereas the main reaction proposed to take place in the biocathodes was H₂ production mediated by *Rhodobacter capsulatus* (Puig et al., 2017). Another feasible approach exploring this possibility was performed by Deutzmann and Spormann, defining consortium of Fe(0)-corroding strain IS4 (*Desulfopila corrodens* DSM 15630) with hydrogenotrophic methane-producer *Methanococcus maripaludis* or with the homoacetogen *Acetobacterium woodii*. The authors demonstrated that the strain IS4 conforming a monospecific biofilm in the electrode was able to evolve efficiently H₂ that was consumed by *M. maripaludis* or *A. woodii*. Moreover, they demonstrated an increase in the overall production rates of methane and acetate and a reduction of cathode potentials (more than 0.2 V) (Deutzmann & Spormann, 2017).

The advantages of using synthetic consortia are the control of the existing microbial members and the possible interaction occurring between them, normally being limited, traceable, and adjustable (Song et al., 2014). This approach serves to integrate diverse metabolic pathways not provided by a sole microorganism, enhancing the robustness of BES and increasing the product spectrum (Höffner & Barton, 2014). Furthermore, defined co-cultures offer the possibility to engineer each member introducing new and desirable features (non-natural reactions) or improving an existing function (Rosenbaum & Henrich, 2014; Song et al., 2014; Yang et al., 2015). Nevertheless, significant efforts are still to be implemented in order to obtain partners that result in stable, obligate, partnership and remain in the long run. The application synthetic biology methods to selected strains, may help in this process and is currently being proposed in many experimental projects.

3. Putting all elements together: The *Desulfovibrio* scenario

Controlling gene expression levels in microorganisms is attractive for many reasons, from understanding the gene function and regulation, to create more efficient organisms for many biotechnological areas. Recently, huge advances in synthetic biology have substantially improved our ability to program quickly and cheaply microbes to be used on large scale with greater control (Johns et al., 2016). Diverse applications can benefit from the ability of tuning the expression levels in a programmable way (Vigouroux & Bikard, 2020). Especially in the field of industrial and environmental biotechnology, genetic engineering may serve for the overproduction of a whole range of chemicals such as, synthesis feedstocks, chemicals, medicines, fuels, and remediation of waste products or toxins (Johns et al., 2016; Tian et al.,

2017). To this end, genome editing, and gene expression control are performed and can be crucial for the development of mature MES platforms. The applicability of genetic engineering in microbial electrocatalysts has to face the challenge of setting up new and appropriate tools, since well-established and versatile techniques optimized for model organisms such as *E. coli* or *Saccharomyces cerevisiae* may not be fully functional for non-model organisms (Rosenbaum & Henrich, 2014). Recently, the utilization of CRISPR/Cas platform as a suitable way to genetically modify bacteria has been taking the interest of the scientific community and has resulted in both successful and frustrating experiences. CRISPR (clustered regularly interspace short palindromic repeats) technology is considered a revolutionary methodology for genetic engineering which unprecedentedly facilitated strain engineering with high impact on industrial applications for gene knock-outs, editing, repression, or activation of genetic traits (Tian et al., 2017). Despite CRISPR has been proven straightforward for applications within eukaryotes, application of this methodology in bacteria seems to be more challenging (Fokum et al., 2019).

To develop a strategy towards increasing bio-H₂ production of two *Desulfovibrio* strains via genetic modification, was our target. The obtained results in [Chapter 2](#) made evident the promising role of *Desulfovibrio* strains, especially *D. paquesii* DSM 16681 as a sustainable bio-H₂ evolving platform. Therefore, the main purpose in [Chapter 3](#) was to improve H₂ evolution on *D. paquesii* cells by overexpressing genes putatively involved in this process (hydrogenases and cytochromes). [Fe]-only hydrogenase and tetraheme cytochrome *c*₃ were selected and four vectors were constructed containing these genes for the model strain *D. vulgaris* DSM 644 and *D. paquesii* DSM 16681. Up to eight different conditions based on described protocols for *D. vulgaris*, *Clostridium ljungdablii*, and *Geobacter sulfurreducens* were used in both *D. paquesii* and *D. vulgaris* towards inducing cell competence and transformation (electroporation). Unfortunately, no transformants were obtained in any of the conditions, indicating that further efforts are still needed. Although CRISPR/Cas application has been thought as a possible tool to be used, to our knowledge no implementation of the technology has been used for genetic engineering in *Desulfovibrio* strains representing an enormous challenge considering our objective. Therefore, optimization of culture (medium composition and culture growth control) and transformation conditions (initial cell amount, DNA concentration, and electroporation parameters) may focus the next step in this study.

Increasing the H₂ levels when utilizing very negative potentials for microbial electrosynthesis may sound like a not necessary step in BES research. However, having a resilient platform to sustain the production and availability over the time of H₂ is essential if working with

lower energy-demanding potentials is desired. The application of a defined co-culture, a resilient bio-H₂ production platform together with other microbial catalysts, especially those tuned to produce high-value chemicals, may contribute to further improve bioelectrochemical processes.

4. Outlook and future perspectives

MET-based platforms offer multiple functional possibilities (*i.e.*, bioproduction, bioremediation, wastewater treatment, biosensing) and their low environmental impact has been attracting the interest of the scientific community since they can be involved in the transition to a more sustainable world. The proposed strategies in this Ph.D. Thesis to enhance bioproduction and applicability of bioelectrochemical processes are mainly focused on microorganisms' roles during these processes, and how can they be improved. Our scientific contributions may pave the way for new and more optimal advances in METs. However, some of the shortcomings still to be addressed in MES, at both laboratory and technological scale, are:

- The mechanisms of communication at the molecular level between both cell-electrode and cell-cell.

Relevant cellular components and enzymatic functions related to electron uptake mechanisms remain unknown, being highly dependent on the microorganisms and on regulatory effects triggered by operational BES conditions. It seems clear that further efforts have to be done to increase the current knowledge and/or to elucidate how microorganisms communicate with conductive surfaces since interactions at the molecular level are still subject to basic studies.

- The limitation of biofilm growth and biocompatible electrodes.

Biofilm formation and electrode composition are co-dependent limiting factors affecting the performance of MES. In the recent years, optimization of MES performance have been achieved through surface modification of commercial electrode materials (*i.e.*, modified carbon cloth with chitosan, gold, or nickel among others) or purposely built ones (*i.e.*, graphene) increasing their biocompatibility and, with the addition of conductive or semi-conductive particles into the catholyte (*i.e.*, magnetite). Biocompatibility, high porosity, and surface area enabling bacterial adherence and biofilm formation along with conductivity are the main characteristics to be considered for electrodes. Therefore, the recent advances in additive manufacturing technologies (3D-printing) might be a new opportunity for MES applicability and scaling-up.

- The relatively short product spectrum, production rate and selectivity focused on the production of low-economical value compounds (C2 molecules).

Up to now, acetate is the main product achieved through MES with higher selectivity (more than 90%) and at higher rates than other chemicals ($>100 \text{ g}\cdot\text{m}^{-2}\cdot\text{day}^{-1}$). But the economic viability of its production in MES is limited by its low market value (Dessi et al., 2021). Improvements, in this sense, are limited by the amount of electricity required for the generation of larger carbon products subject to the highly-energy demanding metabolic pathways (reductive carbon fixation pathways) used by microorganisms for the *de novo* formation of C-C bonds (Jourdin et al., 2020; Tremblay & Zhang, 2015). However, as highlighted in this PhD. Thesis, application of genetically engineered microorganisms to target specific added-value carbon products and/or integration of defined consortia for MES have great potential for its near-future applications. Also, coupling MES with other existing technologies as a multi-step bioconversion approach might be a feasible solution to integrate electrochemical technologies in the industry.

- The applicability of new and promising tools such as synthetic biology or defined consortia.

Benefits of genetic engineering microorganism, as well as co-culturing, are subject to further and intense research related to several of the points presented since now, but they still have high applicability potential. Insufficient knowledge on the fundamental mechanisms that rule MES together with the lack of accessible and efficient molecular toolkits and experimental protocols enabling genetic modification in any microorganism of interest are limiting the application of genetic engineering approaches in electricity-driven metabolic pathways. On the other hand, co-culturing requires further knowledge on specific interactions occurring between the consortia members prior to its application in BES that, at the same time, are limited if insufficient information is known about the individual populations.

CONCLUDING REMARKS

This Ph.D. Thesis contributed improving the knowledge on H₂-mediated events during microbial electrosynthesis. Special attention was given to microbial physiology and genetics to understand how bioelectrochemical processes could be improved.

Specific conclusions drawn in this Ph.D. Thesis are:

1. *Methanobacterium* spp. were the main biocatalysts in mesophilic electromethanogenic reactor.

The electromethanogenic microbial community (DNA-based analysis), and the portion remaining in active state (cDNA-based analysis), were highly enriched in a single *Methanobacterium* spp. sequence variant (>70%) and were directly involved in methane production. Archaea served as model microorganisms to study if the expression of [NiFe]-hydrogenases was affected by cathode connection and could be directly involved in electron transfer events.

2. Selected [NiFe]-hydrogenases (*chaB*, *ehbL*, *mvhA*, *hdrA*, *frhA*, and *hypD*) were constitutively expressed.

No significant differences in expression levels were found for those enzymes comparing closed *vs.* open electric circuits. Suspected mechanisms for direct electron transfer in *Methanobacterium* based on reversible hydrogenases could not be assessed at the transcriptional level.

3. Electroactivity and the ability to increase biotic production of H₂ seems to be a common trait for anaerobes.

Eight out of the ten bacterial strains tested were able to increase biotically hydrogen evolution in cathodes and showed some electroactivity considering cyclic voltammetry results. Only *Rhodobacter capsulatus* DSM 152, isolate C1S119.2, *Desulfovibrio desulfuricans* DSM 642 and *Desulfovibrio paquesii* DSM 16681 showed specific hydrogen production rates markedly higher compared to pure electrochemical.

4. *Desulfovibrio* spp. were the most interesting strains for a sustained biohydrogen production over time in biocathodes.

Desulfovibrio desulfuricans DSM 642 and *Desulfovibrio paquesii* DSM 16681 presented the higher net H₂ production rates in comparison with abiotic conditions. *D. paquesii* DSM 16681 could feasibly evolve H₂ at a less reducing potential (-0.8 V *vs.* Ag/AgCl), being the most promising candidate to be further studied. Even though, specific rates

(per unit biomass) were comparable among strains suggesting higher productivities could be due to differences in the biofilm formation.

5. Improvements are still needed to establish a reliable protocol for genetic modification of *Desulfovibrio*.

Tested conditions towards genetic modification of *Desulfovibrio paquesii* DSM 16681 and *Desulfovibrio vulgaris* DSM 644 through chemical competence and transformation via electroporation resulted not suitable to introduce foreign DNA.

6. Acquired knowledge in this Ph.D. Thesis will contribute to new and promising experimental approaches in microbial electrosynthesis.

The application of defined co-cultures and genetically modified organisms in BES are expected to be explored in the near future. Application of novel synthetic biology approaches and exploitation of structured (compartmentalized) reactors are needed as a step forward in future BES development towards a competitive technology.

- Acinas, S. G., Marcelino, L. A., Klepac-Ceraj, V., & Polz, M. F. (2004). Divergence and Redundancy of 16S rRNA Sequences in Genomes with Multiple *rrn* Operons. *Journal of Bacteriology*, *186*(9), 2629–2635. <https://doi.org/10.1128/JB.186.9.2629-2635.2004>
- Agostino, V., & Rosenbaum, M. A. (2018). Sulfate-reducing electroautotrophs and their applications in bioelectrochemical systems. *Frontiers in Energy Research*. <https://doi.org/10.3389/fenrg.2018.00055>
- Aryal, N., Tremblay, P. L., Lizak, D. M., & Zhang, T. (2017). Performance of different *Sporomusa* species for the microbial electrosynthesis of acetate from carbon dioxide. *Bioresource Technology*, *233*, 184–190. <https://doi.org/10.1016/j.biortech.2017.02.128>
- Aulenta, F., Catapano, L., Snip, L., Villano, M., & Majone, M. (2012). Linking bacterial metabolism to graphite cathodes: electrochemical insights into the H₂-producing capability of *Desulfovibrio* sp. *ChemSusChem*, *5*(6), 1080–1085. <https://doi.org/10.1002/cssc.201100720>
- Bajracharya, S., Ter Heijne, A., Dominguez Benetton, X., Vanbroekhoven, K., Buisman, C. J. N., Strik, D. P. B. T. B., & Pant, D. (2015). Carbon dioxide reduction by mixed and pure cultures in microbial electrosynthesis using an assembly of graphite felt and stainless steel as a cathode. *Bioresource Technology*, *195*, 14–24. <https://doi.org/10.1016/j.biortech.2015.05.081>
- Battle-Vilanova, P., Ganigué, R., Ramió-Pujol, S., Bañeras, L., Jiménez, G., Hidalgo, M., Balaguer, M.D., Colprim, J., Puig, S. (2017). Microbial electrosynthesis of butyrate from carbon dioxide: Production and extraction. *Bioelectrochemistry*, *117*, 57–64. <https://doi.org/10.1016/j.bioelechem.2017.06.004>
- Battle-Vilanova, P., Puig, S., Gonzalez-Olmos, R., Balaguer, M. D., & Colprim, J. (2016). Continuous acetate production through microbial electrosynthesis from CO₂ with microbial mixed culture. *Journal of Chemical Technology & Biotechnology*, *91*(4), 921–927. <https://doi.org/10.1002/jctb.4657>
- Battle-Vilanova, P., Puig, S., Gonzalez-Olmos, R., Vilajeliu-Pons, A., Balaguer, M. D., & Colprim, J. (2015). Deciphering the electron transfer mechanisms for biogas upgrading to biomethane within a mixed culture biocathode. *RSC Advances*, *5*(64), 52243–52251. <https://doi.org/10.1039/C5RA09039C>
- Battle-Vilanova, P., Puig, S., Gonzalez-Olmos, R., Vilajeliu-Pons, A., Bañeras, L., Balaguer, M. D., & Colprim, J. (2014). Assessment of biotic and abiotic graphite cathodes for hydrogen production in microbial electrolysis cells. *International Journal of Hydrogen Energy*, *39*(3), 1297–1305. <https://doi.org/10.1016/j.ijhydene.2013.11.017>
- Beese-Vasbender, P. F., Nayak, S., Erbe, A., Stratmann, M., & Mayrhofer, K. J. J. (2015).

REFERENCES

- Electrochemical characterization of direct electron uptake in electrical microbially influenced corrosion of iron by the lithoautotrophic SRB *Desulfopila corrodens* strain IS4. *Electrochimica Acta*, 167, 321–329. <https://doi.org/10.1016/j.electacta.2015.03.184>
- Beimgraben, C., Gutekunst, K., Opitz, F., & Appel, J. (2014). HypD as a marker for [NiFe]-hydrogenases in microbial communities of surface waters. *Applied and Environmental Microbiology*, 80(12), 3776–3782. <https://doi.org/10.1128/AEM.00690-14>
- Bender, K. S., Yen, H. C. B., Hemme, C. L., Yang, Z., He, Z., He, Q., Zhou, J., Huang, K.H., Alm, E.J., Hazen, T.C., Arkin A.P., Wall, J. D. (2007). Analysis of a ferric uptake regulator (Fur) mutant of *Desulfovibrio vulgaris* Hildenborough. *Applied and Environmental Microbiology*, 73(17), 5389–5400. <https://doi.org/10.1128/AEM.00276-07>
- Berg, G., Rybakova, D., Fischer, D., Cernava, T., Vergès, M. C. C., Charles, T., ... Schloter, M. (2020). Microbiome definition re-visited: old concepts and new challenges. *Microbiome*, 8(1), 1–22. <https://doi.org/10.1186/s40168-020-00875-0>
- Blanchard, L., Marion, D., Pollock, B., Voordouw, G., Wall, J., Bruschi, M., & Guerlesquin, F. (1993). Overexpression of *Desulfovibrio vulgaris* Hildenborough cytochrome c553 in *Desulfovibrio desulfuricans* G200: Evidence of conformational heterogeneity in the oxidized protein by NMR. *European Journal of Biochemistry*, 218(2), 293–301. <https://doi.org/10.1111/j.1432-1033.1993.tb18377.x>
- Blanchet, E., Duquenne, F., Rafrafi, Y., Etcheverry, L., Erable, B., & Bergel, A. (2015). Importance of the hydrogen route in up-scaling electrosynthesis for microbial CO₂ reduction. *Energy & Environmental Science*, 8(12), 3731–3744. <https://doi.org/10.1039/C5EE03088A>
- Blasco-Gómez, R., Batlle-Vilanova, P., Villano, M., Balaguer, M., Colprim, J., & Puig, S. (2017). On the Edge of Research and Technological Application: A Critical Review of Electromethanogenesis. *International Journal of Molecular Sciences*, 18(4), 874. <https://doi.org/10.3390/ijms18040874>
- Blasco-Gómez, R., Ramió-Pujol, S., Bañeras, L., Colprim, J., Balaguer, M. D., Puig, S. (2019). Unravelling the factors that influence the bio-electrorecycling of carbon dioxide towards biofuels. *Green Chemistry*, 21(3), 684–691. <https://doi.org/10.1039/c8gc03417f>
- Bose, A., Gardel, E. J., Vidoudez, C., Parra, E. A., & Girguis, P. R. (2014). Electron uptake by iron-oxidizing phototrophic bacteria. *Nature Communications*, 5, 3391. <https://doi.org/10.1038/ncomms4391>
- Botheju, D. (2011). Oxygen Effects in Anaerobic Digestion – A Review. *The Open Waste Management Journal*, 4(1), 1–19. <https://doi.org/10.2174/1876400201104010001>

REFERENCES

- Caffrey, S. M., Park, H. S., Voordouw, J. K., He, Z., Zhou, J., & Voordouw, G. (2007). Function of periplasmic hydrogenases in the sulfate-reducing bacterium *Desulfovibrio vulgaris* hildenborough. *Journal of Bacteriology*, *189*(17), 6159–6167. <https://doi.org/10.1128/JB.00747-07>
- Call, D., & Logan, B. E. (2008). Hydrogen production in a single chamber microbial electrolysis cell lacking a membrane. *Environmental Science and Technology*, *42*(9), 3401–3406. <https://doi.org/10.1021/es8001822>
- Caporaso, J. G., Bittinger, K., Bushman, F. D., DeSantis, T. Z., Andersen, G. L., & Knight, R. (2010). PyNAST: a flexible tool for aligning sequences to a template alignment. *Bioinformatics (Oxford, England)*, *26*(2), 266–267. <https://doi.org/10.1093/bioinformatics/btp636>
- Carlozzi, P., & Lambardi, M. (2009). Fed-batch operation for bio-H₂ production by *Rhodospseudomonas palustris* (strain 42OL). *Renewable Energy*, *34*(12), 2577–2584. <https://doi.org/10.1016/j.renene.2009.04.016>
- Cheng, S., Xing, D., Call, D. F., & Logan, B. E. (2009). Direct Biological Conversion of Electrical Current into Methane by Electromethanogenesis. *Environmental Science & Technology*, *43*(10), 3953–3958. <https://doi.org/10.1021/es803531g>
- Choi, O., & Sang, B.-I. B. I. (2016). Extracellular electron transfer from cathode to microbes: Application for biofuel production. *Biotechnology for Biofuels*, *9*(1), 1–14. <https://doi.org/10.1186/s13068-016-0426-0>
- Clauwaert, P., Aelterman, P., Pham, T. H., De Schampelaire, L., Carballa, M., Rabaey, K., & Verstraete, W. (2008, July). Minimizing losses in bio-electrochemical systems: The road to applications. *Applied Microbiology and Biotechnology*. <https://doi.org/10.1007/s00253-008-1522-2>
- Coppi, M. V., Leang, C., Sandler, S. J., & Lovley, D. R. (2001). Development of a Genetic System for *Geobacter sulfurreducens*. *Applied and Environmental Microbiology*, *67*(7), 3180–3187. <https://doi.org/10.1128/AEM.67.7.3180-3187.2001>
- Cordas, C. M., Moura, I., & Moura, J. J. G. (2008). Direct electrochemical study of the multiple redox centers of hydrogenase from *Desulfovibrio gigas*. *Bioelectrochemistry*, *74*(1), 83–89. <https://doi.org/10.1016/j.bioelechem.2008.04.019>
- Costa, K. C., Lie, T. J., & Jacobs, M. A. (2013). H₂ independent growth *Methanococcus maripaludis*. *Microbiology*, *4*(2), 1–7. <https://doi.org/10.1128/mBio.00062-13>.Editor
- Croese, E., Pereira, M. A., Euverink, G.-J. J. W. J. W., Stams, A. J. M. M., & Geelhoed, J. S. (2011). Analysis of the microbial community of the biocathode of a hydrogen-producing microbial electrolysis cell. *Applied Microbiology and Biotechnology*, *92*(5), 1083–1093. <https://doi.org/10.1007/s00253-011-3583-x>

REFERENCES

- Deng, X., Dohmae, N., Neilson, K. H., Hashimoto, K., & Okamoto, A. (2018). Multi-heme cytochromes provide a pathway for survival in energy-limited environments. *Science Advances*, 4(2), 1–9. <https://doi.org/10.1126/sciadv.aao5682>
- Dessi, P., Rovira-Alsina, L., Sánchez, C., Dinesh, G. K., Tong, W., Chatterjee, P., Tedesco, M., Farràs, P., Hamelers, H.M.V., Puig, S. (2021). Microbial electrosynthesis: Towards sustainable biorefineries for production of green chemicals from CO₂ emissions. *Biotechnology Advances*. <https://doi.org/10.1016/j.biotechadv.2020.107675>
- Deutzmann, J. S., Sahin, M., & Spormann, A. M. (2015). Extracellular enzymes facilitate electron uptake in biocorrosion and bioelectrosynthesis. *MBio*, 6(2), 1–8. <https://doi.org/10.1128/mBio.00496-15>
- Deutzmann, J. S., & Spormann, A. M. (2017). Enhanced microbial electrosynthesis by using defined co-cultures. *ISME Journal*, 11(3), 704–714. <https://doi.org/10.1038/ismej.2016.149>
- Dolfing, J. (2014). Syntrophy in microbial fuel cells. *ISME Journal*, 8(1), 4–5. <https://doi.org/10.1038/ismej.2013.198>
- Dower, W. ., Miller, J. ., & Ragsdale, C. W. (1988). High efficiency transformation of *E. coli* by high voltage electroporation. *Nucleic Acids Research*, 16(13), 6127–6145. <https://doi.org/10.1093/nar/16.13.6127>
- Dubé, C.-D., & Guiot, S. R. (2015). Direct Interspecies Electron Transfer in Anaerobic Digestion: A Review. In *Biogas Science and Technology* (pp. 101–115). https://doi.org/10.1007/978-3-319-21993-6_4
- Edgar, R. C. (2010). Search and clustering orders of magnitude faster than BLAST. *Bioinformatics*, 26(19), 2460–2461. <https://doi.org/10.1093/bioinformatics/btq461>
- Edgar, R. C., & Flyvbjerg, H. (2015). Error filtering, pair assembly and error correction for next-generation sequencing reads. *Bioinformatics (Oxford, England)*, 31(21), 3476–3482. <https://doi.org/10.1093/bioinformatics/btv401>
- Ergal, Í., Fuchs, W., Hasibar, B., Thallinger, B., Bochmann, G., & Rittmann, S. K. M. R. (2018). The physiology and biotechnology of dark fermentative biohydrogen production. *Biotechnology Advances*, 36(8), 2165–2186. <https://doi.org/10.1016/j.biotechadv.2018.10.005>
- Escapa, A., Mateos, R., Martínez, E. J., & Blanes, J. (2016). Microbial electrolysis cells: An emerging technology for wastewater treatment and energy recovery. from laboratory to pilot plant and beyond. *Renewable and Sustainable Energy Reviews*, 55, 942–956. <https://doi.org/10.1016/j.rser.2015.11.029>
- Faraghiparapari, N., & Zengler, K. (2017). Production of organics from CO₂ by microbial

REFERENCES

- electrosynthesis (MES) at high temperature. *Journal of Chemical Technology and Biotechnology*, *92*(2), 375–381. <https://doi.org/10.1002/jctb.5015>
- Fokum, E., Zabed, H. M., Guo, Q., Yun, J., Yang, M., Pang, H., An, Y., li, W., Qi, X. (2019). Metabolic engineering of bacterial strains using CRISPR/Cas9 systems for biosynthesis of value-added products. *Food Bioscience*, *28*(December 2018), 125–132. <https://doi.org/10.1016/j.fbio.2019.01.003>
- Fourmond, V. (2016). QSoas: A Versatile Software for Data Analysis. *Analytical Chemistry*, *88*(10), 5050–5052. <https://doi.org/10.1021/acs.analchem.6b00224>
- Fud, R., & Voordouw, G. (1997). Targeted gene-replacement mutagenesis of *dcrA*, encoding an oxygen sensor of the sulfate-reducing bacterium *Desulfovibrio vulgaris* Hildenborough. *Microbiology*, *143*(6), 1815–1826. <https://doi.org/10.1099/00221287-143-6-1815>
- Ganigué, R., Puig, S., Batlle-Vilanova, P., Balaguer, M. D., & Colprim, J. (2015). Microbial electrosynthesis of butyrate from carbon dioxide. *Chem. Commun. Chem. Commun*, *51*(51), 3235–3238. <https://doi.org/10.1039/c4cc10121a>
- Gebicki, J., Modigell, M., Schumacher, M., Van Der Burg, J., & Roebroek, E. (2010). Comparison of two reactor concepts for anoxygenic H₂ production by *Rhodobacter capsulatus*. *Journal of Cleaner Production*, *18*(SUPPL. 1). <https://doi.org/10.1016/j.jclepro.2010.05.023>
- Geelhoed, J. S., & Stams, A. J. M. (2011). Electricity-assisted biological hydrogen production from acetate by *Geobacter sulfurreducens*. *Environmental Science & Technology*, *45*(2), 815–820. <https://doi.org/10.1021/es102842p>
- Goers, L., Freemont, P., & Polizzi, K. M. (2014). Co-culture systems and technologies: taking synthetic biology to the next level. *Journal of The Royal Society Interface*, *11*(96), 20140065. <https://doi.org/10.1098/rsif.2014.0065>
- Greening, C., Biswas, A., Carere, C. R., Jackson, C. J., Taylor, M. C., Stott, M. B., Cook, G.M., Morales, S. E. (2016). Genomic and metagenomic surveys of hydrogenase distribution indicate H₂ is a widely utilised energy source for microbial growth and survival. *ISME Journal*, *10*(3), 761–777. <https://doi.org/10.1038/ismej.2015.153>
- Guiral-Brugna, M., Giudici-Ortoni, M.-T., Bruschi, M., & Bianco, P. (2001). Electrocatalysis of the hydrogen production by [Fe] hydrogenase from *Desulfovibrio vulgaris* Hildenborough. *Journal of Electroanalytical Chemistry*, *510*(1–2), 136–143. [https://doi.org/10.1016/S0022-0728\(01\)00502-2](https://doi.org/10.1016/S0022-0728(01)00502-2)
- Gupta, D., Guzman, M. S., & Bose, A. (2020). Extracellular electron uptake by autotrophic microbes: physiological, ecological, and evolutionary implications. *Journal of Industrial Microbiology and Biotechnology*, *47*(9–10), 863–876. <https://doi.org/10.1007/s10295-020-02309-0>

REFERENCES

- Guzman, M. S., Rengasamy, K., Binkley, M. M., Jones, C., Ranaivoarisoa, T. O., Singh, R., Fike, D.A., Meacham, J.M., Bose, A. (2019). Phototrophic extracellular electron uptake is linked to carbon dioxide fixation in the bacterium *Rhodospseudomonas palustris*. *Nature Communications*, 10(1). <https://doi.org/10.1038/s41467-019-09377-6>
- Harnisch, F., & Freguia, S. (2012, March 5). A basic tutorial on cyclic voltammetry for the investigation of electroactive microbial biofilms. *Chemistry - An Asian Journal*. <https://doi.org/10.1002/asia.201100740>
- Harnisch, F., Rosa, L. F. M., Kracke, F., Viridis, B., & Krömer, J. O. (2015). Electrifying white biotechnology: Engineering and economic potential of electricity-driven bio-production. *ChemSusChem*, 8(5), 758–766. <https://doi.org/10.1002/cssc.201402736>
- Heidelberg, J. F., Seshadri, R., Haveman, S. A., Hemme, C. L., Paulsen, I. T., Kolonay, J. F., ... Fraser, C. M. (2004). The genome sequence of the anaerobic, sulfate-reducing bacterium *Desulfovibrio vulgaris* Hildenborough. *Nature Biotechnology*, 22(5), 554–559. <https://doi.org/10.1038/nbt959>
- Hendrickson, E. L., Haydock, A. K., Moore, B. C., Whitman, W. B., & Leigh, J. A. (2007). Functionally distinct genes regulated by hydrogen limitation and growth rate in methanogenic Archaea. *Proceedings of the National Academy of Sciences*, 104(21), 8930–8934. <https://doi.org/10.1073/pnas.0701157104>
- Höffner, K., & Barton, P. I. (2014). Design of Microbial Consortia for Industrial Biotechnology. In *Computer Aided Chemical Engineering* (Vol. 34, pp. 65–74). Elsevier. <https://doi.org/10.1016/B978-0-444-63433-7.50008-0>
- Ishii, Shun'ichi, Suzuki, S., Norden-Krichmar, T. M., Tenney, A., Chain, P. S. G., Scholz, M. B., ... Bretschger, O. (2013). A novel metatranscriptomic approach to identify gene expression dynamics during extracellular electron transfer. *Nature Communications*, 4(1), 1601. <https://doi.org/10.1038/ncomms2615>
- Ishii, Shun'ichi, Suzuki, S., Tenney, A., Nealson, K. H., & Bretschger, O. (2018). Comparative metatranscriptomics reveals extracellular electron transfer pathways conferring microbial adaptivity to surface redox potential changes. *ISME Journal*. <https://doi.org/10.1038/s41396-018-0238-2>
- Ishii, Shun'ichi, Suzuki, S., Tenney, A., Norden-Krichmar, T. M., Nealson, K. H., & Bretschger, O. (2015). Microbial metabolic networks in a complex electrogenic biofilm recovered from a stimulus-induced metatranscriptomics approach. *Scientific Reports*, 5(1), 14840. <https://doi.org/10.1038/srep14840>
- Jian, C., Luukkonen, P., Yki-Järvinen, H., Salonen, A., & Korpela, K. (2020). Quantitative PCR provides a simple and accessible method for quantitative microbiota profiling. *PLoS ONE*,

REFERENCES

- 15(1), 1–10. <https://doi.org/10.1371/journal.pone.0227285>
- Johns, N. I., Blazjewski, T., Gomes, A. L. L. C., & Wang, H. H. (2016). Principles for designing synthetic microbial communities. *Current Opinion in Microbiology*, 31(31), 146–153. <https://doi.org/10.1016/j.mib.2016.03.010>
- Johnson, J. S., Spakowicz, D. J., Hong, B. Y., Petersen, L. M., Demkowicz, P., Chen, L., ... Weinstock, G. M. (2019). Evaluation of 16S rRNA gene sequencing for species and strain-level microbiome analysis. *Nature Communications*, 10(1), 1–11. <https://doi.org/10.1038/s41467-019-13036-1>
- Jourdin, L., Freguia, S., Donose, B. C., & Keller, J. (2015). Autotrophic hydrogen-producing biofilm growth sustained by a cathode as the sole electron and energy source. *Bioelectrochemistry*, 102, 56–63. <https://doi.org/10.1016/j.bioelechem.2014.12.001>
- Jourdin, L., Grieger, T., Monetti, J., Flexer, V., Freguia, S., Lu, Y., Chen, J., Romano, M., Wallace, G.G. & Keller, J. (2015). High Acetic Acid Production Rate Obtained by Microbial Electrosynthesis from Carbon Dioxide. *Environmental Science and Technology*, 49(22), 13566–13574. <https://doi.org/10.1021/acs.est.5b03821>
- Jourdin, L., Sousa, J., Stralen, N. van, & Strik, D. P. B. T. B. (2020). Techno-economic assessment of microbial electrosynthesis from CO₂ and/or organics: An interdisciplinary roadmap towards future research and application. *Applied Energy*. <https://doi.org/10.1016/j.apenergy.2020.115775>
- Kaster, A.-K., Goenrich, M., Seedorf, H., Liesegang, H., Wollherr, A., Gottschalk, G., & Thauer, R. K. (2011). More Than 200 Genes Required for Methane Formation from H₂ and CO₂ and Energy Conservation Are Present in *Methanothermobacter marburgensis* and *Methanothermobacter thermautotrophicus*. *Archaea*, 2011(1), 1–23. <https://doi.org/10.1155/2011/973848>
- Kato, S., Hashimoto, K., & Watanabe, K. (2012). Methanogenesis facilitated by electric syntrophy via (semi)conductive iron-oxide minerals. *Environmental Microbiology*, 14(7), 1646–1654. <https://doi.org/10.1111/j.1462-2920.2011.02611.x>
- Keller, K. L., Bender, K. S., & Wall, J. D. (2009). Development of a markerless genetic exchange system for *Desulfovibrio vulgaris* Hildenborough and its use in generating a strain with increased transformation efficiency. *Applied and Environmental Microbiology*, 75(24), 7682–7691. <https://doi.org/10.1128/AEM.01839-09>
- Keller, K. L., Wall, J. D., & Chhabra, S. (2011). Methods for Engineering Sulfate Reducing Bacteria of the Genus *Desulfovibrio*. In *Synthetic Biology* (1st ed., Vol. 497, pp. 503–517). Elsevier Inc. <https://doi.org/10.1016/B978-0-12-385075-1.00022-6>

REFERENCES

- Kennedy, K., Hall, M. W., Lynch, M. D. J., Moreno-Hagelsieb, G., & Neufeld, J. D. (2014). Evaluating bias of Illumina-based bacterial 16S rRNA gene profiles. *Applied and Environmental Microbiology*, *80*(18), 5717–5722. <https://doi.org/10.1128/AEM.01451-14>
- Kim, M.-S., Kim, D.-H., Cha, J., & Lee, J. K. (2012). Effect of carbon and nitrogen sources on photo-fermentative H₂ production associated with nitrogenase, uptake hydrogenase activity, and PHB accumulation in *Rhodobacter sphaeroides* KD131. *Bioresource Technology*, *116*, 179–183. <https://doi.org/10.1016/j.biortech.2012.04.011>
- Koch, C., & Harnisch, F. (2016). Is there a Specific Ecological Niche for Electroactive Microorganisms? *ChemElectroChem*. <https://doi.org/10.1002/celec.201600079>
- Koku, H., Erolu, I., Gunduz, U., Yucel, M., & Turker, L. (2002). Aspect of the metabolism of hydrogen production by *Rhodobacter sphaeroides*. *Int J Hydrogen Energy*, *27*, 1315–1329. [https://doi.org/10.1016/S0360-3199\(02\)00127-1](https://doi.org/10.1016/S0360-3199(02)00127-1)
- Kotelnikova, S., Macraio, A. J. L., & Pedersen, K. (1998). *Methanobacterium subterraneum* sp. nov., a new alkaliphilic, eurythermic and halotolerant methanogen isolated from deep granitic groundwater. *International Journal of Systematic Bacteriology*, *48*, 357–367.
- Kozich, J. J., Westcott, S. L., Baxter, N. T., Highlander, S. K., & Schloss, P. D. (2013). Development of a dual-index sequencing strategy and curation pipeline for analyzing amplicon sequence data on the miseq illumina sequencing platform. *Applied and Environmental Microbiology*, *79*(17), 5112–5120. <https://doi.org/10.1128/AEM.01043-13>
- Kracke, F., Vassilev, I., & Krömer, J. O. (2015). Microbial electron transport and energy conservation - The foundation for optimizing bioelectrochemical systems. *Frontiers in Microbiology*, *6*(JUN), 1–18. <https://doi.org/10.3389/fmicb.2015.00575>
- Kracke, F., Wong, A. B., Maegaard, K., Deutzmann, J. S., Hubert, M. A., Hahn, C., Jaramillo, T.F. & Spormann, A. M. (2019). Robust and biocompatible catalysts for efficient hydrogen-driven microbial electrosynthesis. *Communications Chemistry*, *2*(1), 45. <https://doi.org/10.1038/s42004-019-0145-0>
- Kundu, A., Sahu, J. N., Redzwan, G., & Hashim, M. A. (2013). An overview of cathode material and catalysts suitable for generating hydrogen in microbial electrolysis cell. *International Journal of Hydrogen Energy*, *38*(4), 1745–1757. <https://doi.org/10.1016/j.ijhydene.2012.11.031>
- LaBarge, N., Yilmazel, Y. D., Hong, P. Y., & Logan, B. E. (2017). Effect of pre-acclimation of granular activated carbon on microbial electrolysis cell startup and performance. *Bioelectrochemistry*, *113*, 20–25. <https://doi.org/10.1016/j.bioelechem.2016.08.003>
- Langille, M. G. I., Zaneveld, J., Caporaso, J. G., McDonald, D., Knights, D., Reyes, J. A., ...

REFERENCES

- Huttenhower, C. (2013). Predictive functional profiling of microbial communities using 16S rRNA marker gene sequences. *Nature Biotechnology*, *31*(9), 814–821. <https://doi.org/10.1038/nbt.2676>
- Laudadio, I., Fulci, V., Palone, F., Stronati, L., Cucchiara, S., & Carissimi, C. (2018). Quantitative Assessment of Shotgun Metagenomics and 16S rDNA Amplicon Sequencing in the Study of Human Gut Microbiome. *OMICS A Journal of Integrative Biology*, *22*(4), 248–254. <https://doi.org/10.1089/omi.2018.0013>
- Letunic, I., & Bork, P. (2016). Interactive tree of life (iTOL) v3: an online tool for the display and annotation of phylogenetic and other trees. *Nucleic Acids Research*, *44*(W1), W242–5. <https://doi.org/10.1093/nar/gkw290>
- Li, H., Opgenorth, P. H. P. H., Wernick, D. G. D. G., Rogers, S., Wu, T. Y. T.-Y., Higashide, W., Malati, P., Huo, Y., Cho, K.M. & Liao, J. C. (2012). Integrated Electromicrobial Conversion of CO₂ to Higher Alcohols. *Science*, *335*(6076), 1596–1596. <https://doi.org/10.1126/science.1217643>
- Li, X., Luo, Q., Wofford, N. Q., Keller, K. L., McInerney, M. J., Wall, J. D., & Krumholz, L. R. (2009). A Molybdopterine Oxidoreductase Is Involved in H₂ Oxidation in *Desulfovibrio desulfuricans* G20. *Journal of Bacteriology*, *191*(8), 2675–2682. <https://doi.org/10.1128/JB.01814-08>
- Lie, T. J., Costa, K. C., Lupa, B., Korpole, S., Whitman, W. B., & Leigh, J. A. (2012). Essential anaerobic role for the energy-converting hydrogenase Eha in hydrogenotrophic methanogenesis. *Proceedings of the National Academy of Sciences*, *109*(38), 15473–15478. <https://doi.org/10.1073/pnas.1208779109>
- Lienemann, M., Deutzmann, J. S., Milton, R. D., Sahin, M., & Spormann, A. M. (2018). Mediator-free enzymatic electrosynthesis of formate by the *Methanococcus marisnigri* heterodisulfide reductase supercomplex. *Bioresource Technology*, *254*(November 2017), 278–283. <https://doi.org/10.1016/j.biortech.2018.01.036>
- Light, S. H., Su, L., Rivera-Lugo, R., Cornejo, J. A., Louie, A., Iavarone, A. T., Ajo-Franklin, C.M. & Portnoy, D. A. (2018). A flavin-based extracellular electron transfer mechanism in diverse Gram-positive bacteria. *Nature*, *562*(7725), 140–144. <https://doi.org/10.1038/s41586-018-0498-z>
- Liu, Z., Wang, K., Chen, Y., Tan, T., & Nielsen, J. (2020). Third-generation biorefineries as the means to produce fuels and chemicals from CO₂. *Nature Catalysis*, *3*(3), 274–288. <https://doi.org/10.1038/s41929-019-0421-5>
- Llirós, M., Casamayor, E. O., & Borrego, C. (2008). High archaeal richness in the water column of a

REFERENCES

- freshwater sulfurous karstic lake along an interannual study. *FEMS Microbiology Ecology*, *66*(2), 331–342. <https://doi.org/10.1111/j.1574-6941.2008.00583.x>
- Logan, B. E., Call, D., Cheng, S., Hamelers, H. V. M., Sleutels, T. H. J. A., Jeremiasse, A. W., & Rozendal, R. A. (2008). Microbial Electrolysis Cells for High Yield Hydrogen Gas Production from Organic Matter. *Environmental Science & Technology*, *42*(23), 8630–8640. <https://doi.org/10.1021/es801553z>
- Logan, B. E., & Rabaey, K. (2012). Conversion of Wastes into Bioelectricity and Chemicals by Using Microbial Electrochemical Technologies. *Science*, *337*(6095), 686–690. <https://doi.org/10.1126/science.1217412>
- Logan, B. E., Rossi, R., Ragab, A., & Saikaly, P. E. (2019). Electroactive microorganisms in bioelectrochemical systems. *Nature Reviews Microbiology*, *17*(5), 307–319. <https://doi.org/10.1038/s41579-019-0173-x>
- Lohner, S. T., Deutzmann, J. S., Logan, B. E., Leigh, J., & Spormann, A. M. (2014). Hydrogenase-independent uptake and metabolism of electrons by the archaeon *Methanococcus maripaludis*. *The ISME Journal*, *8*(8), 1673–1681. <https://doi.org/10.1038/ismej.2014.82>
- Lojou, E., Durand, M. C., Dolla, A., & Bianco, P. (2002). Hydrogenase activity control at *Desulfovibrio vulgaris* cell-coated carbon electrodes: Biochemical and chemical factors influencing the mediated bioelectrocatalysis. *Electroanalysis*, *14*(13), 913–922. [https://doi.org/10.1002/1521-4109\(200207\)14:13<913::AID-ELAN913>3.0.CO;2-N](https://doi.org/10.1002/1521-4109(200207)14:13<913::AID-ELAN913>3.0.CO;2-N)
- López-Gutiérrez, J. C., Henry, S., Hallet, S., Martin-Laurent, F., Catroux, G., & Philippot, L. (2004). Quantification of a novel group of nitrate-reducing bacteria in the environment by real-time PCR. *Journal of Microbiological Methods*, *57*(3), 399–407. <https://doi.org/10.1016/j.mimet.2004.02.009>
- Lovley, D. R. (2011). Live wires: Direct extracellular electron exchange for bioenergy and the bioremediation of energy-related contamination. *Energy and Environmental Science*, *4*(12), 4896–4906. <https://doi.org/10.1039/c1ee02229f>
- Lovley, D. R. (2012). Electromicrobiology. *Annual Review of Microbiology*, *66*(1), 391–409. <https://doi.org/10.1146/annurev-micro-092611-150104>
- Lovley, D. R. (2017). Syntrophy Goes Electric: Direct Interspecies Electron Transfer. *Annual Review of Microbiology*, *71*(1), 643–664. <https://doi.org/10.1146/annurev-micro-030117-020420>
- Lovley, D. R., & Holmes, D. E. (2020). Protein Nanowires: the Electrification of the Microbial World and Maybe Our Own. *Journal of Bacteriology*, *202*(20). <https://doi.org/10.1128/JB.00331-20>
- Lovley, D. R., & Nevin, K. P. (2013). Electrobiocommodities: Powering microbial production of

REFERENCES

- fuels and commodity chemicals from carbon dioxide with electricity. *Current Opinion in Biotechnology*, 24(3), 385–390. <https://doi.org/10.1016/j.copbio.2013.02.012>
- Lovley, D. R., & Walker, D. J. F. (2019). *Geobacter* Protein Nanowires. *Frontiers in Microbiology*, 10(September). <https://doi.org/10.3389/fmicb.2019.02078>
- Lozupone, C., & Knight, R. (2005). UniFrac: a New Phylogenetic Method for Comparing Microbial Communities. *Applied and Environmental Microbiology*, 71(12), 8228–8235. <https://doi.org/10.1128/AEM.71.12.8228-8235.2005>
- Major, T. A., Liu, Y., & Whitman, W. B. (2010). Characterization of Energy-Conserving Hydrogenase B in *Methanococcus maripaludis*. *Journal of Bacteriology*, 192(15), 4022–4030. <https://doi.org/10.1128/JB.01446-09>
- Mansure, J. J., & Hallenbeck, P. C. (2008). *Desulfovibrio vulgaris* Hildenborough HydE and HydG interact with the HydA subunit of the [FeFe] hydrogenase. *Biotechnology Letters*, 30(10), 1765–1769. <https://doi.org/10.1007/s10529-008-9755-9>
- Marshall, C. W., Ross, D. E., Fichot, E. B., Norman, R. S., & May, H. D. (2012). Electrosynthesis of commodity chemicals by an autotrophic microbial community. *Applied and Environmental Microbiology*, 78(23), 8412–8420. <https://doi.org/10.1128/AEM.02401-12>
- Marshall, C. W., Ross, D. E., Fichot, E. B., Norman, R. S., & May, H. D. (2013). Long-term operation of microbial electrosynthesis systems improves acetate production by autotrophic microbiomes. *Environmental Science and Technology*. <https://doi.org/10.1021/es400341b>
- Marshall, C. W., Ross, D. E., Handley, K. M., Weisenhorn, P. B., Edirisinghe, J. N., Henry, C. S., ... Handley, K. M. (2017). Metabolic Reconstruction and Modeling Microbial Electrosynthesis. *Scientific Reports*, 7(1), 8391. <https://doi.org/10.1038/s41598-017-08877-z>
- Martin, W. F. (2012). Hydrogen, metals, bifurcating electrons, and proton gradients: The early evolution of biological energy conservation. *FEBS Letters*, 586(5), 485–493. <https://doi.org/10.1016/j.febslet.2011.09.031>
- May, H. D., Evans, P. J., & Labelle, E. V. (2016). ScienceDirect The bioelectrosynthesis of acetate. *Current Opinion in Biotechnology*, 42, 225–233. <https://doi.org/10.1016/j.copbio.2016.09.004>
- Molitor, B., Kirchner, K., Henrich, A. W., Schmitz, S., & Rosenbaum, M. A. (2016). Expanding the molecular toolkit for the homoacetogen *Clostridium ljungdablii*. *Scientific Reports*, 6, 1–10. <https://doi.org/10.1038/srep31518>
- Morris, B. E. L., Henneberger, R., Huber, H., & Moissl-Eichinger, C. (2013). Microbial syntrophy: Interaction for the common good. *FEMS Microbiology Reviews*, 37(3), 384–406. <https://doi.org/10.1111/1574-6976.12019>

REFERENCES

- Moscoviz, R., Toledo-Alarcón, J., Trably, E., & Bernet, N. (2016). Electro-Fermentation: How To Drive Fermentation Using Electrochemical Systems. *Trends in Biotechnology*, *34*(11), 856–865. <https://doi.org/10.1016/j.tibtech.2016.04.009>
- Nevin, K. P., Hensley, S. A., Franks, A. E., Summers, Z. M., Ou, J., Woodard, T. L., Snoeyenbos-West, O.L. & Lovley, D. R. (2011). Electrosynthesis of organic compounds from carbon dioxide is catalyzed by a diversity of acetogenic microorganisms. *Applied and Environmental Microbiology*, *77*(9), 2882–2886. <https://doi.org/10.1128/AEM.02642-10>
- Nevin, K. P., Woodard, T. L., Franks, A. E., Summers, Z. M., & Lovley, D. R. (2010). Microbial Electrosynthesis: Feeding Microbes Electricity To Convert Carbon Dioxide and Water to Multicarbon Extracellular Organic Compounds. *MBio*, *1*(2), 1–4. <https://doi.org/10.1128/mBio.00103-10>
- Parks, J. M., Johs, A., Podar, M., Bridou, R., Hurt, R. A., Smith, S. D., ... Liang, L. (2013). The genetic basis for bacterial mercury methylation. *Science*, *339*(6125), 1332–1335. <https://doi.org/10.1126/science.1230667>
- Patil, S. A., Gildemyn, S., Pant, D., Zengler, K., Logan, B. E., & Rabaey, K. (2015). A logical data representation framework for electricity-driven bioproduction processes. *Biotechnology Advances*, *33*(6), 736–744. <https://doi.org/10.1016/j.biotechadv.2015.03.002>
- Pham, T. H., Boon, N., De Maeyer, K., Höfte, M., Rabaey, K., & Verstraete, W. (2008). Use of *Pseudomonas* species producing phenazine-based metabolites in the anodes of microbial fuel cells to improve electricity generation. *Applied Microbiology and Biotechnology*, *80*(6), 985–993. <https://doi.org/10.1007/s00253-008-1619-7>
- Philips, J. (2020). Extracellular Electron Uptake by Acetogenic Bacteria: Does H₂ Consumption Favor the H₂ Evolution Reaction on a Cathode or Metallic Iron? *Frontiers in Microbiology*, *10*(January), 1–13. <https://doi.org/10.3389/fmicb.2019.02997>
- PrévotEAU, A., Carvajal-Arroyo, J. M., Ganigué, R., & Rabaey, K. (2020). Microbial electrosynthesis from CO₂: forever a promise? *Current Opinion in Biotechnology*, *62*, 48–57. <https://doi.org/10.1016/j.copbio.2019.08.014>
- Puig, S., Ganigué, R., Batlle-Vilanova, P., Balaguer, M. D., Bañeras, L., & Colprim, J. (2017). Tracking bio-hydrogen-mediated production of commodity chemicals from carbon dioxide and renewable electricity. *Bioresour Technol*, *228*, 201–209. <https://doi.org/10.1016/j.biortech.2016.12.035>
- Rabaey, K., & Rozendal, R. A. (2010). Microbial electrosynthesis — revisiting the electrical route for microbial production. *Nature Reviews Microbiology*, *8*(10), 706–716. <https://doi.org/10.1038/nrmicro2422>

REFERENCES

- Ragab, A., Shaw, D. R., Katuri, K. P., & Saikaly, P. E. (2020). Effects of set cathode potentials on microbial electrosynthesis system performance and biocathode methanogen function at a metatranscriptional level. *Scientific Reports*, *10*(1), 1–15. <https://doi.org/10.1038/s41598-020-76229-5>
- Ragsdale, S. W., & Pierce, E. (2008, December). Acetogenesis and the Wood-Ljungdahl pathway of CO₂ fixation. *Biochimica et Biophysica Acta - Proteins and Proteomics*. <https://doi.org/10.1016/j.bbapap.2008.08.012>
- Rajeev, L., Luning, E. G., Zane, G. M., Juba, T. R., Kazakov, A. E., Novichkov, P. S., Wall, J.D. & Mukhopadhyay, A. (2019). LurR is a regulator of the central lactate oxidation pathway in sulfate-reducing *Desulfovibrio* species. *PLoS ONE*, *14*(4), 1–14. <https://doi.org/10.1371/journal.pone.0214960>
- Rapp-Giles, B. J., Casalot, L., English, R. S., Ringbauer, J. A., Dolla, A., & Wall, J. D. (2000). Cytochrome c3 mutants of *Desulfovibrio desulfuricans*. *Applied and Environmental Microbiology*, *66*(2), 671–677. <https://doi.org/10.1128/AEM.66.2.671-677.2000>
- Raskin, L., Stromley, J. M., Rittmann, B. E., & Stahl, D. a. (1994). Group-Specific 16S Ribosomal-Rna Hybridization Probes To Describe Natural Communities of Methanogens. *Applied and Environmental Microbiology*, *60*(4), 1232–1240. [https://doi.org/0099-2240/94/\\$04.00+0](https://doi.org/0099-2240/94/$04.00+0)
- Ray, J., Keller, K. L., Catena, M., Juba, T. R., Zemla, M., Rajeev, L., ... Mukhopadhyay, A. (2014). Exploring the role of CheA3 in *Desulfovibrio vulgaris* Hildenborough motility. *Frontiers in Microbiology*, *5*(March), 1–9. <https://doi.org/10.3389/fmicb.2014.00077>
- Rosenbaum, M. A., & Henrich, A. W. (2014). Engineering microbial electrocatalysis for chemical and fuel production. *Current Opinion in Biotechnology*, *29*(1), 93–98. <https://doi.org/10.1016/j.copbio.2014.03.003>
- Rosenbaum, M., Aulenta, F., Villano, M., & Angenent, L. T. (2011). Cathodes as electron donors for microbial metabolism: Which extracellular electron transfer mechanisms are involved? *Bioresource Technology*, *102*(1), 324–333. <https://doi.org/10.1016/j.biortech.2010.07.008>
- Rotaru, A.-E. E., Shrestha, P. M., Liu, F., Markovaite, B., Chen, S., Nevin, K. P., & Lovley, D. R. (2014). Direct interspecies electron transfer between *Geobacter metallireducens* and *Methanosarcina barkeri*. *Applied and Environmental Microbiology*, *80*(15), 4599–4605. <https://doi.org/10.1128/AEM.00895-14>
- Rotaru, A. E., Shrestha, P. M., Liu, F., Ueki, T., Nevin, K., Summers, Z. M., & Lovley, D. R. (2012). Interspecies electron transfer via hydrogen and formate rather than direct electrical connections in cocultures of *Pelobacter carbinolicus* and *Geobacter sulfurreducens*. *Applied and Environmental Microbiology*, *78*(21), 7645–7651. <https://doi.org/10.1128/AEM.01946-12>

REFERENCES

- Rousset, M., Dermoun, Z., Chippaux, M., & Bélaich, J. P. (1991). Marker exchange mutagenesis of the hydN genes in *Desulfovibrio fructosovorans*. *Molecular Microbiology*, *5*(7), 1735–1740. <https://doi.org/10.1111/j.1365-2958.1991.tb01922.x>
- Rousset, Marc, Casalot, L., Rapp-Giles, B. J., Dermoun, Z., De Philip, P., Bélaich, J. P., & Wall, J. D. (1998). New shuttle vectors for the introduction of cloned DNA in *Desulfovibrio*. *Plasmid*, *39*(2), 114–122. <https://doi.org/10.1006/plas.1997.1321>
- Rovira-Alsina, L., Balaguer, M. D., & Puig, S. (2021). Thermophilic bio-electro carbon dioxide recycling harnessing renewable energy surplus. *Bioresource Technology*, *321*, 124423. <https://doi.org/10.1016/j.biortech.2020.124423>
- Rowe, A. R., Rajeev, P., Jain, A., Pirbadian, S., Okamoto, A., Gralnick, J. A., El-Naggar, M.Y. & Neelson, K. H. (2018). Tracking Electron Uptake from a Cathode into *Shewanella* Cells: Implications for Energy Acquisition from Solid-Substrate Electron Donors. *MBio*, *9*(1), 1–19. <https://doi.org/10.1128/mBio.02203-17>
- Sánchez, C., Dessì, P., Duffy, M., & Lens, P. N. L. (2020). Microbial electrochemical technologies: Electronic circuitry and characterization tools. *Biosensors and Bioelectronics*, *150*(September 2019). <https://doi.org/10.1016/j.bios.2019.111884>
- Schievano, A., Pepé Sciarria, T., Vanbroekhoven, K., De Wever, H., Puig, S., Andersen, S. J., Rabaey, K. & Pant, D. (2016). Electro-Fermentation - Merging Electrochemistry with Fermentation in Industrial Applications. *Trends in Biotechnology*. <https://doi.org/10.1016/j.tibtech.2016.04.007>
- Schröder, U., Harnisch, F., & Angenent, L. T. (2015). Microbial electrochemistry and technology: Terminology and classification. *Energy and Environmental Science*, *8*(2), 513–519. <https://doi.org/10.1039/c4ee03359k>
- Schuchmann, K., & Müller, V. (2014). Autotrophy at the thermodynamic limit of life: A model for energy conservation in acetogenic bacteria. *Nature Reviews Microbiology*, *12*(12), 809–821. <https://doi.org/10.1038/nrmicro3365>
- Selembo, P. A., Merrill, M. D., & Logan, B. E. (2010). Hydrogen production with nickel powder cathode catalysts in microbial electrolysis cells. *International Journal of Hydrogen Energy*, *35*(2), 428–437. <https://doi.org/10.1016/j.ijhydene.2009.11.014>
- Sherba, J. J., Hogquist, S., Lin, H., Shan, J. W., Shreiber, D. I., & Zahn, J. D. (2020). The effects of electroporation buffer composition on cell viability and electro-transfection efficiency. *Scientific Reports*, 1–9. <https://doi.org/10.1038/s41598-020-59790-x>
- Shrestha, P. M., Rotaru, A.-E., Summers, Z. M., Shrestha, M., Liu, F., & Lovley, D. R. (2013). Transcriptomic and Genetic Analysis of Direct Interspecies Electron Transfer. *Applied and*

REFERENCES

- Environmental Microbiology*, 79(7), 2397–2404. <https://doi.org/10.1128/AEM.03837-12>
- Søndergaard, D., Pedersen, C. N. S., & Greening, C. (2016). HydDB: A web tool for hydrogenase classification and analysis. *Scientific Reports*, 6, 1–8. <https://doi.org/10.1038/srep34212>
- Song, H., Ding, M. Z., Jia, X. Q., Ma, Q., & Yuan, Y. J. (2014). Synthetic microbial consortia: From systematic analysis to construction and applications. *Chemical Society Reviews*, 43(20), 6954–6981. <https://doi.org/10.1039/c4cs00114a>
- Stoeck, T., Bass, D., Nebel, M., Christen, R., Jones, M. D. M., Breiner, H.-W., & Richards, T. A. (2010). Multiple marker parallel tag environmental DNA sequencing reveals a highly complex eukaryotic community in marine anoxic water. *Molecular Ecology*, 19 Suppl 1(SUPPL. 1), 21–31. <https://doi.org/10.1111/j.1365-294X.2009.04480.x>
- Stokkermans, J. P. W. G., Houba, P. H. J., Pierik, A. J., Hagen, W. R., Dongen, W. M. A. M., & Veerger, C. (1992). Overproduction of prismane protein in *Desulfovibrio vulgaris* (Hildenborough): evidence for a second $S = 1/2$ -spin system in the one-electron reduced state. *European Journal of Biochemistry*, 210(3), 983–988. <https://doi.org/10.1111/j.1432-1033.1992.tb17503.x>
- Subramanian, P., Pirbadian, S., El-Naggar, M. Y., & Jensen, G. J. (2018). Ultrastructure of *Shewanella oneidensis* MR-1 nanowires revealed by electron cryotomography. *Proceedings of the National Academy of Sciences*, 115(14), E3246–E3255. <https://doi.org/10.1073/pnas.1718810115>
- Summers, Z. M., Fogarty, H. E., Leang, C., Franks, A. E., Malvankar, N. S., & Lovley, D. R. (2010). Direct exchange of electrons within aggregates of an evolved syntrophic coculture of anaerobic bacteria. *Science*, 330(6009), 1413–1415. <https://doi.org/10.1126/science.1196526>
- Sun, D., Call, D. F., Kiely, P. D., Wang, A., & Logan, B. E. (2012). Syntrophic interactions improve power production in formic acid fed MFCs operated with set anode potentials or fixed resistances. *Biotechnology and Bioengineering*, 109(2), 405–414. <https://doi.org/10.1002/bit.23348>
- Sydow, A., Krieg, T., Mayer, F., Schrader, J., & Holtmann, D. (2014). Electroactive bacteria—molecular mechanisms and genetic tools. *Applied Microbiology and Biotechnology*, 98(20), 8481–8495. <https://doi.org/10.1007/s00253-014-6005-z>
- Ter Heijne, A., Hamelers, H. V. M., De Wilde, V., Rozendal, R. A., & Buisman, C. J. N. (2006). A bipolar membrane combined with ferric iron reduction as an efficient cathode system in microbial fuel cells. *Environmental Science and Technology*, 40(17), 5200–5205. <https://doi.org/10.1021/es0608545>
- Tersteegen, A., & Hedderich, R. (1999). *Methanobacterium thermoautotrophicum* encodes two multisubunit membrane-bound [NiFe] hydrogenases. Transcription of the operons and sequence analysis of

REFERENCES

- the deduced proteins. *European Journal of Biochemistry*, 264(3), 930–943. <https://doi.org/10.1046/j.1432-1327.1999.00692.x>
- Thauer, R. K. (2012). The Wolfe cycle comes full circle. *Proceedings of the National Academy of Sciences*, 109(38), 15084–15085. <https://doi.org/10.1073/pnas.1213193109>
- Thauer, R. K., Kaster, A.-K., Goenrich, M., Schick, M., Hiromoto, T., & Shima, S. (2010). Hydrogenases from methanogenic archaea, nickel, a novel cofactor, and H₂ storage. *Annual Review of Biochemistry*, 79(1), 507–536. <https://doi.org/10.1146/annurev.biochem.030508.152103>
- Tian, P., Wang, J., Shen, X., Rey, J. F., Yuan, Q., & Yan, Y. (2017). Fundamental CRISPR-Cas9 tools and current applications in microbial systems. *Synthetic and Systems Biotechnology*, 2(3), 219–225. <https://doi.org/10.1016/j.synbio.2017.08.006>
- Tremblay, P.-L., Faraghiparapari, N., & Zhang, T. (2019). Accelerated H₂ Evolution during Microbial Electrosynthesis with *Sporomusa ovata*. *Catalysts*, 9(2), 166. <https://doi.org/10.3390/catal9020166>
- Tremblay, P.-L., & Zhang, T. (2015). Electrifying microbes for the production of chemicals. *Frontiers in Microbiology*, 6(MAR), 1–10. <https://doi.org/10.3389/fmicb.2015.00201>
- Van Eerten-Jansen, M. C. A. A., Veldhoen, A. B., Plugge, C. M., Stams, A. J. M., Buisman, C. J. N., & Ter Heijne, A. (2013). Microbial Community Analysis of a Methane-Producing Biocathode in a Bioelectrochemical System. *Archaea*, 2013, 1–12. <https://doi.org/10.1155/2013/481784>
- Vandenberg, W., Stokkermans, J., & Vandongen, W. (1993). The operon for the Fe-hydrogenase in *Desulfovibrio vulgaris* (Hildenborough): Mapping of the transcript and regulation of expression. *FEMS Microbiology Letters*, 110(1), 85–90. [https://doi.org/10.1016/0378-1097\(93\)90246-X](https://doi.org/10.1016/0378-1097(93)90246-X)
- Vigouroux, A., & Bikard, D. (2020). CRISPR Tools To Control Gene Expression in Bacteria. *Microbiology and Molecular Biology Reviews*, 84(2). <https://doi.org/10.1128/MMBR.00077-19>
- Vilar-Sanz, A., Pous, N., Puig, S., Balaguer, M. D., Colprim, J., & Bañeras, L. (2018). Denitrifying nirK-containing alphaproteobacteria exhibit different electrode driven nitrite reduction capacities. *Bioelectrochemistry*, 121, 74–83. <https://doi.org/10.1016/j.bioelechem.2018.01.007>
- Voordouw, G., Pollock, W. B., Bruschi, M., Guerlesquin, F., Rapp-Giles, B. J., & Wall, J. D. (1990). Functional expression of *Desulfovibrio vulgaris* Hildenborough cytochrome c3 in *Desulfovibrio desulfuricans* G200 after conjugational gene transfer from *Escherichia coli*. *Journal of Bacteriology*, 172(10), 6122–6126. <https://doi.org/10.1128/jb.172.10.6122-6126.1990>
- Vu, M. T., Noori, M. T., & Min, B. (2020). Conductive magnetite nanoparticles trigger syntrophic methane production in single chamber microbial electrochemical systems. *Bioresource Technology*,

REFERENCES

- 296(October 2019), 122265. <https://doi.org/10.1016/j.biortech.2019.122265>
- Wang, H., & Ren, Z. J. (2013). A comprehensive review of microbial electrochemical systems as a platform technology. *Biotechnology Advances*, *31*(8), 1796–1807. <https://doi.org/10.1016/j.biotechadv.2013.10.001>
- Wood, J. L., Osman, A., & Wade, S. A. (2019). An efficient, cost-effective method for determining the growth rate of sulfate-reducing bacteria using spectrophotometry. *MethodsX*, *6*(June), 2248–2257. <https://doi.org/10.1016/j.mex.2019.09.036>
- Wu, S. C., Liou, S. Z., & Lee, C. M. (2012). Correlation between bio-hydrogen production and polyhydroxybutyrate (PHB) synthesis by *Rhodospirillum rubrum* WP3-5. *Bioresource Technology*, *113*, 44–50. <https://doi.org/10.1016/j.biortech.2012.01.090>
- Yang, Y., Wu, Y., Hu, Y., Cao, Y., Poh, C. L., Cao, B., & Song, H. (2015). Engineering Electrode-Attached Microbial Consortia for High-Performance Xylose-Fed Microbial Fuel Cell. *ACS Catalysis*, *5*(11), 6937–6945. <https://doi.org/10.1021/acscatal.5b01733>
- Ye, J., Coulouris, G., Zaretskaya, I., Cutcutache, I., Rozen, S., & Madden, T. L. (2012). Primer-BLAST: a tool to design target-specific primers for polymerase chain reaction. *BMC Bioinformatics*, *13*(1), 134. <https://doi.org/10.1186/1471-2105-13-134>
- Yu, Lin, Duan, J., Zhao, W., Huang, Y., & Hou, B. (2011). Characteristics of hydrogen evolution and oxidation catalyzed by *Desulfovibrio caledoniensis* biofilm on pyrolytic graphite electrode. *Electrochimica Acta*, *56*(25), 9041–9047. <https://doi.org/10.1016/j.electacta.2011.05.086>
- Yu, Linpeng, Yuan, Y., Tang, J., & Zhou, S. (2017). Thermophilic *Moorella thermoautotrophica*-immobilized cathode enhanced microbial electrosynthesis of acetate and formate from CO₂. *Bioelectrochemistry*, *117*, 23–28. <https://doi.org/10.1016/j.bioelechem.2017.05.001>
- Zane, G. M., Yen, H. B., & Wall, J. D. (2010). Effect of the Deletion of qmoABC and the Promoter-Distal Gene Encoding a Hypothetical Protein on Sulfate Reduction in *Desulfovibrio vulgaris* Hildenborough. *Applied and Environmental Microbiology*, *76*(16), 5500–5509. <https://doi.org/10.1128/AEM.00691-10>
- Zaybak, Z., Logan, B. E., & Pisciotta, J. M. (2018). Electrotrophic activity and electrosynthetic acetate production by *Desulfobacterium autotrophicum* HRM2. *Bioelectrochemistry*, *123*, 150–155. <https://doi.org/10.1016/j.bioelechem.2018.04.019>